

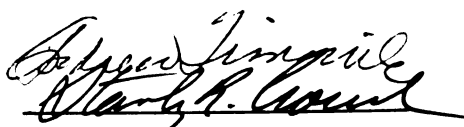
This is to certify that the
thesis entitled
SOME EXPERIMENTAL AND THEORETICAL STUDIES OF
CORRECTIONS FOR ABSORPTION INTERFERENCES
IN RIGHT-ANGLE FLUORIMETRY

presented by

David R. Christmann

has been accepted towards fulfillment
of the requirements for

Ph.D. degree in Chemistry


Major professor

Date October 6, 1980



OVERDUE FINES:

25¢ per day per item

RETURNING LIBRARY MATERIALS:

Place in book return to remove
charge from circulation records

--	--	--

SOME THEORETICAL AND EXPERIMENTAL STUDIES OF CORRECTIONS
FOR ABSORPTION INTERFERENCES IN RIGHT-ANGLE FLUORIMETRY

By

David Ray Christmann

A DISSERTATION

Submitted to

Michigan State University

in partial fulfillment of the requirements

for the degree of

DOCTOR OF PHILOSOPHY

Department of Chemistry

1980

ABSTRACT

SOME EXPERIMENTAL AND THEORETICAL STUDIES OF CORRECTIONS FOR ABSORPTION INTERFERENCES IN RIGHT-ANGLE FLUORIMETRY

By

David R. Christmann

A correction factor has been developed for errors caused by absorption and reflection of the exciting and fluorescence radiation in a dispersive right-angle fluorimeter. The correction factor is a function of the sample transmittance and cell reflectance at both the excitation and emission wavelengths and of a set of geometric window parameters characteristic of the instrument. Experiments are described which show the equation to be accurate to one percent or better up to a sample absorbance of 2.0 when the reemission of absorbed fluorescence by the sample is negligible. For samples containing fluorophores with highly overlapping absorption and emission bands, positive errors can occur in the corrected fluorescence at concentrations greater than about 10^{-5} M due to reemission phenomena.

The instrumental conditions required for implementation of the absorption and reflection correction procedure include: 1) that stray light be low; 2) that the bandwidths of excitation and emission be narrow compared to the sample absorption bands; and 3) that the beams of exciting and fluorescence radiation be highly collimated.

These requirements will preclude the use of the correction equation in conventional filter fluorimetry.

A major practical limitation of the absorption and reflection correction procedure is the need to make transmittance measurements at the excitation and emission wavelengths for each sample. To eliminate this problem, a unique fluorescence instrument has been constructed in which the fluorescence sample cell is shifted with respect to the excitation and emission optics. From fluorescence measurements obtained at three cell positions, the sample transmittance values at the excitation and emission wavelengths and the corrected fluorescence are computed. A microcomputer is employed in the instrument to control cell positioning, data acquisition, wavelength scanning, and to transmit the acquired data to a minicomputer for permanent storage and data reduction. Automation of the cell shift procedure has resulted in a reduction in measurement time, elimination of cell positioning as a source of error, and in simplification and improved accuracy of the window calibration procedure.

With this instrument, a critical study of the precision and accuracy of absorption- and reflection-corrected fluorescence by the cell shift method has been carried out. Experiments are described which show the method to be accurate to two percent or better up to a sample absorbance of 2.7. Reemission and scattering phenomena must be negligible, however, and the bandwidths of excitation and emission must be narrow. Accuracy limitations are demonstrated when each of these conditions do not exist.

Analytical precision has been shown theoretically and experimentally to be reduced by the cell shift correction procedure, but

only by a factor of about two. The sensitivity of the cell shift method is poorer than normal fluorimetric methods because of the high degree of excitation and emission beam collimation required. This is thought to be the major practical limitation of the correction procedure.

To Dad, to Margaret, and
to Mom

ACKNOWLEDGMENTS

The author gratefully acknowledges the guidance and sincere friendship of Professors Andrew Timnick and Stanley R. Crouch over the last four years.

The author wishes to thank Ron Haas and Marty Rabb for their help on electronic matters, Tom Atkinson for his help with MULPLT and computer problems, and master instrument maker, Len Eisele, for his excellent work on the cell positioner.

Thanks are due to many fellow members of the Crouch Group: to Rytis for keeping the 8/e running, to Charlie for always lending an ear, to Gene for his many valuable suggestions concerning this research, to Clay and Rob and Frank for their friendship, and to Jim for saving the author from the Xerox machine.

The author expresses his thanks to Michigan State University, the Department of Chemistry, and Professor Frederick Horne for providing financial support in the form of teaching assistantships and fellowships, to the National Science Foundation for research support, and to the American Chemical Society and Perkin Elmer Corporation for an American Chemical Society Analytical Division Fellowship.

Finally, the author expresses his deepest thanks to his family for their support and for remaining so close when so far away, to Scott and Ken for their companionship on the lakes and streams, and to his wife, Margaret, for her love and patience and her capacity to put up with him.

TABLE OF CONTENTS

Chapter	Page
LIST OF TABLES.	viii
LIST OF FIGURES	ix
CHAPTER I - INTRODUCTION.	1
CHAPTER II - HISTORICAL	6
A. Problems Caused by Excessive Sample Absorption	6
1. Absorption Effects on Quantitative Fluorescence Measurements.	6
2. Absorption Effects on Fluorescence Spectra and Quantum Yield Measure- ments	9
3. Absorption Effects on Synchronous Fluorescence Spectra.	11
4. Absorption Effects on Other Fluores- cence Measurements.	12
B. Conventional Methods for Dealing with Excessive Sample Absorption	13
1. Dilution of the Sample.	14
2. Use of Different Excitation and Emission Wavelengths.	14
3. Different Detection Geometries.	15
4. Special Sample Cells.	17
5. Two-Photon Excitation	18
C. Mathematical Corrections for Sample Absorption.	19
1. Absorption Corrections for Trans- mission Geometry.	19

Chapter	Page
2. Absorption Corrections for Front-Surface Geometry.	21
3. Absorption Corrections for Right-angle Geometry.	24
CHAPTER III - CORRECTION OF RIGHT-ANGLE MOLECULAR FLUORESCENCE MEASUREMENTS FOR ABSORPTION OF FLUORESCENCE RADIATION	28
A. Introduction.	28
B. Theory.	30
1. Cell Geometry	30
2. Some Initial Assumptions.	30
3. The Attenuation by Secondary Absorption.	32
4. Absorption Effects on the Measured Fluorescence Signal	35
5. The Correction Factor	35
C. Experimental	
1. Instrumentation	39
2. Reagents.	39
D. Results and Discussion.	39
1. Measurement Conditions.	39
2. Determination of the Excitation Window Parameters	40
3. Further Verification of the Secondary Absorption Correction	43
4. A Limitation of the Absorption Correction Procedure.	46
5. A Comparison of Correction Factors	48
CHAPTER IV - THE EFFECT OF REFLECTIONS ON RIGHT-ANGLE MOLECULAR FLUORESCENCE MEASUREMENTS	53
A. Introduction	53
B. Theory	54

Chapter	Page
1. Reflections at the Exciting Wavelength	54
2. Reflections at the Emission Wavelength	57
3. Determination of the Cell Reflectance.	59
C. Experimental.	60
D. Results and Discussion.	61
CHAPTER V - AN AUTOMATED INSTRUMENT FOR ABSORPTION-CORRECTED FLUORESCENCE MEASUREMENTS BY THE CELL SHIFT METHOD	64
A. Introduction.	64
B. Theory.	66
C. Instrument Design	70
1. General Description	70
2. The Microcomputer	72
3. Data Acquisition.	74
4. The Cell Positioner	78
5. Alignment and Calibration	83
D. Results and Discussion.	88
1. Determination of the Sample Transmittance	88
2. Fluorimetric Determination of Aluminum.	91
3. Correction of Fluorescence Emission Spectra.	94
CHAPTER VI - PRECISION AND ACCURACY OF ABSORPTION- CORRECTED MOLECULAR FLUORESCENCE MEASUREMENTS BY THE CELL SHIFT METHOD.	99
A. Introduction.	99
B. Experimental.	100

Chapter	Page
1. Instrumentation	100
2. Reagents.	101
C. Results and Discussion.	101
1. Correction Accuracy When Reemission is Negligible	101
2. Effect of Reemission.	109
3. Effect of Light Scattering.	114
4. Effect of Spectral Bandwidth.	116
5. Correction Precision.	118
CHAPTER VII - CONCLUSIONS	123
A. Summary	123
B. Suggestions for Further Work.	128
REFERENCES.	131
APPENDIX A - The IM6100 PROM Monitor.	135
APPENDIX B - Microcomputer Control of the Fluorimeter.	153

LIST OF TABLES

Table	Page
1 Definition of Symbols in Equation (3.10).	36
2 Definition of Symbols in Equation (4.1)	56
3 Test of Reflection Corrections.	62
4 Cell Position Reproducibility	84
5 Comparison of Sample Absorbance Estimates	90
6 Recovery of Aluminum in the Presence of Iron	93
A1 Identity of Circuit Components in Figures A1-A4	140
B1 Identity of Interface Circuit Components.	157
B2 I/O Instructions for the Fluorimeter.	159
B3 Keyboard Commands for Program DRC3.	174

LIST OF FIGURES

Figure		Page
1	<p>Geometry for right-angle fluorimetry with a square cell of internal dimensions $b \times b$ cm. Pathlength (cm) for absorption of exciting radiation at λ nm = x_{β} (max.) and x_{α} (min.). Pathlength (cm) for absorption of fluorescence radiation at λ' nm = y_{β} (max.) and y_{α} (min.).</p>	31
2	<p>Fluorescence of quinine sulfate at 436 nm as a function of fluorescein absorbance at 436 nm. A. Source and blank corrected fluorescence. B. Primary absorption corrected fluorescence. C. Primary and secondary absorption corrected fluorescence. D. Results of applying the correction factor $(T_{\lambda,})^{-(\Theta_{\alpha} + \Theta_{\beta})/2}$ to Curve B</p>	42
3	<p>Fluorescence emission spectra of 10^{-4} M quinine sulfate (-) and 10^{-4} M quinine sulfate + 2.5×10^{-5} M fluorescein (*)</p> <p>A. Corrected for blank, source intensity, and primary absorption. B. Corrected</p>	

Figure		Page
	for fluorescein emission and secondary absorption	45
4	Fluorescence Analytical Curve of Fluorescein. (▲) measured fluo- rescence intensity; (■) primary absorption- corrected intensity; (◆) primary and secondary absorption-corrected intensity; (—) theoretical response	47
5	Fluorescence analytical curve of quinine sulfate. A. Blank and source corrected fluorescence, $\omega_{\beta} = 0.451$, $\omega_{\alpha} = 0.246$. B. Primary absorption corrected fluo- rescence using the factor $(\omega_{\beta} - \omega_{\alpha}) \ln T_{\lambda} /$ $(T_{\lambda})^{\omega_{\beta}} - (T_{\lambda})^{\omega_{\alpha}}$. C. Primary absorption cor- rected fluorescence using the factor $(T_{\lambda})^{-(\omega_{\alpha} + \omega_{\beta})/2}$	51
6	Cell positions for the cell shift method. EX = excitation window, EM = emission window	67
7	Instrument components and their arrangement.	71
8	Block diagram of computer network.	73
9	Fluorescence S/N vs fluorescence photoanodic current. (x) + 22°C, (o) -30° C	76

Figure		Page
10	RMS dark current noise vs temperature for Hamamatsu R666 PMT at 600 V.	77
11	Photograph of the cell positioner.	79
12	Components of the cell positioner.	80
13	Cell displacement in y-dimension as a function of lead screw rotation	82
14	Fluorescence profile of the cell in the y-dimension.	85
15	Fluorescence profile of the cell in the x-dimension.	87
16	Absorbance at excitation wavelength vs. fluorophore concentration. (x) calculated from F_1 and F_2 , (-) regression line cal- culated from spectrophotometric data	89
17	Uncorrected fluorescence emission spectra of 10^{-6} M rhodamine B in ethanol. (o) cell position 1, (Δ) cell position 2, (\square) cell position 3.	95
18	Uncorrected and absorption-corrected fluorescence emission spectra of 10^{-5} M rhodamine B in ethanol, (1) Response from cell position 1. (2) Response from cell position 2. (3) Response from cell position 3	96

Figure		Page
19	Normalized absorption-corrected fluorescence emission spectra of rhodamine B in ethanol. (o) 10^{-6} M, (Δ) 2×10^{-6} M, (\square) 6×10^{-6} M, (\diamond) 10^{-5} M.	97
20	Correction for absorption of exciting radiation by the fluorophore. A - Fluorescence of quinine sulfate vs absorbance at the exciting wavelength, (\blacksquare) corrected fluorescence; (\blacktriangle) measured fluorescence for cell positions 2 and 3; (\bullet) measured fluorescence for cell position 1. B - RSD of corrected fluorescence vs absorbance.	103
21	Correction for absorption of exciting radiation by the sample matrix. A - Fluorescence of a constant amount of quinine sulfate in the presence of increasing amounts of gentisic acid, (\blacktriangle) corrected fluorescence; (\blacksquare) measured fluorescence for cell positions 2 and 3; (\bullet) measured fluorescence for cell position 1. B - RSD of corrected fluorescence vs absorbance	105
22	Correction for absorption of exciting and fluorescence radiation. A - Fluorescence of a constant amount of quinine	

22	sulfate in the presence of increasing amounts of fluorescein; (●) corrected fluorescence; (▲) measured fluorescence for cell position 1; (■) measured fluorescence for cell position 2; (◆) measured fluorescence for cell position 3. B - RSD of corrected fluorescence vs absorbance.	107
23	Effect of reemission on the corrected fluorescence (▲) and apparent sample absorbance at the excitation wavelength (■) when fluorescence is monitored outside the overlap region.	110
24	Effect of reemission on the corrected fluorescence (▲) and apparent sample absorbance at the excitation (■) and emission (◆) wavelengths when fluorescence is monitored in the overlap region	111
25	Absorption-corrected fluorescence emission spectra of rhodamine B in ethanol. (o) 5×10^{-6} M, (Δ) 10^{-5} M, (□) 3×10^{-5} M	113

Figure		Page
26	Corrected fluorescence (Δ) and apparent absorbance (\square), normalized to zero scattering agent, of a constant concentration of quinine sulfate as a function of increasing amounts of soluble starch	115
27	Corrected fluorescence (Δ) and apparent absorbance at the exciting wavelength (\square) vs concentration for quinine sulfate excited with a Xe-Hg arc lamp and Corning 7-60 filter	117
28	Normalized RSD of corrected fluorescence as a function of absorbance. (\bullet) $(\sigma_{F_C}/F_C)/(\sigma_{F_C}/F_2)$, (---) theoretical result from Equation (6.6) for $\xi = 1/2$	121
A1	Data Bus Buffering and Address Circuitry	137
A2	PROM Board Memory and Decoding Circuitry	138
A3	Control Panel Interrupt and Voltage Regulation Circuitry.	139
A4	PROM Board Component Layout	141

Figure		Page
B1	I/O Instruction Decoding Circuitry.	155
B2	Device Select Circuitry	156
B3	Photocurrent Amplifier Circuitry.	160
B4	Sample-and-Hold and Multiplexer Circuitry	162
B5	Analog-to-Digital Conversion Circuitry	164
B6	Cell Position and Chopper Wheel Monitoring Circuitry.	166
B7	Cell Positioner Control Circuitry. R1 = 2.2K, R2-R5 = VR1 - VR4 = 1K, Q1-Q8 = 2N6043.	168
B8	Monochromator Scanning Circuitry.	172

CHAPTER I

INTRODUCTION

Over the past 25 years, fluorimetric analysis has steadily gained popularity as a method for obtaining qualitative and quantitative information about molecules in solution. An increase in the volume of scientific literature on the subject is evidence of this (1). Basically, fluorimetry involves illuminating a sample solution with ultraviolet or visible radiation and measuring the intensity of fluorescence radiation that is emitted. The fluorescence intensity is usually measured at a right-angle to the direction of excitation to discriminate against scattered exciting light.

Several reasons for the increased use of fluorimetric analytical methods can be given. First, because only a limited number of compounds fluoresce, those that do can usually be determined selectively in a complex sample matrix. For samples containing several fluorescent compounds, measurement selectivity is often greater than for molecular absorption spectrophotometry because there are two analytical wavelengths to manipulate.

A second and very important reason for the increased use of fluorimetric methods is that they are typically more sensitive than spectrophotometric methods by a factor of about 10^3 . Because the measured fluorescence photon flux is usually low, very sensitive,

high gain detector-amplifier combinations and photon counting techniques can be used. The fluorescence analytical signal is also directly proportional to the intensity of illumination. Sensitivity is, therefore, increased by the use of a more intense excitation source.

Improvements in fluorescence instrumentation have also contributed greatly to the increased popularity of fluorimetric analytical methods. For many years the reproducibility of fluorimetric measurements was poor due to such instrumental distortions as the instability and spectral distribution of the excitation source intensity and the transmission characteristics of the excitation optical system. In most modern spectrofluorimeters these problems are corrected by ratioing the fluorescence signal to a reference signal that is proportional to the illuminating photon flux. The reference signal is obtained by employing a beam splitter directly before the sample cell to direct a known fraction of the exciting light to a quantum counter and detector. Other instrumental distortions due to the characteristics of the emission optical system and the wavelength dependence of the fluorescence detector sensitivity are eliminated by calibrating the detection system against a standard spectral source and applying corrections to the fluorescence data. This procedure is often carried out automatically in modern instruments by a micro-computer. The development of more intense excitation sources (including lasers), high-throughput holographic grating monochromators, low noise photomultiplier tubes, solid state amplifiers, and digital data acquisition systems has improved the sensitivity, precision,

and accuracy of fluorescence measurements. Further developments in these areas and in applications of fiber optics, array detectors, and microcomputers will continue to expand the use of fluorimetric methods.

Although the state of fluorimetric methodology has improved greatly in recent years, many problems remain to be solved. A major problem that continues to plague fluorimetric methods is the distortion of chemical information from a sample due to excessive absorption by the sample components. The errors that result can be classified as either primary absorption interferences, which involve absorption of the exciting radiation, or as secondary absorption interferences, which involve absorption of the fluorescence radiation.

In the second chapter of this thesis the errors caused by primary and secondary absorption processes are discussed in detail. The experimental techniques that have been used to reduce absorption errors in fluorimetry are also reviewed. Because no experimental method has been a complete solution to the problems of excess sample absorption, much work has been devoted to the development of mathematical corrections for absorption errors. Chapter II concludes with a review of the previous work on absorption-corrected fluorescence.

The remaining chapters of this thesis describe several studies which were conducted with the purpose of eliminating sample absorption as a source of error in right-angle fluorimetry. Chapter III presents a detailed theory that extends the work of previous investigators (2) in explaining the effects of both primary and secondary absorption processes on right-angle fluorescence measurements. A correction factor for secondary absorption interferences is derived and tested,

and the conditions necessary for its implementation are identified. The theory is extended in Chapter IV to include the effects of reflections within the sample cell at the excitation and emission wavelengths. Correction factors for reflection effects are derived and shown to improve the accuracy of the absorption correction procedure. These treatments form the basis for the work described in the following chapters.

In Chapter V, the design of a unique absorption-corrected right-angle spectrofluorimeter is described. A microcomputer is employed to shift the fluorescence sample cell so that the effective path-lengths of excitation and emission are independently varied. From fluorescence measurements at three cell positions, corrections for both primary and secondary absorption interferences are computed. Direct measurement of the sample transmittance is not required. The theory of the cell shift method is explained, and the performance of the instrument is evaluated.

In the next chapter, a critical study of the precision and accuracy of absorption-corrected fluorescence measurements by the cell shift method is described. Accuracy limitations of the correction procedure are demonstrated when wide spectral bandwidths are involved and also when scattering and reemission phenomena occur. When these conditions are absent, the method is shown to be highly accurate. Analytical precision is reduced slightly by the absorption correction procedure, but the effect is generally insignificant. From these findings it is clear that, although limitations exist, in many fluorimetric analytical methods interferences due to all types of

sample absorption can be totally eliminated.

Finally, the significance of this work is summarized, and some recommendations for future work in the area of absorption-corrected right-angle fluorimetry are made. It is hoped that this work will serve to promote the use of absorption correction procedures and to improve the accuracy of many fluorimetric analytical methods.

CHAPTER II

HISTORICAL

A. Problems Caused by Excessive Sample Absorption

In this section, absorption interferences in molecular fluorescence spectrometry are discussed according to their effects on quantitative fluorescence measurements and on fluorescence spectral data. The discussion initially focuses on right-angle detection geometry, but other detection methods are also considered.

1. Absorption Effects on Quantitative Fluorescence Measurements

Primary absorption by the fluorescence analyte is a necessary process in all fluorimetric methods. It can also be the cause of analytical error. The most obvious effect of primary absorption on quantitative fluorescence measurements is that the measured fluorescence intensity is not a linear function of the fluorophore concentration. This fact is usually emphasized in fluorescence monographs (3,4) and textbooks of analytical chemistry (5,6) by the equation

$$F = K\phi I_0(1 - 10^{-\epsilon bc}) \quad (2.1)$$

where F is the intensity of fluorescence emission, K is a constant

that accounts for instrumental factors, ϕ is the fluorescence quantum efficiency, and I_0 is the intensity of monochromatic illumination. The quantities ϵ , b , and c have their usual Beer's law meanings. As the fluorophore concentration approaches zero, Equation 2.1 approaches the linear form

$$F = 2.303K I_0 \epsilon bc \quad (2.2)$$

Because fluorescence measurements can be made at very low concentrations, therefore, the relationship between fluorescence intensity and concentration is usually assumed to be linear. However, some degree of error is always introduced by this assumption (7).

When the primary absorbance of the fluorophore exceeds a value of 0.01, the fluorescence analytical curve begins to bend noticeably toward the concentration axis. At higher fluorophore concentrations the curve passes through a maximum and the fluorescence response begins to decrease (8). Holland (9) has explained this behavior as the result of a shift of the most intensely fluorescing region of sample solution toward the excitation face of the cell as the penetration depth of the exciting radiation is reduced by increased absorption. Because the emission window must be chosen so that the cell walls are masked to prevent distortions from reflection and scattering phenomena, at high enough analyte concentrations not all of the radiation from the most strongly emitting region of solution passes through the geometrical detection window of the fluorimeter, and fewer fluorescence photons are observed. Ohnesorge (10) has shown

that the emission window dimensions and location affect the curvature of the fluorescence response.

If fluorescence is monitored on the short wavelength side of an emission band, absorption of the fluorescence radiation by the fluorophore due to the overlap of its absorption and emission bands, i.e., self-absorption, will also cause the fluorescence analytical curve to bend through a maximum at higher concentrations. This occurs because the fraction of light transmitted by the solution at the emission wavelength decreases exponentially as the fluorophore concentration is increased (11). Monitoring fluorescence in this spectral region is not a recommended practice, but may be necessary to avoid interferences from other chromophores or fluorophores in the sample.

As a consequence of these effects, a nonlinear analytical curve must be used or the samples must be diluted to make use of the linear portion of the curve at lower concentrations. Both of these alternatives are inconvenient and involve possible sources of error. It would be most desirable if fluorescence measurements could be corrected to zero sample absorption so that a linear calibration curve would result.

Other absorption problems can be encountered in quantitative fluorimetry if the sample contains primary or secondary absorbing components other than the fluorophore. If the calibration standards are not prepared in this same matrix, the attenuation of the sample fluorescence by primary or secondary absorption is not compensated, and a serious negative error in the analysis can result. Hemoglobin is known to interfere in this manner with the determination of zinc

protoporphyrin in blood (12) and in the determination of serum calcium (13). Often the sample matrix cannot be exactly duplicated and may vary between samples. Separation procedures prior to the fluorimetric analysis may be necessary to avoid the error. This has the disadvantages of increasing the amount of sample treatment, increasing the analysis time, and introducing an additional source of error.

2. Absorption Effects on Fluorescence Spectra and Quantum Yield Measurements

It is well known that instrumental factors such as the spectral energy distribution of the excitation source and the spectral sensitivity of the detection system can severely distort fluorescence excitation and emission spectra unless corrections for their effects are made (14-21). Parker and Rees (14) have shown that primary and secondary absorption processes can cause spectral distortions which are just as serious.

Theoretically, the fluorescence excitation spectrum of a compound should be identical to its absorption spectrum (3,22). To observe this for a given sample, however, the measured fluorescence intensity must vary linearly with the sample absorbance. As discussed above, this behavior is approached accurately only when the primary absorbance of the fluorophore is 0.01 or less. When the absorbance exceeds this limit the fluorescence excitation spectrum sags below the absorption spectrum (23). The problem is compounded if the absorbance of the sample is higher than 0.01. The shift of the fluorescing region of solution out of the detection window of the

instrument can cause a further decrease of fluorescence intensity and possibly a minimum in the excitation spectrum in the spectral region of an absorption peak. Clearly, under conditions in which the sample primary absorbance exceeds 0.01 the true fluorescence excitation spectrum will not be observed.

Primary absorption processes also affect fluorescence emission spectra. The decrease in emission intensity caused by primary absorption affects all emission wavelengths so that the entire emission spectrum is attenuated by a constant factor. Parker and Rees (21) have noted that this will cause a negative error in the relative quantum yield determined from the area under the spectrum. They suggest: 1) keeping the primary absorbance of the sample below 0.02 to reduce the error to four percent or less, or 2) matching the absorbance of the quantum yield standard to that of the sample.

Secondary absorption by the fluorophore causes a loss of intensity on the short wavelength end of fluorescence emission spectra (21). Because of this, a serious negative error, which Demas and Crosby (24) have called the "reabsorption error", will exist in the quantum yield determined from such a spectrum. Similarly, secondary absorption by other components of the sample will lead to decreased intensity and possibly minima in the observed emission spectrum in the spectral regions where they absorb. This also causes the measured quantum yield to be low and precludes accurate quantum yield measurements on all but pure fluorophore solutions.

3. Absorption Effects on Synchronous Fluorescence Spectra

In recent years, a new modification of the fluorescence method called synchronous fluorescence spectrometry has come into use (25). In this method, the excitation and emission wavelengths are scanned in tandem with a constant wavelength difference between them. The result is a unique fluorescence emission spectrum that is often a better fingerprint of a compound than its normal emission spectrum. The qualitative power of the synchronous method has been demonstrated by its use to identify crude oil samples (26) and traces of rubber (27) as well as its use in a wide range of forensic applications (28-30). Vo-Dinh (31) was able to resolve completely and identify as many as five polycyclic aromatic hydrocarbons in the synchronous spectrum of a mixture for which the normal emission spectral components were hopelessly overlapped.

Theories of the synchronous emission spectrum have been published by Lloyd and Evett (32) and by Vo-Dinh (31). From these discussions, it is clear that a synchronous signal is observed only in the spectral region in which the normal fluorescence excitation and emission spectra overlap. A combination of the extent of overlap, the features of the overlapping spectra, and the spectral position of the overlap make the synchronous spectrum unique for each compound. However, these same factors make the synchronous spectrum highly subject to primary and secondary absorption interferences.

Because the synchronous signal is derived from the region of spectral overlap, secondary absorption by the fluorophore will

inevitably attenuate the signal and distort the observed spectrum. This fact has been the subject of a recent controversy about the usefulness of the synchronous method (33-35). Since the excitation and emission processes in the overlap region are not as efficient, higher than normal sample concentrations must be used to obtain detectable signals. This step increases secondary absorption interference and may cause primary absorption by the fluorophore to become significant. The synchronous method appears to be useful on complex samples for which the normal emission spectral components overlap. But in these types of solutions, primary and secondary absorption by the other sample components attenuate the synchronous fluorescence signal in the same way that they affect the normal emission spectrum (33).

The synchronous emission spectrum may be a valuable qualitative tool, but it is not likely to be of significant quantitative value unless the primary and secondary absorption interferences can be corrected. No quantitative applications of synchronous fluorescence measurements are presently known, and indeed, the data of White (36) suggest that the relationship between the synchronous fluorescence signal and fluorophore concentration is not linear.

4. Absorption Effects on Other Fluorescence Measurements

Molecular fluorescence spectrometry is often used to determine chemical equilibrium constants and related thermodynamic quantities such as ΔG , ΔH , and ΔS for both ground state and excited state molecules (37). It is assumed in these studies that the fluorescence

signal is linearly related to the fluorophore concentration. Linearity is not always verified with a calibration curve, however. When a calibration curve is used it may not compensate for absorption interferences due to the sample matrix if the matrix is not duplicated for the calibration standards. Accurate experimental results can be very difficult to obtain.

Fluorescence detection is also used to monitor rates of reaction from which rate laws, rate constants, and activation parameters are determined. Here also, it is fundamentally assumed that the fluorescence signal is a linear function of the analyte concentration. Primary and secondary absorption interferences can cause the signal-concentration relationship to be far from linear, and the degree of interference can change as the reaction proceeds. Thus, it could be difficult to extract a meaningful rate constant from the observed rate behavior, and all calculated results could unknowingly be in error.

B. Conventional Methods for Dealing with Excessive Sample Absorption

Many investigators have found ways to overcome absorption interferences in particular experimental situations by altering their experimental procedure or fluorescence instrumentation. These methods and their limitations are discussed in this section and are compared to normal right-angle fluorimetric methods when appropriate.

1. Dilution of the Sample

The most widely recommended and used procedure for dealing with primary and secondary absorption interferences is to dilute the sample until the magnitude of the absorption effect is reduced to an acceptable level (3,4). In many situations this is a simple and practical remedy. It will not always be satisfactory, however. Dilution of the fluorophore almost always involves a loss of sensitivity. It is possible that to reduce the sample absorbance to an acceptable level the fluorophore must be diluted to a concentration that is difficult to detect. For example, for a sample containing a weak fluorophore and a strong primary or secondary absorbing chromophore, the fluorescence signal might be near the detection limit and dilution would not be possible.

Other disadvantages of sample dilution procedures are that they increase the amount of sample treatment and the analysis time and can be a source of error. Although it should be possible to keep dilution errors small, it is best to avoid them altogether. Finally, dilution can shift solution equilibria. The use of dilution procedures in some types of studies and analyses may be impossible for this reason.

2. Use of Different Excitation and Emission Wavelengths

With modern spectrofluorimeters it is often possible to choose an excitation and emission wavelength at which primary and secondary absorption interferences are negligible. Although this is usually

a convenient remedy, with complicated samples it may not be possible to avoid the absorption interference of one chromophore without encountering absorption interferences from other chromophores or spectral interferences from other fluorophores. Another limitation of this procedure is that sensitivity is usually lost by moving the excitation or emission wavelengths away from the fluorescence excitation or emission maximum.

3. Different Detection Geometries

Another common method of dealing with absorption interferences is to use a different detection geometry, of which there are two types: "in-line" or "transmission" geometry and "front-surface" geometry.

a. Transmission Geometry - In the transmission geometry arrangement, the fluorescence detector views the cell face through which the exciting light leaves the cell. The advantage of this geometry is that primary absorption interferences are less severe. As the primary absorbance of the sample is increased, the fluorescing region of the solution moves toward the excitation face of the cell but always remains in the detection window. The curvature of the fluorescence analytical curve and the resulting errors are, therefore, reduced.

There are also several disadvantages of transmission detection geometry. First, primary absorption interferences are only reduced and not eliminated. Of more importance, secondary absorption

interferences are usually more severe than with right-angle geometry (38). This is due to the fact that some of the fluorescence light must travel the entire width of the cell through the sample to reach the detector. Secondary absorption interferences can be even worse if the primary absorbance of the sample is high. As the fluorescing region of solution moves toward the excitation face, the average path-length through the sample for the fluorescence emission is increased and can approach the full width of the cell. Distortions of fluorescence excitation spectra recorded with transmission geometry have been reported and blamed on this effect (39).

b. Front-surface Geometry - "Front-surface" or "reflection" geometry involves observing fluorescence emission through the front or excitation face of the sample cell. It is often used to avoid absorption interferences in fluorescence emission spectra. For very highly absorbing solutions, the exciting light is almost completely absorbed at the cell wall-solution interface. The depth of penetration of the exciting radiation into the solution decreases with increasing analyte concentration. The path for fluorescence radiation out of the solution is, therefore, very short. Also, the fluorescing region of solution always remains in the instrument detection window. These conditions help to reduce primary and secondary absorption errors. To maintain these conditions, however, highly concentrated samples must always be used, and because of this, secondary absorption and quenching errors can occur (24). McDonald and Selinger (39) have shown that large secondary absorption errors, similar to those which

plague right-angle measurements, can exist in fluorescence emission spectra obtained with the front surface arrangement. Berlman (40) and Parker (3) have suggested that the fluorophore be excited at its most intense absorption peak to reduce the concentration of fluorophore required. This does not eliminate the interference but does make it less serious than in right-angle measurements (38).

Another limitation of front-surface fluorescence detection geometry that has been noted (24,38) is that the emission spectra recorded are more subject to distortion due to the reemission of absorbed fluorescence by the sample. Quantum yields up to 50 percent greater than the true value have been measured for 9,10-diphenylanthracene because of this effect (41,42).

4. Special Sample Cells

Several variations of the fluorescence sample cell that take advantage of shorter pathlengths for the exciting and fluorescence radiation into and out of the sample have been shown to be effective for reducing absorption interferences. Chen and Hayes (43) were able to extend the linear portion of the fluorescence calibration curve of NADPH by almost an order of magnitude in concentration by placing a square cuvette eccentrically in the sample compartment of an Aminco-Bowman spectrofluorimeter. Similar improvements were obtained when a 3 mm microcell was used in place of a normal 1 cm cuvette. With both arrangements, however, the sample absorption interferences were only reduced and not eliminated. Another problem is that interferences from light scattered and fluoresced by the cell walls is greater than

for the normal right-angle arrangement, especially with the micro-cell.

Mitchell, Garden, and Aldous (44) described a fluorimetric cell in which a single fiber optic bundle carries the exciting light to and the fluorescence light from the sample solution. This also reduces the pathlengths for absorption. Compared to a right-angle fluorimeter, they were able to reduce the measurement error on a solution with a primary absorbance of 0.25 from 63 percent to 21 percent with this cell. Although this is a significant improvement, more improvement is desirable. It is doubtful that this fiber optic design will be of significant use for dealing with absorption interferences in fluorimetry.

5. Two-Photon Excitation

Recently, Wirth and Lytle (45) used the method of two-photon excitation to overcome primary absorption interferences in optically dense solutions. In this mode of excitation the fluorophore must simultaneously absorb two photons which are of half the energy required for single-photon absorption. Two-photon absorption does not follow the Beer-Lambert absorption law and is characterized by a very low absorption cross section. These facts make fluorimetry with two-photon excitation essentially immune to errors due to primary absorption by the fluorophore. In one experiment, a constant fluorescence signal was measured for a constant amount of p-terphenyl as the primary absorbance of the solutions for single-photon absorption was increased to 28.

Although these results are promising, several limitations exist. The selection rules for two-photon absorption differ from those for single photon absorption making it difficult to reach some excited energy states. The instrumentation required for two-photon excitation is also more complicated and expensive. A laser excitation source must be used. Also, the method is not immune to secondary absorption interferences. Focusing the exciting laser beam close to the emission face of the sample cell will reduce secondary absorption errors but not eliminate them. Finally, single-photon absorption of the exciting laser light by the sample matrix will cause primary absorption errors. For complicated samples the method may not offer any advantages over conventional fluorimetry.

C. Mathematical Corrections for Sample Absorption

It is evident from the previous discussion that there is no universal experimental method for obtaining absorption-free fluorescence information from a sample. For this reason, many attempts have been made to describe primary and secondary absorption interferences mathematically so that fluorescence measurements can be corrected for their effects. These efforts are reviewed here according to the detection geometries used.

1. Absorption Corrections for Transmission Geometry

Probably the first attempt to describe the effects of absorption on transmission type fluorescence measurements mathematically was

made by Weber in 1930 (46). Two equations were proposed to describe the fluorescence intensity as a function of the primary absorbance of the sample. Measured fluorescence intensities from a transmission type filter fluorimeter were compared with values calculated from the proposed relationships, but without much success. More recent work has shown that the equations were too simple to describe the experimental results accurately.

In 1938, Sen-Gupta and Ghosh (47,48) derived equations to describe transmission as well as front-surface and right-angle fluorescence measurements in terms of both the primary and secondary absorbances of the sample. Although these equations were more carefully conceived, the fact that radiation absorbed by the sample matrix will not contribute to the observed fluorescence intensity was neglected. No further work based on this study is known. However, in 1944, Rollefson and Dodgen (49) independently derived an equivalent expression. Using measured solution absorbances at the excitation and emission wavelengths, they obtained good agreement between calculated and observed fluorescence intensities from solutions of fluorescein and of acridone. The correction appeared to be accurate for solutions of a single fluorophore, but was not tested with other primary absorbing components present in the sample.

In 1973, van Slageren and workers (50) published a third independent derivation of the same absorption expressions for transmission type fluorescence measurements. Theoretical plots of the fluorescence response as a function of sample absorbance were presented, but no experimental verification was attempted or has been described

since the work was published. The authors did clearly state that for the expressions to be accurate, the excitation light must be homogeneous, monochromatic, and collimated. The fluorescence light reaching the detector must also be monochromatic and collimated.

It appears that a good theoretical description of the effects of primary absorption by the fluorophore on transmission type fluorescence measurements is available. It is not clear, however, that the equations are accurate when a second absorbing component is present in the sample. No applications of the correction equations have been reported, probably because of the more widespread use of other detection geometries.

2. Absorption Corrections for Front-Surface Geometry

Many papers on absorption-corrected fluorescence have dealt with front-surface detection geometry. The first work of this sort was by Sen-Gupta and Ghosh (47,48) who derived an expression for the fluorescence intensity in terms of the molar absorptivities of the sample at the excitation and emission wavelengths. An equation of the same functional form was published by van Slageren et al. (50). In 1951, Förster (51) derived an expression of similar form but not identical to these equations. In all three cases, no experimental verification of the proposed relationships was described.

In 1956, Budo and Ketskemety (52,53) initiated a series of papers (54,55) that described a complicated correction for primary and secondary absorption and also reemission errors in front-surface

fluorimetric measurements. Their equation was similar to that of Sen-Gupta (48) but included a factor $(1 + K)$ to compensate for re-emission of absorbed fluorescence. The factor K was defined to be the ratio of the reemitted light to that of the direct fluorescence light and was calculated by evaluating a complex integral. These workers maintained that by replacing the factor $(1 + K)$ with a factor $1/(1 - K)$ multiple reabsorption and reemission effects could be corrected. They offered some experimental evidence as proof (55). The results seem to substantiate the accuracy of the correction procedure, but the conditions under which the correction can be used are unclear. The calculation of the factor K was also very complicated and not explained well.

In 1961, Melhuish (41) modified the equations of Budo et al. (52) to include a correction for the movement of the fluorescing region of solution away from the front face of the sample cell as the sample is diluted. The limiting forms of the equation at high and low primary absorbance were discussed, and the former was applied to correct Stern-Volmer plots for anthracene and perylene to linearity. More recently, a point by point correction of the emission spectrum of perylene has been published (56).

The remainder of the literature on absorption-corrected fluorescence for front-surface geometry has focused on correcting fluorescence quantum yields for absorption interferences. Birks (38) described a simple correction which involves multiplying the observed quantum yield ϕ by a factor $1/(1 - a)$, where a is a quantity called the "self-absorption probability". This factor was determined from

the integrated emission spectrum both in the presence and in the absence of self-absorption phenomena. The correction was later extended to cover interference due to reemission of absorbed fluorescence by letting the correction factor be $1/(1 - a + a\phi)$. This correction factor was claimed to be valid for all observation geometries except the front-surface case when ϕ exceeds the value of 0.3 (57). If ϕ is greater than 0.3, the difference between the true and observed quantum yields is great enough to make the correction inaccurate. For the correction to be exact, the true quantum yield would have to be used to calculate the correction factor.

A quite different approach was taken by Rohatgi and Singhal (58) in 1962. These authors described the "average molar absorptivity for self-absorption" which was derived from a simple exponential attenuation model of secondary absorption interference. They showed how this parameter could be determined experimentally, and later derived a relatively simple, new expression to correct the observed quantum yield from measured values of the parameter (59). A linear Stern-Volmer plot was presented to verify the reliability of the method. The simplicity of the calculations was stressed.

Finally, Alan Mode and Sisson (60) described a correction scheme in which an integral was numerically evaluated to obtain a correction factor for primary absorption interference in front-surface quantum yield measurements. They were successful in obtaining constant corrected quantum yields from quinine sulfate solutions in which the primary absorbance varied from 2 to 24. This required repeating the numerical evaluation for each value of the sample absorbance.

Reemission and secondary absorption interferences, which others have found to be significant, were not considered in their treatment.

3. Absorption Corrections for Right-Angle Geometry

Many of the first attempts to describe the effects of primary and secondary absorption on right-angle fluorescence measurements were inaccurate because of a failure to account for absorption by sample components other than the fluorophore and because of geometrical simplifications that do not represent the true experimental arrangement. The equations given by Sen-Gupta (47) and by Förster (51) are of doubtful validity because they were derived from the assumption that the observed fluorescence originates from a point source. This is a poor approximation of the conditions in a real right-angle fluorimeter. Braunsberg and Osborn (61) and Lauer (62) neglected the excitation and emission window dimensions, which are usually chosen to mask the cell walls. Henderson (11) considered the experimental geometry of the fluorescence emission window more carefully, but ignored the finite width of the excitation beam. He found good agreement between calculated fluorescence values and a measured analytical curve for biacetyl and claimed this to be satisfactory verification of his equation. The experiment did show that his consideration of primary absorption interference by the fluorophore was probably correct, but did not test the expression for primary absorption by other sample components. The test also did not extend to high secondary absorbance values at which the geometrical simplification

that was made might create errors.

Thomas and coworkers (63) have presented a more complete consideration of the measurement geometry in deriving an equation for the right-angle fluorescence intensity. Several calculated and measured analytical curves were presented which agreed well below a primary absorbance of about 0.5, but showed large discrepancies at higher absorbances. The differences between the observed and calculated signals were attributed to inaccurate absorption measurements on the more concentrated solutions. The equation was claimed to be accurate, but as in Henderson's work (11), the equation considered only primary absorption by the fluorophore and was not tested under conditions in which the secondary absorbance of the sample was significant.

St. John et al. (64) included expressions for the effects of primary and secondary absorption in a theory of signal-to-noise ratio in luminescence spectrometry. Their equations were adapted in part from a theory of self-absorption in flame photometry (65). It is not clear that this extension of the theory is valid, however.

Leese and Wehry (66) have presented derivations of correction factors for primary and secondary absorption errors in determinations of Stern-Volmer quenching constants by right-angle and front-surface fluorimetry. Although their data support the validity of their method, the correction factors involve complex integrals that must be evaluated numerically. The equations are also only applicable to Stern-Volmer quenching data. This work is clearly not a general solution to the absorption interference problem in right-angle fluorimetry.

Other workers have made more significant contributions to absorption corrected right-angle fluorimetry. In 1957, Parker and Barnes (23) proposed a unique primary absorption correction factor that is a function of only the emission window dimensions and the absorbance of the sample at the excitation wavelength. The factor was claimed to be valid for not only primary absorption by the fluorophore, but also for primary absorption by the sample matrix. The theoretical origin of the expression and the experimental conditions under which it would be valid were not explained. Gill (67) attempted to answer these questions but was able only to justify Parker's equation partially. More recently, an accurate explanation of the theoretical basis of the primary absorption correction factor, experimental evidence of its validity, and the experimental conditions necessary for its implementation have been published (2,68).

Van Slageren et al. (50) have described the attenuation of right-angle fluorescence intensity by primary and secondary absorption in a manner that also accounts for reflections within the sample cell. Their equations appear to account completely for the measurement geometry and for all primary and secondary absorbing components in the sample. The conditions under which the equations apply were clearly stated and closely approximate those found in most modern spectrofluorimeters. Unfortunately, no experimental verification of their theory was attempted. Based on this work, however, Novak (69) recently derived and tested expressions to correct right-angle fluorescence measurements for all absorption interferences without requiring the direct measurement of the sample absorbance. Two procedures were

described by which the sample absorbance or transmittance at the excitation and emission wavelengths can be computed from only fluorescence measurements. One procedure involves measuring the fluorescence with a second sample cell in the excitation or emission light path. The second procedure, called the cell shift method, involves shifting the sample cell with respect to the instrument window optics and measuring the fluorescence at three cell positions. The absorbance values computed from these measurements were used to compute a correction factor for total sample absorption. Some evidence for the accuracy of these correction procedures was presented, but a critical evaluation of the method has not been published. This is the subject of later chapters in this thesis.

CHAPTER III

CORRECTION OF RIGHT-ANGLE MOLECULAR FLUORESCENCE MEASUREMENTS FOR ABSORPTION OF FLUORESCENCE RADIATION

A. Introduction

In previous work by Holland et al. (2) and Kelly (68), a correction factor for primary absorption interferences in right-angle fluorimetry similar to that presented and applied by Parker and Barnes (23) was derived and tested. It was demonstrated that right-angle molecular fluorescence measurements can be accurately corrected for primary absorption interferences when the sample absorbance at the excitation wavelength is as high as 2.0. However, the usefulness of these corrected measurements is limited unless a correction for secondary absorption interference can also be made. The primary absorption-corrected fluorescence intensity is directly proportional to the fluorophore concentration, the desired result, only if the sample is completely transparent to the emitted fluorescence. Many real samples contain components that absorb the analyte fluorescence. The precision and accuracy of the primary absorption-corrected measurement can be seriously degraded as a result.

As discussed in the previous chapter, a correction procedure for secondary absorption interference in front-surface fluorimetry

has been developed and verified by several investigators, but the literature is not consistent on a correction procedure for right-angle detection geometry. Several different mathematical descriptions of the interference have been published for the right-angle case, but no experimental support is given for some of these models. Where experimental results are reported, the accuracy of the model is not clearly demonstrated. A major matter of dispute is whether the fluorescing volume of solution viewed by the detector can be treated as a point source of light (11). This assumption leads to a simplified correction scheme (66), but one of questionable accuracy for a real fluorimeter. Only for the cell shift method proposed by Novak (69) is clear experimental evidence given of the accuracy of a secondary absorption correction procedure.

To clear up the confusion that exists in the literature, and to establish a basis for an investigation of the cell shift method, a detailed study of secondary absorption interferences in right-angle fluorimetry was undertaken. In this chapter, a general theory of secondary absorption interference for a right-angle fluorimeter equipped with a square fluorescence cell is described which incorporates the primary absorption theory of Holland et al. (2). For the specific case of a dispersive instrument, a correction factor for secondary absorption interference is derived, and experimental results are presented to verify its effectiveness. The superiority of this method is demonstrated by comparing experimental results with those obtained by using a correction factor consistent with the point source assumption.

B. Theory

1. Cell Geometry

Figure 1 is a top view representation of the cell geometry that is typically used in right-angle fluorimetry. The fluorescence cell is square with sides of length b cm. The thickness of the cell walls is assumed to be negligible for simplicity. The excitation beam enters the cell through the excitation window which is defined by baffle edges at distances y_{β} and y_{α} cm from the plane of the emission face of the cell. Similarly, the emission beam leaves the cell through the emission window which is defined by baffle edges at distances x_{β} and x_{α} cm from the plane of the excitation face.

2. Some Initial Assumptions

In addition to the cell geometry shown in Figure 1, it is initially convenient to make the following assumptions.

- (a) The excitation beam is homogeneous, collimated, and monochromatic with a wavelength λ nm.
- (b) The emission beam is collimated and monochromatic with a wavelength λ' nm.
- (c) Fluorescence photons which are absorbed in the cell are not remitted by the sample.
- (d) Scattered light, refractive index effects, and reflections within the cell are negligible.
- (e) The sample is homogeneous and contains a single fluorophore although other chromophores may be present.

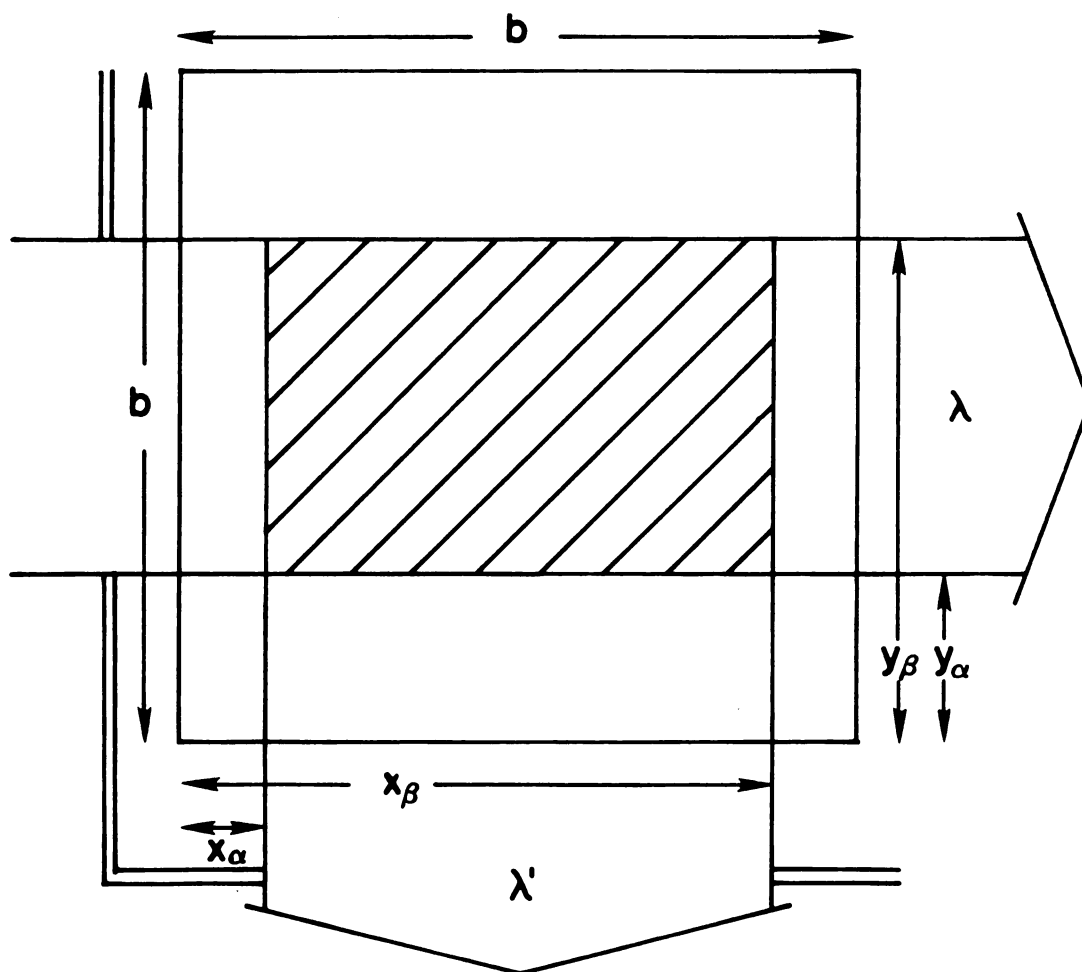


Figure 1. Geometry for right-angle fluorimetry with a square cell of internal dimensions $b \times b$ cm. Pathlength (cm) for absorption of exciting radiation at λ nm = x_β (max.) and x_α (min.). Pathlength (cm) for absorption of fluorescence radiation at λ' nm = y_β (max.) and y_α (min.).

3. The Attenuation by Secondary Absorption

In Figure 1, the fluorescing volume of solution which is viewed by the detector can be represented as a collection of n parallel and equally spaced plane sources of light, each of which is characterized by its distance y_i cm from the emission face of the cell. Each plane contributes a component of radiant power p_i watts to the emission beam such that the power P contained in the beam at the cell face is given by

$$P = \sum_{i=1}^n p_i \quad (3.1)$$

If assumptions 1, 2, and 5 are valid and there is no secondary absorption, each plane will contribute an equal component to the emission beam, i.e., $p_i = p$. The power P_0 of the unattenuated emission beam is then

$$P_0 = \sum_{i=1}^n p = np \quad (3.2)$$

When secondary absorption occurs, the power contributed by each plane is attenuated according to the Beer-Lambert law so that $p_i = p 10^{-y_i \Sigma \epsilon c}$. The quantity $\Sigma \epsilon c$ is the absorbance of the sample per centimeter at the emission wavelength. In terms of the sample transmittance,

$$p_i = p T^{\ominus i} \quad (3.3)$$

where $T = 10^{-b \sum \epsilon c}$ and $\Theta_i = y_i/b$, the fractional distance across the excitation face of the cell. From Equations (3.1) and (3.3), the power P of the attenuated emission beam is given by,

$$P = p \sum_{i=1}^n T^{\Theta_i} \quad (3.4)$$

and the fraction of radiant power in the emission beam that is transmitted to the cell wall is

$$f = \frac{P}{P_0} = \frac{\sum_{i=1}^n T^{\Theta_i}}{n} \quad (3.5)$$

Obviously, if Equation (3.5) is to be meaningful, its limiting form must be determined as the number of planes becomes infinite.

If $\Theta_\beta = y_\beta/b$ and $\Theta_\alpha = y_\alpha/b$, by letting $\Delta\Theta = \Theta_\beta - \Theta_\alpha$ and $\Theta_i = (\Delta\Theta/n-1)(i-1) + \Theta_\alpha$, Equation (3.5) can be rewritten as

$$f = \frac{\sum_{i=1}^n T^{\Theta_\alpha + (\Delta\Theta/n-1)(i-1)}}{n} = \frac{\sum_{j=0}^{n-1} T^{\Theta_\alpha + (\Delta\Theta/n-1)j}}{n} \quad (3.6)$$

By simple division it can be shown that $\sum_{j=0}^{n-1} t^j = \frac{t^n - 1}{t - 1}$. Applying this identity to Equation (3.6) gives

$$f = \frac{T^{\Theta_\alpha} (T^{\Delta\Theta/n-1})_{-1}}{n (T^{\Delta\Theta/n-1})_{-1}} \quad (3.7)$$

or,

$$f = \frac{T^{\Theta_{\alpha}}(T^{\Delta\Theta}T^{\Delta\Theta/(n-1)}-1)}{n(T^{\Delta\Theta/(n-1)}-1)} \quad (3.8)$$

If n is large, $T^{\Delta\Theta/(n-1)} \approx 1 + \frac{\Delta\Theta}{n-1} \ln T$, and as n approaches infinity it follows that

$$\lim_{n \rightarrow \infty} f = \frac{T^{\Theta_{\beta}} - T^{\Theta_{\alpha}}}{\Delta\Theta \ln T} \quad (3.9)$$

Therefore, the fraction of radiant power in the emission beam that is transmitted to the cell wall is an explicit function of the sample transmittance at the emission wavelength and of the excitation window parameters Θ_{β} and Θ_{α} . By expanding the numerator in Equation (3.9) as a Maclaurin series, it is easily shown that the expression becomes unity as the transmittance approaches 1, the required result. Also in support of Equation (3.9), it is noted that a similar expression, but in terms of the sample absorbance and actual beam dimensions, has been briefly derived in a different manner by van Slageren et al. (50) for a similar set of assumptions.

4. Absorption Effects on the Measured Fluorescence Signal

For this discussion to be realistic it is clear that the conditions of assumptions 1 and 2 must be relaxed. In a real fluorimeter, the excitation and emission beams may be very nearly collimated, especially over small distances in the sample cell, but they are never truly monochromatic as Leese and Wehry (66) recently emphasized. Therefore, based on the formality of Winefordner et al. (70), the following general expression can be written to describe the fluorescence photoanodic current produced by any right-angle fluorimeter equipped with a square fluorescence cell:

$$i_{fpa} = \int_0^\infty \int_0^\infty ((\phi_\lambda F_{ex\lambda} + \phi_{st\lambda}) f_\lambda [2.303 A_{f\lambda} \frac{(T_\lambda)^{\omega_\beta} - (T_\lambda)^{\omega_\alpha}}{\ln T_\lambda}] Y_{\lambda\lambda'}) \times$$

$$K \left[\frac{(T_{\lambda'})^{\theta_\beta} - (T_{\lambda'})^{\theta_\alpha}}{(\theta_\beta - \theta_\alpha) \ln T_{\lambda'}} \right] f_{\lambda'} F_{em\lambda'} + \phi_{st\lambda'}) S_{\lambda'} d\lambda d\lambda' \quad (3.10)$$

All symbols and their units are defined in Table 1.

5. The Correction Factor

From Equation (3.10) it is clear that primary and secondary absorption interferences are very complicated for filter type fluorimeters. For dispersive instruments, however, several simplifications can be made. With a good set of monochromators the stray light power terms $\phi_{st\lambda}$ and $\phi_{st\lambda'}$ will be small compared to the source

Table 1. Definition of Symbols in Equation (3.10).

i_{fpa}	= fluorescence photoanodic current, A
ϕ_{λ}	= source spectral radiant flux collected by the instrument, W nm^{-1}
$F_{\text{ex}\lambda}$	= transmission factor of excitation wavelength isolation device, dimensionless
	= $F_{\lambda} t_{\text{s}\lambda}$
F_{λ}	= excitation monochromator slit function, dimensionless
$t_{\text{s}\lambda}$	= transmission factor of monochromator optics, dimensionless
$\phi_{\text{st}\lambda}$	= excitation stray light spectral radiant flux, W nm^{-1}
f	= transmission factor of focusing optics and cell wall, dimensionless
$[2.303 A_{\text{f}\lambda} \frac{(T_{\lambda})^{\omega_{\beta}} - (T_{\lambda})^{\omega_{\alpha}}}{\ln T_{\lambda}}]$	= fraction of power in excitation beam at wavelength λ nm absorbed by the fluorophore in the region of the cell viewed by the detector (see Reference 2)
$A_{\text{f}\lambda}$	= absorbance of the fluorophore at wavelength λ nm
T_{λ}	= sample transmittance at wavelength λ nm
$\omega_{\beta} = x_{\beta}/b$	= emission window parameter, dimensionless

Table 1. Continued.

$\omega_{\alpha} = x_{\alpha}/b$	
$Y_{\lambda\lambda'}$	= luminescence spectral power yield, dimensionless
	= fraction of power absorbed by fluorophore at wavelength λ nm which is emitted at λ' nm
K	= instrumental constant, dimensionless
	= fraction of fluorescence radiation collected as the emission beam
$\left[\frac{(T_{\lambda'})^{\theta_{\beta}} - (T_{\lambda'})^{\theta_{\alpha}}}{(\theta_{\beta} - \theta_{\alpha}) \ln T_{\lambda'}} \right]$	= secondary absorption transmission factor (see text and Equation (3.9))
$T_{\lambda'}$	= sample transmittance at wavelength λ' nm
$f_{\lambda'}$	= transmission factor of cell wall and collection optics, dimensionless
$F_{em\lambda'}$	= transmission factor of emission wavelength isolation device, dimensionless
$\phi_{st\lambda'}$	= emission stray light spectral radiant flux, $W\ nm^{-1}$
$S_{\lambda'}$	= detector sensitivity factor, $A\ W^{-1}$

radiant power ϕ_λ and can therefore be neglected. The limits of integration will then be defined by the monochromator slit functions, assuming a continuum source. If the spectral bandpasses for excitation and emission are made sufficiently narrow so that the sample transmittances T_λ and $T_{\lambda'}$ do not vary significantly over the respective bandpasses, the fluorescence signal current will be given by

$$i_{fpa} = 2.303 K A_f \left[\frac{(T_\lambda)^{\omega_\beta} - (T_\lambda)^{\omega_\alpha}}{\ln T_\lambda} \right] \left[\frac{(T_{\lambda'})^{\theta_\beta} - (T_{\lambda'})^{\theta_\alpha}}{(\theta_\beta - \theta_\alpha) \ln T_{\lambda'}} \right] \iint \dots \quad (3.11)$$

where all wavelength dependent factors in Equation (3.10) remain in the integral. In the limit as T_λ and $T_{\lambda'}$ approach unity, the fluorescence signal becomes totally absorption-free and is given by

$$i_o = 2.303 K A_{f\lambda} (\omega_\beta - \omega_\alpha) \iint \dots \quad (3.12)$$

It follows directly from Equations (3.11) and (3.12) that the absorption-free fluorescence signal is related to the measured signal by

$$i_o = \left[\frac{(\omega_\beta - \omega_\alpha) \ln T_\lambda}{(T_\lambda)^{\omega_\beta} - (T_\lambda)^{\omega_\alpha}} \right] \left[\frac{(\theta_\beta - \theta_\alpha) \ln T_{\lambda'}}{(T_{\lambda'})^{\theta_\beta} - (T_{\lambda'})^{\theta_\alpha}} \right] i_{fpa} \quad (3.13)$$

The first factor in this equation is the primary absorption correction factor (2). The second factor is defined to be the secondary absorption correction factor.

C. Experimental

1. Instrumentation

All fluorescence and absorption measurements described were obtained with a minicomputer controlled spectrofluorimeter capable of simultaneous absorption and fluorescence measurements (68). A Corning 7-60 bandpass filter was placed directly before the quantum counter-reference detector to reduce stray light interference from the sample fluorescence.

2. Reagents

All reagents were of analytical grade and were used without further purification. House distilled water was used to prepare all aqueous solutions.

D. Results and Discussion

1. Measurement Conditions

To test the validity of Equation (3.13), it was necessary to make the measurement conditions conform to the assumptions that are made in its derivation. Some of these conditions already existed in the spectrofluorimeter. Both monochromators have a stray light rating of 0.1 percent and a maximum spectral bandpass of 4 nm. These parameters are sufficient for molecular absorption spectrometry and were therefore

assumed to be satisfactory for this work. They apply to all measurements which are presented here. Also, the emission optical system of the instrument allows a variation of less than two percent in the path length of the emission beam through the sample (2). This enabled assumption 2 to be closely satisfied.

To meet the requirements of assumption 1, a quartz lens (1.5 inch diameter, $f/3$) was used to collimate the radiation from the excitation monochromator. A set of baffles was placed between this lens and the cell to define the width of the excitation beam. The homogeneity of the beam was judged by visual inspection and was optimized by positioning the lens and the light source. The divergence of the beam was measured and found to be less than four percent over its path through the cell.

2. Determination of the Excitation Window Parameters

The spectrofluorimeter used in this study employs an oscillating mirror assembly to move the excitation beam continuously between reference and sample cells (68). However, it was possible to adjust the sample and reference flag signal circuits to arrange for data acquisition to occur at a reproducible point in this movement so that θ_α and θ_β were constant. The point of maximum displacement of the beam into the sample cell was chosen for this work because this enabled θ_α to be measured. The other parameter θ_β could not be measured directly, but was estimated from the measured beam width $\Delta\theta$ by the relationship $\Delta\theta = \theta_\beta - \theta_\alpha$.

Because a real spectrofluorimeter will only approach the required measurement conditions, the effective window parameters for the instrument may differ slightly from those which are actually measured. Therefore, a calibration procedure is necessary. Previously (68), a method was described for determining the emission window parameters ω_{α} and ω_{β} . A Simplex optimization routine, program RTFACT, was used to fit experimental data to a theoretical absorption-free curve. The same method was used in this study to determine Θ_{α} and Θ_{β} .

Solutions of 0 to 5×10^{-5} M fluorescein (sodium salt) and a constant concentration of 10^{-5} M quinine sulfate in 0.1 N H_2SO_4 were prepared. The solutions were excited at 365 nm, and the fluorescence of the quinine sulfate was measured at 436 nm where fluorescein has an absorption maximum in acidic solution and does not itself fluoresce. This selection of wavelengths ensured that assumption 3 was valid over the emission bandpass. The measured fluorescence signals are plotted against the absorbance of the solutions at 436 nm in Figure 2 (Curve A). Each point is the average of 2000 measurements and is source and blank corrected. Severe attenuation by both primary and secondary absorption is evident in these data as the fluorescein concentration is increased. Curve B shows the measured signals after correction for primary absorption interference. Because fluorescein was present in concentrations too low to quench the quinine sulfate fluorescence, the error remaining in Curve B is due only to secondary absorption. These data were submitted to the computerized optimization routine which varied the window parameters

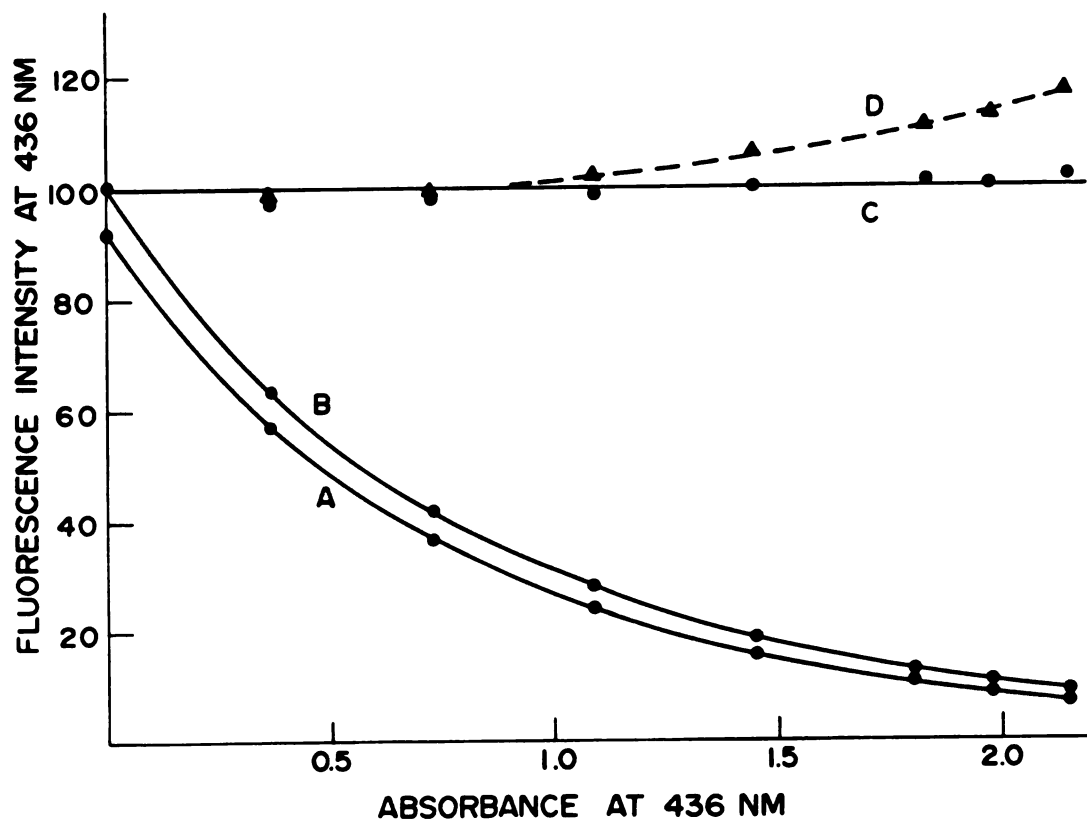


Figure 2. Fluorescence of quinine sulfate at 436 nm as a function of fluorescein absorbance at 436 nm.
 A. Source and blank corrected fluorescence.
 B. Primary absorption corrected fluorescence.
 C. Primary and secondary absorption corrected fluorescence.
 D. Results of applying the correction factor $(T_{\lambda})^{-(\theta_{\alpha} + \theta_{\beta})/2}$ to Curve B.

in the secondary absorption correction factor to obtain a constant absorption corrected response. The results are shown in Curve C. The secondary absorption corrected data are constant to within three percent up to an absorbance of about 2.0. No data were collected beyond this limit because of a decrease in the accuracy of the primary absorption correction (2). The best fit values of $\Theta_{\alpha} = 0.337$ and $\Delta\Theta = 0.364$ agreed well with the measured estimates of $\Theta_{\alpha} = 0.30$ and $\Delta\Theta = 0.35$. This indicates that Equation (3.13) was followed in the experiment. The small differences between the estimated and best fit parameters may be due to the divergence of the emission beam and to the effect of reflections in the cell which have been ignored in this treatment. The effect of reflections is discussed in Chapter IV.

3. Further Verification of the Secondary Absorption Correction

As a further test of Equation (3.13), solutions of 10^{-4} M quinine sulfate, 2.5×10^{-5} M fluorescein, and 10^{-4} M quinine sulfate plus 2.5×10^{-5} M fluorescein were prepared in 0.1 N H_2SO_4 . Each solution was excited at 365 nm and its fluorescence emission spectrum was recorded from 370 to 600 nm. In addition, the absorption spectrum of the quinine sulfate-fluorescein mixture was recorded for use in the correction process. The bandpass filter before the quantum counter was removed for this procedure. Figure 3A shows the emission spectra of the quinine sulfate solution and the quinine sulfate-fluorescein mixture, both of which are corrected for the solvent blank, source intensity, detector response, and primary absorption interference. The location of the fluorescein absorption band is

Figure 3. Fluorescence emission spectra of 10^{-4} M quinine sulfate (-) and 10^{-4} M quinine sulfate + 2.5×10^{-5} M fluorescein (*)

A. Corrected for blank, source intensity, and primary absorption. B. Corrected for fluorescein emission and secondary absorption.

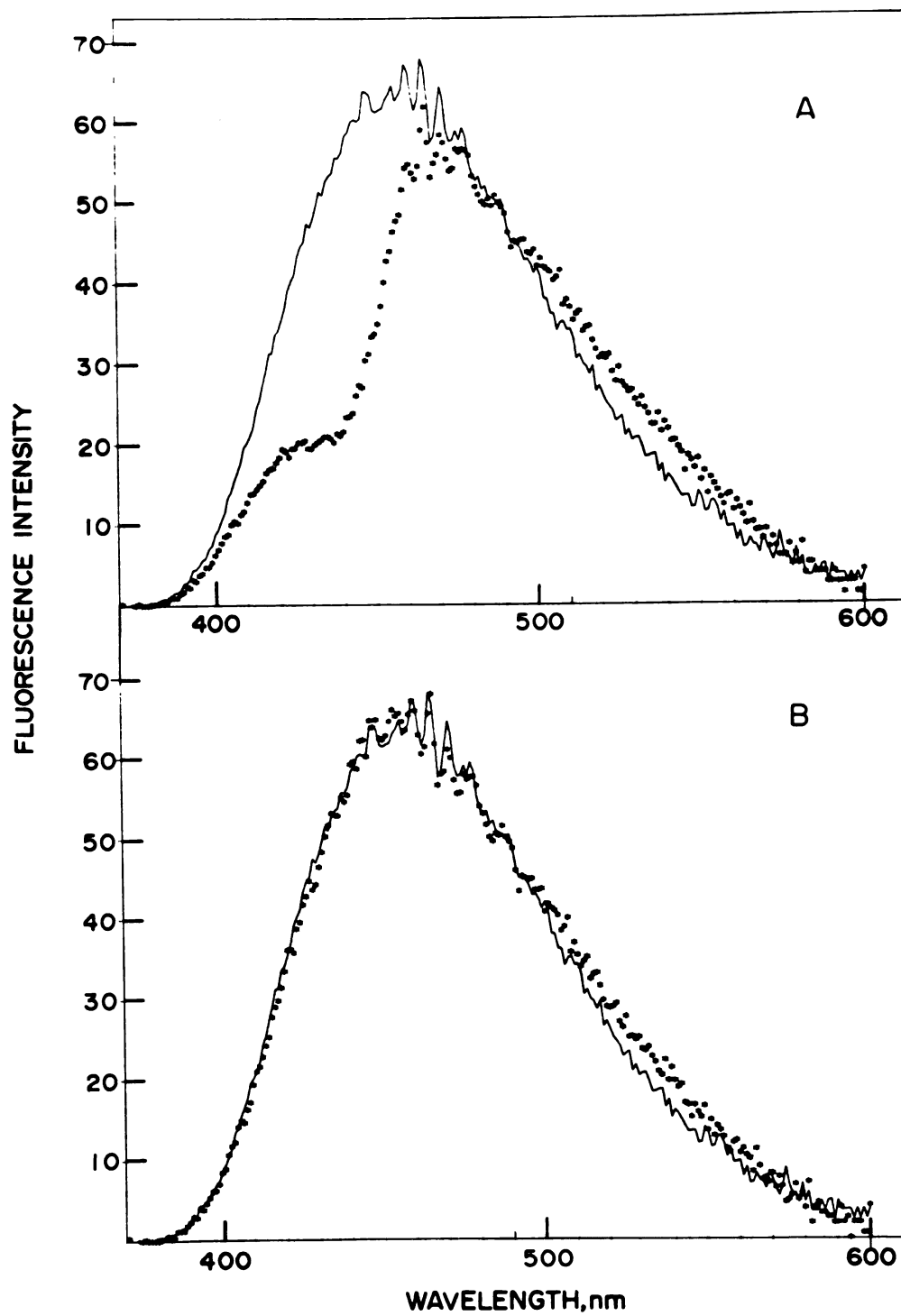


Figure 3

Figure 3. Fluorescence emission spectra of 10^{-4} M quinine sulfate (-) and 10^{-4} M quinine sulfate + 2.5×10^{-5} M fluorescein (*)

A. Corrected for blank, source intensity, and primary absorption. B. Corrected for fluorescein emission and secondary absorption.

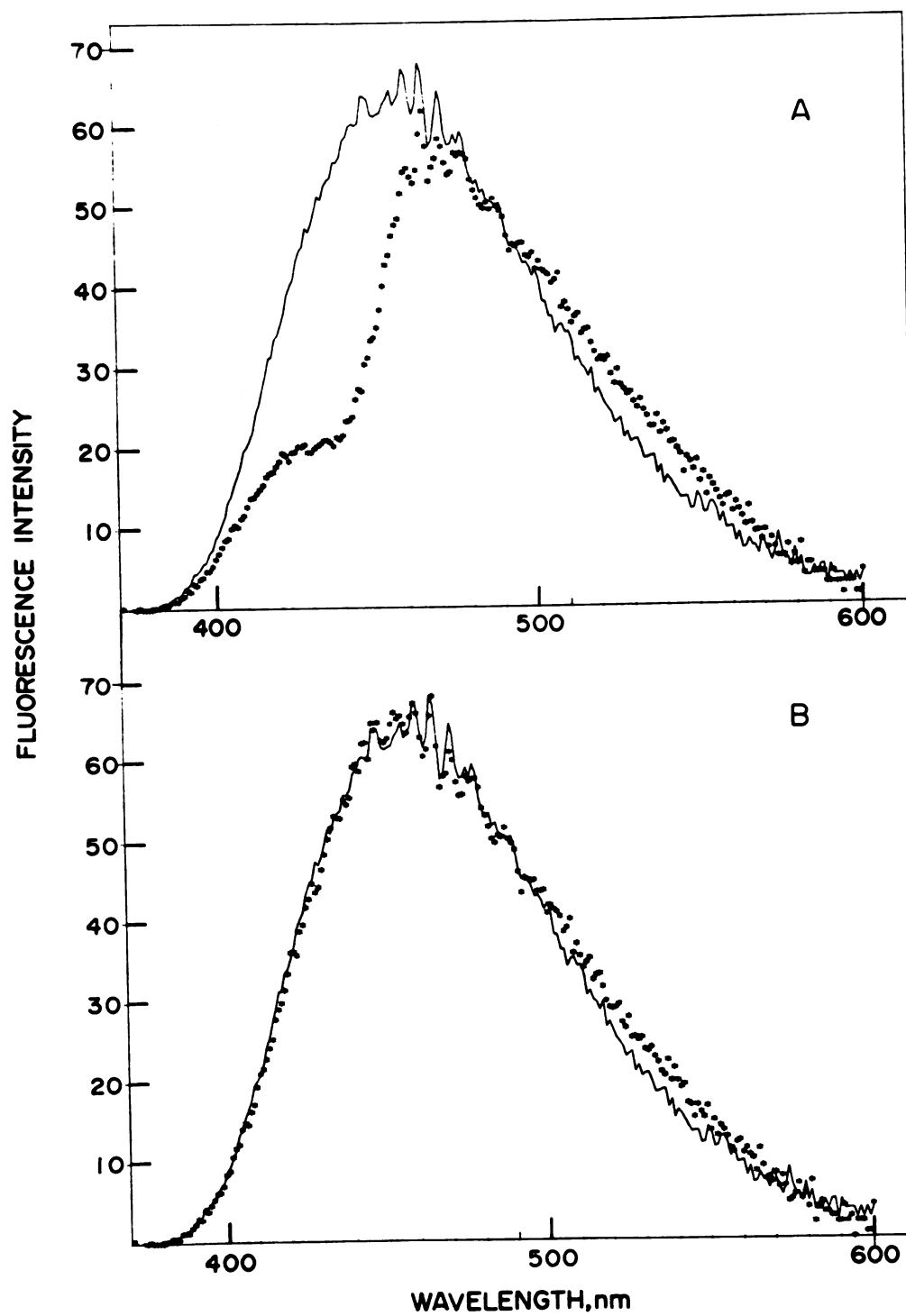


Figure 3

detailed by the decreased intensity in the mixture spectrum at wavelengths smaller than 490 nm. At wavelengths greater than 490 nm, the increase in intensity is due to fluorescein emission. Figure 3B shows the mixture spectrum after the corrected emission of the fluorescein solution was subtracted and the secondary absorption correction applied. The spectrum of the quinine sulfate solution is repeated in Figure 3B for comparison. The accuracy with which the quinine sulfate emission is restored at wavelengths less than 490 nm clearly illustrates the validity of the secondary absorption correction.

4. A Limitation of the Absorption Correction Procedure

At wavelengths larger than 490 nm in Figure 3B, a residual component of fluorescein emission can be distinguished which is due to the excitation of fluorescein by the quinine sulfate emission. This is a violation of assumption 3 and illustrates the failure of the absorption correction procedure when the absorbed fluorescence is re-emitted by the sample. Reemission appears to be a potentially serious limitation of the absorption correction procedure because many fluorophores have highly overlapping absorption and emission spectra, and therefore, absorb and reemit their own fluorescence. The effect of reemission is shown more clearly in Figure 4 which shows the absorption-corrected fluorescence analytical curve of fluorescein in 0.1 N NaOH measured at 510 nm and excited at 313 nm. The straight line in Figure 4 is the corrected fluorescence response extrapolated from concentrations below 6×10^{-6} M for which the sample absorbance at the excitation and emission wavelengths was less than 0.05. Clearly

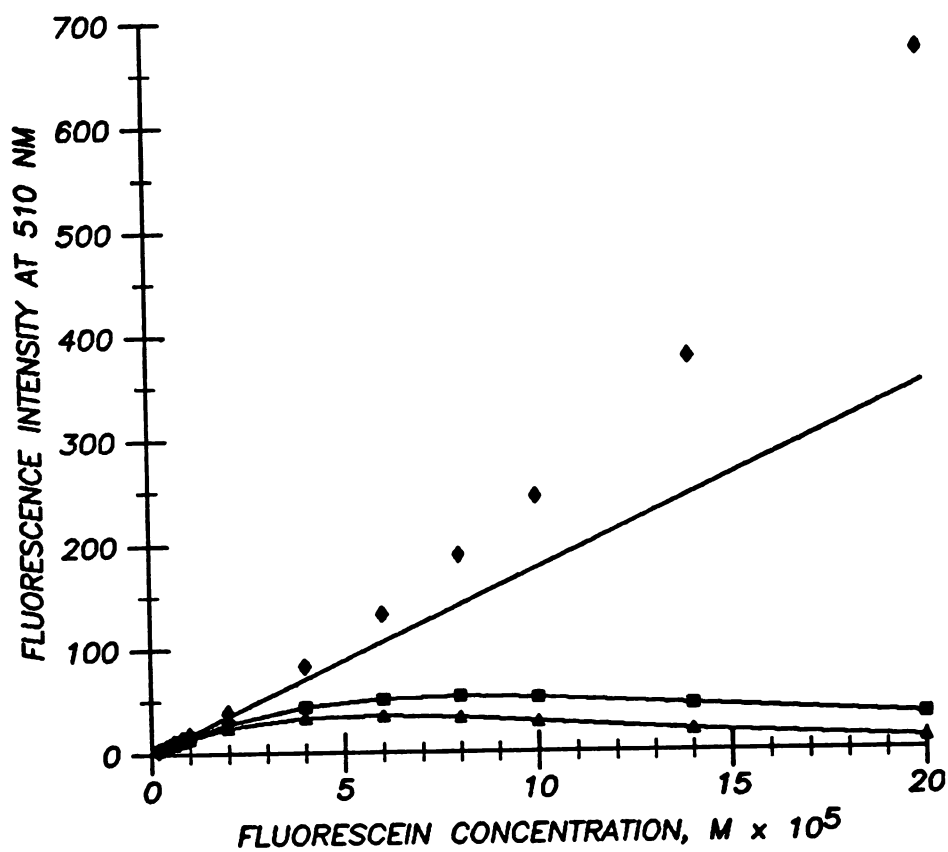


Figure 4. Fluorescence Analytical Curve of Fluorescein.
 (\blacktriangle) Measured fluorescence intensity.
 (\blacksquare) Primary absorption-corrected intensity.
 (\blacklozenge) Primary and secondary absorption-corrected intensity.
 (—) Theoretical response.

the presence of a reemission component in the measured fluorescence signal causes an overcorrection for the effects of primary and secondary absorption. The error increases in magnitude as the fluorophore concentration is increased. An identical effect is observed when fluorescein emission is measured at 550 nm where only primary absorption interference is encountered. At both emission wavelengths, however, the error is insignificant at concentrations of 10^{-5} M and below.

Reemission errors have not been studied previously for right-angle detection geometry, and no method to correct for them is offered in this work. Because of the complexity of the reemission error corrections that have been developed for front-surface fluorimetry (41), it is doubtful that reemission corrections for right-angle fluorimetry could be accomplished in a manner simple enough to be of practical value. Instead, the effects of reemission have been identified to characterize the practical limitations of the absorption correction procedure. A further discussion of reemission errors is given in Chapter VI.

5. A Comparison of Correction Factors

Both primary and secondary absorption errors have been described in previous reports as simple exponential attenuations over an average pathlength through the sample (11,66). This description implies that the fluorescing volume of solution viewed by the detector can be treated as a point source emitter located at the center of the volume element. The secondary absorption correction factor under

this assumption is $(T_{\lambda})^{-(\theta_{\alpha}+\theta_{\beta})/2}$. Figure 2, Curve D shows the result of applying this correction to the data of Curve B. Clearly, at absorbances less than 1 this correction compares well with Equation (3.13), but at higher absorbances a positive error is introduced which becomes significant (>10%) above an absorbance of 1.5. Similarly, Curve C in Figure 5 shows the result of using the factor $(T_{\lambda})^{-(\omega_{\alpha}+\omega_{\beta})/2}$ to correct the analytical curve of quinine sulfate for primary absorption interference. Again, the simple exponential correction compares well with Equation (3.13) (Curve B) at low absorbance but gives a positive error above an absorbance of about 0.5. The reason for this behavior is easily seen from the series expansion of either correction factor. For example, at low absorbance,

$$\frac{(\theta_{\beta}-\theta_{\alpha})\ln T_{\lambda}}{(T_{\lambda})^{\theta_{\beta}} - (T_{\lambda})^{\theta_{\alpha}}} \approx \frac{(\theta_{\beta}-\theta_{\alpha})\ln T_{\lambda}}{(1+\theta_{\beta}\ln T_{\lambda} + \frac{1}{2}\theta_{\beta}^2\ln^2 T_{\lambda}) - (1+\theta_{\alpha}\ln T_{\lambda} + \frac{1}{2}\theta_{\alpha}^2\ln^2 T_{\lambda})} \quad (3.14)$$

$$\approx \frac{(\theta_{\beta}-\theta_{\alpha})\ln T_{\lambda}}{(\theta_{\beta}-\theta_{\alpha})\ln T_{\lambda} + \frac{1}{2}(\theta_{\beta}^2-\theta_{\alpha}^2)\ln^2 T_{\lambda}} \quad (3.15)$$

$$\approx \frac{1}{1 + \frac{1}{2}(\theta_{\alpha}+\theta_{\beta})\ln T_{\lambda}} \quad (3.16)$$

$$\approx (T_{\lambda})^{-(\theta_{\alpha}+\theta_{\beta})/2} \quad (3.17)$$

Figure 5. Fluorescence analytical curve of quinine sulfate

A. Blank and source corrected fluorescence, $\omega_{\beta} = 0.451$,
 $\omega_{\alpha} = 0.246$. B. Primary absorption corrected fluorescence
 using the factor

$$\frac{(\omega_{\beta} - \omega_{\alpha}) \ln T_{\lambda}}{(T_{\lambda})^{\omega_{\beta}} - (T_{\lambda})^{\omega_{\alpha}}}$$

C. Primary absorption corrected fluorescence using the
 factor $(T_{\lambda})^{-(\omega_{\alpha} + \omega_{\beta})/2}$.

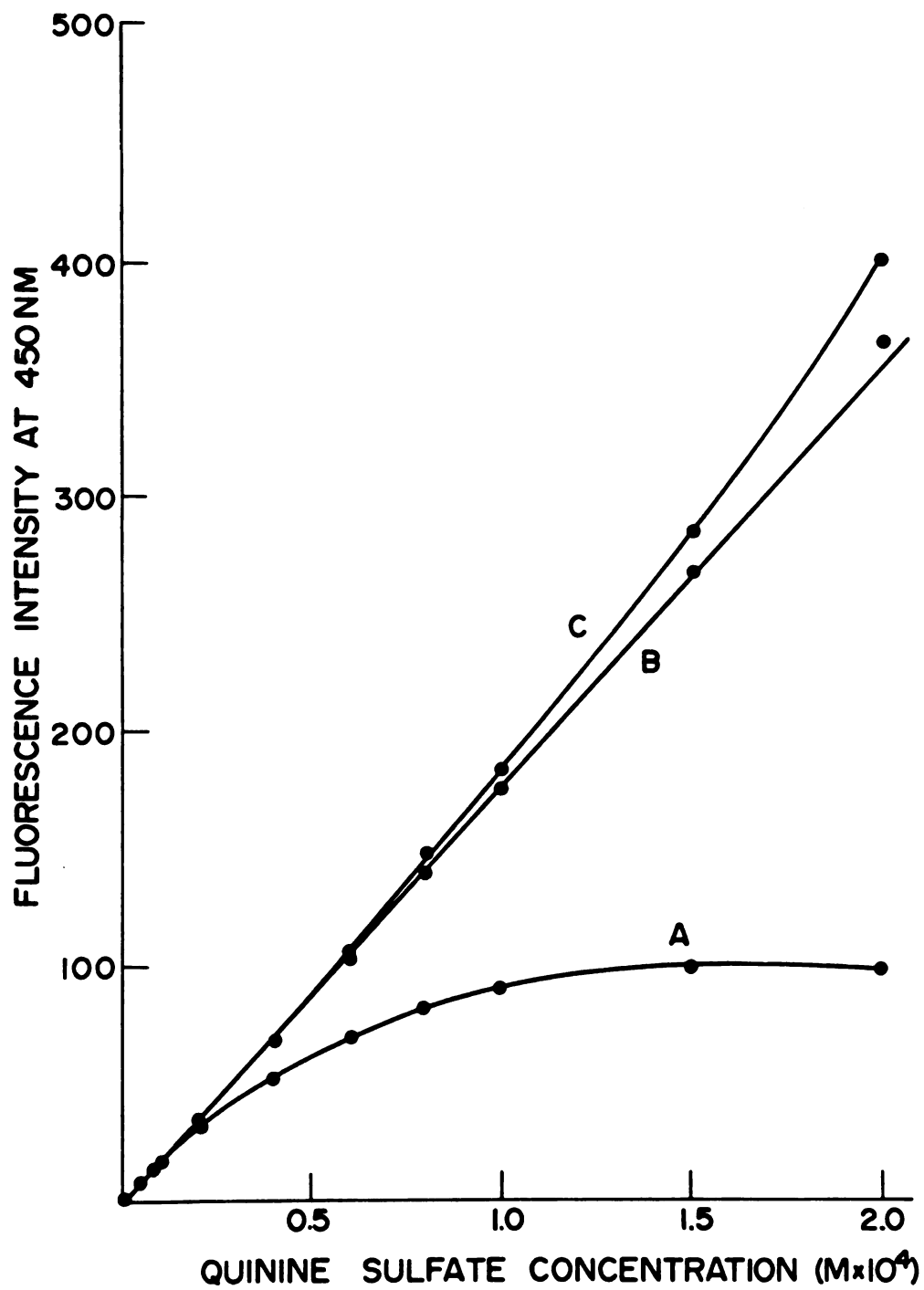


Figure 5

Thus, the simple exponential corrections for primary and secondary absorption are low absorbance limiting forms of the expressions which have been derived here and are in error when cubic and higher order terms of the series expansion become significant. One would expect the magnitude of this error to increase with the width of the window. This has been observed experimentally.

CHAPTER IV

THE EFFECT OF REFLECTIONS ON RIGHT-ANGLE MOLECULAR FLUORESCENCE MEASUREMENTS

A. Introduction

Although the treatment presented in the previous chapter assumes that reflections within the sample cell have a negligible effect on right-angle fluorescence measurements, some simple considerations suggest that this is usually not true. For a typical glass sample cell, four percent of the exciting radiation transmitted by the sample solution will be reflected back into the sample by the air-glass interface of the cell wall. The reflected light will excite the sample and contribute an additional component to the measured fluorescence signal. Similarly, a small fraction of the fluorescence radiation initially emitted in a direction away from the fluorescence detector will be reflected back to the detector to be measured. Logically, the magnitude of these effects will depend on the amount of radiation transmitted to the reflecting surfaces and, therefore, on the sample absorbance. Because these reflection effects could influence the accuracy of the absorption correction procedure, a mathematical model of the reflection phenomena would be valuable so that corrections could be applied.

In this chapter, expressions are developed to describe the

effects of the natural reflection properties of the sample cell in a dispersive right-angle fluorimeter on the measured fluorescence signal. The primary and secondary absorption correction factors described previously are modified to account for reflection effects, and an improvement in the accuracy of the absorption correction procedure resulting from this development is demonstrated. Although equations equivalent to those given here have been proposed by van Slageren et al. (50), this work is presented to clarify the theoretical basis of the expressions and to offer experimental evidence for their validity. Reflections of the exciting radiation are considered first.

B. Theory

1. Reflections at the Exciting Wavelength

To understand the manner in which reflections of the exciting radiation affect the measured fluorescence signal it is easiest to represent the fluorescence photoanodic current as the sum of an infinite number of current components which are generated by successive passes of the exciting radiation through the cell. Absorption and reflection effects at the emission wavelength can initially be ignored because they are totally independent of the exciting wavelength. If all four cell walls are assumed to be identical, the fluorescence photoanodic current from an instrument of the type described in the previous chapter can be represented by

$$i_{fpa} = (1-\rho_r) \left[\left(\frac{(T_\lambda)^{\omega_\beta} - (T_\lambda)^{\omega_\alpha}}{\ln T_\lambda} \right) + \rho_r T_\lambda \left(\frac{(T_\lambda)^{1-\omega_\alpha} - (T_\lambda)^{1-\omega_\beta}}{\ln T_\lambda} \right) + \right. \\ \left. T_\lambda^2 \rho_r^2 \left(\frac{(T_\lambda)^{\omega_\beta} - (T_\lambda)^{\omega_\alpha}}{\ln T_\lambda} \right) + T_\lambda^3 \rho_r^3 \left(\frac{(T_\lambda)^{1-\omega_\alpha} - (T_\lambda)^{1-\omega_\beta}}{\ln T_\lambda} \right) + \dots \right] J_0 \quad (4.1)$$

where all symbols not defined previously are explained in Table 2. The first term in Equation (4.1) represents the signal component generated on the initial pass of the excitation beam through the cell, as described in Chapter III. The second term represents the signal component generated by the first reflection of the excitation beam. Note that the window parameters for this term are different because the direction of excitation is reversed. The factor $\rho_r T_\lambda$ accounts for absorption of the exciting beam on its initial pass through the cell and for the efficiency of the reflection. Successive reflections generate the other terms shown by similar reasoning.

Equation (4.1) can be factored to give Equation (4.2).

$$i_{fpa} = \frac{J_0(1-\rho_r)}{\ln T_\lambda} \left[\{(T_\lambda)^{\omega_\beta} - (T_\lambda)^{\omega_\alpha}\} + \rho_r T_\lambda \{(T_\lambda)^{1-\omega_\alpha} - (T_\lambda)^{1-\omega_\beta}\} \right] \times \\ (1 + \rho_r^2 T_\lambda^2 + \rho_r^4 T_\lambda^4 + \dots) \quad (4.2)$$

Then, by applying the identity $\sum_{n=0}^{\infty} x^n = 1/(1-x)$ and further factoring,

Table 2. Definition of Symbols in Equation (4.1).

$$\rho_r = \frac{r_a + r_b - 2r_a r_b}{1 - r_a r_b}$$

= reflectance of the cell wall at the excitation wavelength,
dimensionless

r_a = reflectivity of air-cell interface at the excitation wavelength,
dimensionless

$$= \frac{(n_a - n_c)^2}{(n_a + n_c)^2}$$

n_a = refractive index of air at the excitation wavelength, dimensionless

n_c = refractive index of cell wall at the excitation wavelength,
dimensionless

r_b = reflectivity of the cell-air interface at the excitation wave-
length, dimensionless

$$= \frac{(n_c - n_a)^2}{(n_c + n_a)^2}$$

$$J_0 = 2.303 A_f K \int_0^\infty \int_0^\infty \phi_\lambda F_{ex\lambda} f_\lambda f_{\lambda'} F_{em\lambda} S_\lambda d\lambda d\lambda'$$

(See Table 1.)

Equation (4.2) can be reduced to Equation (4.3).

$$i_{fpa} = (1 - \rho_r) \left[\frac{(T_\lambda)^{\omega_\beta} - (T_\lambda)^{\omega_\alpha}}{\ln T_\lambda} \right] \left[\frac{1 + \rho_r (T_\lambda)^{2 - \omega_\beta - \omega_\alpha}}{1 - \rho_r^2 T_\lambda^2} \right] \quad (4.3)$$

The second factor in brackets in Equation (4.3) describes the effect of reflections at the excitation wavelength on the measured fluorescence signal. This expression predicts that the magnitude of the reflection effect will depend on the sample absorbance, as reasoned above, on the efficiency of the reflection, and on the excitation window parameters.

2. Reflections at the Emission Wavelength

By the same reasoning and approach used above, Equation (4.3) can be modified to account for the effects of reflections of the fluorescence radiation. This is shown in Equation (4.4).

$$i_{fpa} = \left[\frac{(T_\lambda)^{\omega_\beta} - (T_\lambda)^{\omega_\alpha}}{\ln T_\lambda} \right] \left[\frac{(1 - \rho_r)(1 + \rho_r (T_\lambda)^{2 - \omega_\beta - \omega_\alpha})}{1 - \rho_r^2 T_\lambda^2} \right] (1 - \rho_{r'})$$

$$\left[\frac{(T_{\lambda'})^{\theta_\beta} - (T_{\lambda'})^{\theta_\alpha}}{\Delta \theta \ln T_{\lambda'}} + \rho_{r'} T_{\lambda'} \left(\frac{(T_{\lambda'})^{1 - \theta_\alpha} - (T_{\lambda'})^{1 - \theta_\beta}}{\Delta \theta \ln T_{\lambda'}} \right) \right] \quad (4.4)$$

$$+ (\rho_{r'} T_{\lambda'})^2 \left(\frac{(T_{\lambda'})^{\theta_\beta} - (T_{\lambda'})^{\theta_\alpha}}{\Delta \theta \ln T_{\lambda'}} \right) + (\rho_{r'} T_{\lambda'})^3 \left(\frac{(T_{\lambda'})^{1 - \theta_\alpha} - (T_{\lambda'})^{1 - \theta_\beta}}{\Delta \theta \ln T_{\lambda'}} \right) + \dots \Big] J_0$$

The quantity ρ_r' is the reflectance of the cell wall at the emission wavelength. The odd terms of this sum arise from fluorescence radiation initially emitted toward the fluorescence detector. The even terms are generated by fluorescence radiation initially emitted away from the detector.

Obviously, the series in Equation (4.4) is of the same form as that generated by reflections of the exciting radiation. It follows that Equation (4.4) can be reduced to the form:

$$i_{fpa} = \left[\frac{(T_\lambda)^{\omega_\beta} - (T_\lambda)^{\omega_\alpha}}{\ln T_\lambda} \right] \left[\frac{(1 - \rho_r)(1 + \rho_r(T_\lambda)^{2 - \omega_\beta - \omega_\alpha})}{1 - \rho_r^2 T_\lambda^2} \right] \left[\frac{(T_{\lambda'})^{\Theta_\beta} - (T_{\lambda'})^{\Theta_\alpha}}{\Delta \Theta \ln T_{\lambda'}} \right] \left[\frac{(1 - \rho_r')(1 + \rho_r'(T_{\lambda'})^{2 - \Theta_\beta - \Theta_\alpha})}{1 - (\rho_r' T_{\lambda'})^2} \right] J_0 \quad (4.5)$$

Taking the limit of this expression as T_λ and $T_{\lambda'}$ approach 1, one obtains

$$i_{fpa} = (\omega_\beta - \omega_\alpha) J_0 \quad (4.6)$$

which is consistent with the definition of the absorption-free fluorescence signal defined in Chapter III. From Equations (4.5) and (4.6), a correction factor for absorption and reflection of exciting and fluorescence radiation can be defined as

$$f_{ar} = \left[\frac{\Delta\omega \ln T}{(T_{\lambda})^{\omega_{\beta}} - (T_{\lambda})^{\omega_{\alpha}}} \right] \left[\frac{1 - \rho_r^2 T_{\lambda}^2}{(1 - \rho_r)(1 + \rho_r (T_{\lambda})^{2 - \omega_{\beta} - \omega_{\alpha}})} \right] \left[\frac{\Delta\theta \ln T_{\lambda'}}{(T_{\lambda'})^{\theta_{\beta}} - (T_{\lambda'})^{\theta_{\alpha}}} \right] \\ \left[\frac{1 - (\rho_r' T_{\lambda'})^2}{(1 - \rho_r')(1 + \rho_r' (T_{\lambda'})^{2 - \theta_{\beta} - \theta_{\alpha}})} \right] \quad (4.7)$$

3. Determination of the Cell Reflectance

To apply Equation (4.7) it is necessary to know the values of the cell reflectance at the excitation and emission wavelengths. In most experimental situations these parameters can be determined from the transmittance of the cell filled with solvent measured with respect to air at the appropriate wavelength. If the cell walls do not themselves have an appreciable absorbance, the intensity of radiation transmitted by the solvent filled cell is given by

$$I = I_0 [T_s(1 - \rho_r)^2 + T_s^3(1 - \rho_r)^2 \rho_r^2 + T_s^5(1 - \rho_r)^2 \rho_r^4 + \dots] \quad (4.8)$$

$$= I_0 T_s (1 - \rho_r)^2 [1 + (T_s \rho_r)^2 + (T_s \rho_r)^4 + \dots] \quad (4.9)$$

and

$$I/I_0 = \frac{T_s(1 - \rho_r)^2}{1 - (T_s \rho_r)^2} \quad (4.10)$$

where I_0 is the incident radiation intensity, I is the transmitted radiation intensity, and T_s is the transmittance of the solvent. In

most cases, T_s will have a value close to unity so that Equation (4.10) reduces to

$$I/I_0 = \frac{1 - \rho_r}{1 + \rho_r} \quad (4.11)$$

and ρ_r is given approximately by

$$\rho_r = \frac{1 - (I/I_0)}{1 + (I/I_0)} \quad (4.12)$$

C. Experimental

Fluorescence measurements used to test the validity of Equations (4.5) and (4.7) were obtained with a spectrofluorimeter specially constructed to allow precise and accurate positioning of the sample cell with respect to the excitation and emission windows and to allow accurate, direct measurement of the excitation and emission window parameters. Details of the construction, calibration, and operation of this instrument are given in Chapter V. Transmittance measurements for the absorption corrections and reflectance determinations were obtained with this same instrument by positioning the reference detector to allow the excitation beam intensity transmitted by the sample cell to be measured. Appropriate bandpass filters were placed between the cell and the detector to reduce stray light interference.

D. Results and Discussion

To verify Equations (4.5) and (4.7), solutions of 2×10^{-5} M quinine sulfate plus 0 to 5×10^{-5} M fluorescein in 0.1 N H_2SO_4 were prepared. The solutions were excited at 365 nm and the fluorescence of quinine sulfate was measured at 436 nm. The transmittances of each solution and of the solvent were measured at the excitation and emission wavelengths by the procedure noted above. Correction factors were calculated from Equation (4.7) with reflectance values computed from Equation (4.12). Correction factors were also computed using reflectance values of zero to illustrate the effect of ignoring the reflection corrections. The average corrected fluorescence intensities by each of these procedures are listed in Table 3 along with the experimental standard deviations computed from three measurements. The data show that reflections do have a significant effect on the measured fluorescence intensity and on the accuracy of the absorption correction procedure. For the case in which reflection effects were ignored in the correction calculations, the corrected fluorescence intensity decreased to about 96 percent of its low absorbance value when the secondary absorbance of the sample was 0.35 or greater. When the reflection corrections were included, however, the corrected fluorescence intensity remained constant to better than one percent up to an absorbance of 2.12, as it theoretically should.

At low sample absorbances, Equation (4.5) predicts that multiple reflections within the sample cell will exactly compensate for the excitation radiation lost due to reflection as it enters the cell. It is also predicted that multiple reflections will compensate for

Table 3. Test of Reflection Corrections.

A_{365}	A_{436}	Corrected Fluorescence	
		$\rho_r = \rho_r' = 0$	$\rho_r = 0.0407, \rho_r' = 0.0411$
0.126	0.000	2856 ± 48	2869 ± 48
0.145	0.353	2765 ± 11	2867 ± 11
0.163	0.701	2750 ± 25	2877 ± 27
0.183	1.060	2732 ± 22	2866 ± 23
0.202	1.408	2739 ± 10	2877 ± 11
0.222	1.767	2708 ± 43	2847 ± 45
0.241	2.122	2740 ± 29	2882 ± 31

the fluorescence radiation lost due to reflection as the emission beam leaves the cell. At higher absorbances, however, the signal components generated by multiple reflections are attenuated by the absorption processes causing the measured fluorescence signal to be too small. The error should be of the same magnitude as the cell reflectance, i.e., if $\rho_r' = 0.04$, the error should be four percent. The data in Table 3 confirm this prediction.

It is clear from these results that by including corrections for multiple reflections at the excitation and emission wavelengths the accuracy of the absorption correction procedure is significantly improved. The results presented here are more accurate than those given in Chapter III because reflection effects have been explicitly corrected, while in Chapter III they were removed by a curve fitting procedure. Although the errors caused by reflection phenomena are negligible at low sample absorbances, they could be as high as eight percent for a typical sample cell if the sample absorbances at the excitation and emission wavelengths are both 0.35 or greater. Because of this, reflection effects should be taken into account in absorption-corrected right-angle fluorimetry.

CHAPTER V

AN AUTOMATED INSTRUMENT FOR ABSORPTION-CORRECTED FLUORESCENCE MEASUREMENTS BY THE CELL SHIFT METHOD

A. Introduction

In Chapters III and IV it was shown that the nonlinearity of the signal-concentration relationship in right-angle fluorimetry, due to reflections and absorption of exciting and fluorescence radiation by the sample, can be corrected with a simple mathematical treatment. The measured fluorescence intensity of the sample is multiplied by a correction factor to produce a corrected intensity that is a linear function of the fluorophore concentration even when the sample absorbance is as high as 2.0. The correction factor depends primarily on geometric instrumental parameters, the sample transmittances at the excitation and emission wavelengths, and reflectance parameters of the cell.

Transmittance values needed to compute the correction factor can be obtained with a standard laboratory spectrophotometer. However, this procedure suffers from the following problems: many fluorescent samples undergo spectral changes during the delay between the fluorescence and transmittance measurements; analysis time is increased due to the need for additional measurements; and care must be taken that the spectral bandwidths of excitation and emission are

closely duplicated by the spectrophotometer (69). Ideally, to avoid these problems, the sample transmittance should be measured simultaneously with its fluorescence and with the same instrument so that the same optical system is used.

Simultaneous measurement of sample fluorescence and transmittance at the excitation wavelength has been accomplished in a right-angle fluorimeter by using an oscillating mirror assembly to move the beam of exciting radiation continuously between sample and reference cells and to direct the transmitted radiation to an optical detector (71). The sample transmittance at the emission wavelength must still be determined separately, however. Further development of this design to allow the transmittance at the emission wavelength to be determined has not been attempted because of the complexity of the optical system that would be required.

A unique approach has been recently proposed to overcome this problem. It has been shown (72) that in a right-angle fluorimeter the sample absorbance at the excitation wavelength can be derived from fluorescence intensities measured at two locations along the path of the excitation beam as it passes through the sample cell. The cell is manually moved in a direction parallel to the excitation beam, and fluorescence intensities are obtained at two cell positions. Similarly, the sample absorbance at the emission wavelength can be determined by shifting the cell in a direction perpendicular to the excitation beam to cause a change in the pathlength of the fluorescence radiation through the absorbing solution. The technique is known as the method of "cell shift" (69).

The cell shift approach appears to be an effective and easily implemented method for the correction of absorption errors in right-angle fluorimetry. However, if the sample cell is positioned manually, the procedure can be tedious, time consuming, and subject to significant errors. To reduce these problems and to facilitate further evaluation of the cell shift technique, an absorption-corrected spectrofluorimeter was developed in which a dedicated microcomputer is used to position the sample cell automatically for the cell shift measurements. The microcomputer also integrates the fluorescence and source (reference) signals, scans the excitation and emission monochromators, and transmits the acquired data to a minicomputer for data reduction and permanent storage. In this chapter the basic design and operation of this instrument are described. The theories developed in Chapters III and IV are used to explain the principle of the instrument operation. It is shown that corrections for multiple light reflections are necessary to determine the sample transmittance accurately by the cell shift technique. And finally, the utility of the instrument is demonstrated in an application to the fluorimetric determination of aluminum in the presence of iron.

B. Theory

Figure 6 illustrates the concept of the cell shift method. Baffles are located in the fluorimeter so that only a small, fixed volume of space is excited by the radiation source and viewed by the fluorescence detector. The sample cell is moved to bring the

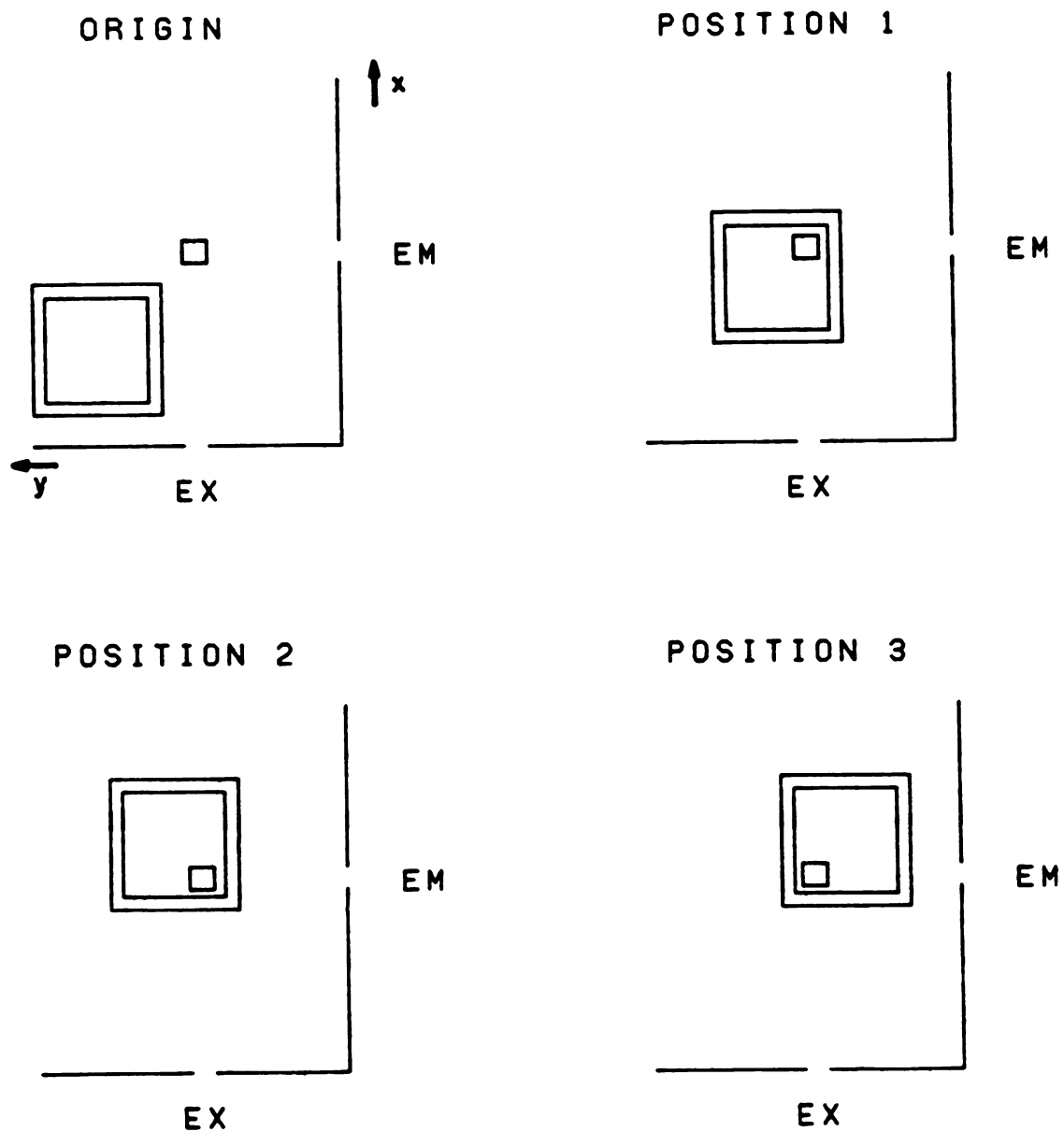


Figure 6. Cell positions for the cell shift method. EX = excitation window, EM = emission window.

sample solution into this region (position 1) and to vary the thickness of solution through which the exciting radiation must pass (position 2). Similarly, the cell is moved to vary the sample thickness through which the fluorescence radiation must pass to reach the detector (position 3).

In accord with the work described in Chapter IV, the fluorescence intensities measured at cell positions 1, 2, and 3 can be described by the expression:

$$F_n = F_0 \left[\frac{(T_\lambda)^{\omega_{\beta n}} - (T_\lambda)^{\omega_{\alpha n}}}{(\omega_{\beta n} - \omega_{\alpha n}) \ln T_\lambda} \right] \left[\frac{(T_{\lambda'})^{\Theta_{\beta n}} - (T_{\lambda'})^{\Theta_{\alpha n}}}{(\Theta_{\beta n} - \Theta_{\alpha n}) \ln T_{\lambda'}} \right] \left[\frac{(1 - \rho_r)(1 + \rho_r(T_\lambda)^{2 - \omega_{\beta n} - \omega_{\alpha n}})}{1 - \rho_r^2 T_\lambda^2} \right] \left[\frac{(1 - \rho_r')(1 + \rho_r'(T_{\lambda'})^{2 - \Theta_{\beta n} - \Theta_{\alpha n}})}{1 - (\rho_r' T_{\lambda'})^2} \right] \quad (5.1)$$

where n designates the cell position ($n = 1, 2$, or 3), F_0 is the absorption-free fluorescence intensity of the sample, and $\omega_{\beta n}$, $\omega_{\alpha n}$, $\Theta_{\beta n}$, and $\Theta_{\alpha n}$ are the instrumental window parameters for the cell position of concern. As for Equation (3.10), Equation (5.1) is valid if the excitation and fluorescence beams are collimated and of narrow spectral bandwidth compared to the sample absorption bands. Stray light, scattering phenomena, and reemission of absorbed fluorescence must also be negligible.

When the fluorescence cell is shifted from position 1 to position 2, the excitation window parameters are not changed, i.e., $\Theta_{\beta 1} = \Theta_{\beta 2}$

and $\Theta_{\alpha 1} = \Theta_{\alpha 2}$. However, the emission window parameters are each decreased by an amount $\delta\omega$ so that $\omega_{\alpha 2} = \omega_{\alpha 1} - \delta\omega$ and $\omega_{\beta 2} = \omega_{\beta 1} - \delta\omega$. Similarly, when the cell is shifted from position 2 to position 3 the emission window parameters are not affected, $\omega_{\beta 3} = \omega_{\beta 2}$ and $\omega_{\alpha 3} = \omega_{\alpha 2}$, but the excitation window parameters are increased by an amount $\delta\Theta$ so that $\Theta_{\beta 3} = \Theta_{\beta 2} + \delta\Theta$ and $\Theta_{\alpha 3} = \Theta_{\alpha 2} + \delta\Theta$. From these relationships and Equation (5.1), it can be shown that T_λ is related to the measured fluorescence intensities F_1 and F_2 by the nonexplicit relationship:

$$T_\lambda = \left[(F_1/F_2) \frac{1 + \rho_r(T_\lambda)^{2-\omega_{\beta 2}-\omega_{\alpha 2}}}{1 + \rho_r(T_\lambda)^{2-\omega_{\beta 1}-\omega_{\alpha 1}}} \right]^{1/\delta\omega} \quad (5.2)$$

If reflection effects are small, however, T_λ is given approximately by

$$T_\lambda \approx (F_1/F_2)^{1/\delta\omega} \quad (5.3)$$

By substituting this relationship into Equation (5.2) to give Equation (5.4), a more accurate estimate of T_λ is obtained.

$$T_\lambda = \left[(F_1/F_2) \frac{1 + \rho_r(F_1/F_2)^{(2-\omega_{\beta 2}-\omega_{\alpha 2})/\delta\omega}}{1 + \rho_r(F_1/F_2)^{(2-\omega_{\beta 1}-\omega_{\alpha 1})/\delta\omega}} \right]^{1/\delta\omega} \quad (5.4)$$

By a similar argument, it can be shown that T_λ' is given by

$$T_{\lambda'} = \left[(F_3/F_2) \frac{1+\rho_{r'}(F_3/F_2)^{(2-\Theta_{\beta 2}-\Theta_{\alpha 2})/\delta\Theta}}{1+\rho_{r'}(F_3/F_2)^{(2-\Theta_{\beta 3}-\Theta_{\alpha 3})/\delta\Theta}} \right]^{1/\delta\Theta} \quad (5.5)$$

The instrument described below automatically measures F_1 , F_2 , and F_3 by shifting the fluorescence sample cell as shown in Figure 6. From known values of ρ_r and $\rho_{r'}$ and the window parameters for each cell position, T_λ and $T_{\lambda'}$ are calculated from Equations (5.4) and (5.5), and Equation (5.1) is solved for the value of F_0 .

C. Instrument Design

1. General Description

The major components of the absorption-corrected spectrofluorimeter and their physical arrangement are shown in Figure 7. Because of the spectral bandwidth and stray light limitations on Equation (5.1), monochromators are used for both excitation and emission wavelength isolation. GCA McPherson model EU-700 monochromators are used at their maximum slit widths (2 mm) and maximum spectral bandwidths (4 nm). A 150 W xenon or a 200 W xenon-mercury arc lamp is used as the excitation source. In the cell compartment, radiation from the excitation monochromator is mechanically chopped at 500 Hz and collimated by a single convex quartz lens (1.5 inch dia., $f/3$). A quartz beam splitter directs a fraction of the collimated beam to a source reference detector, a rhodamine B quantum counter and RCA 1P28 photomultiplier tube. The remainder of the excitation beam is directed to the cell (type A-23 UV quartz, Markson Science, Del Mar, CA)

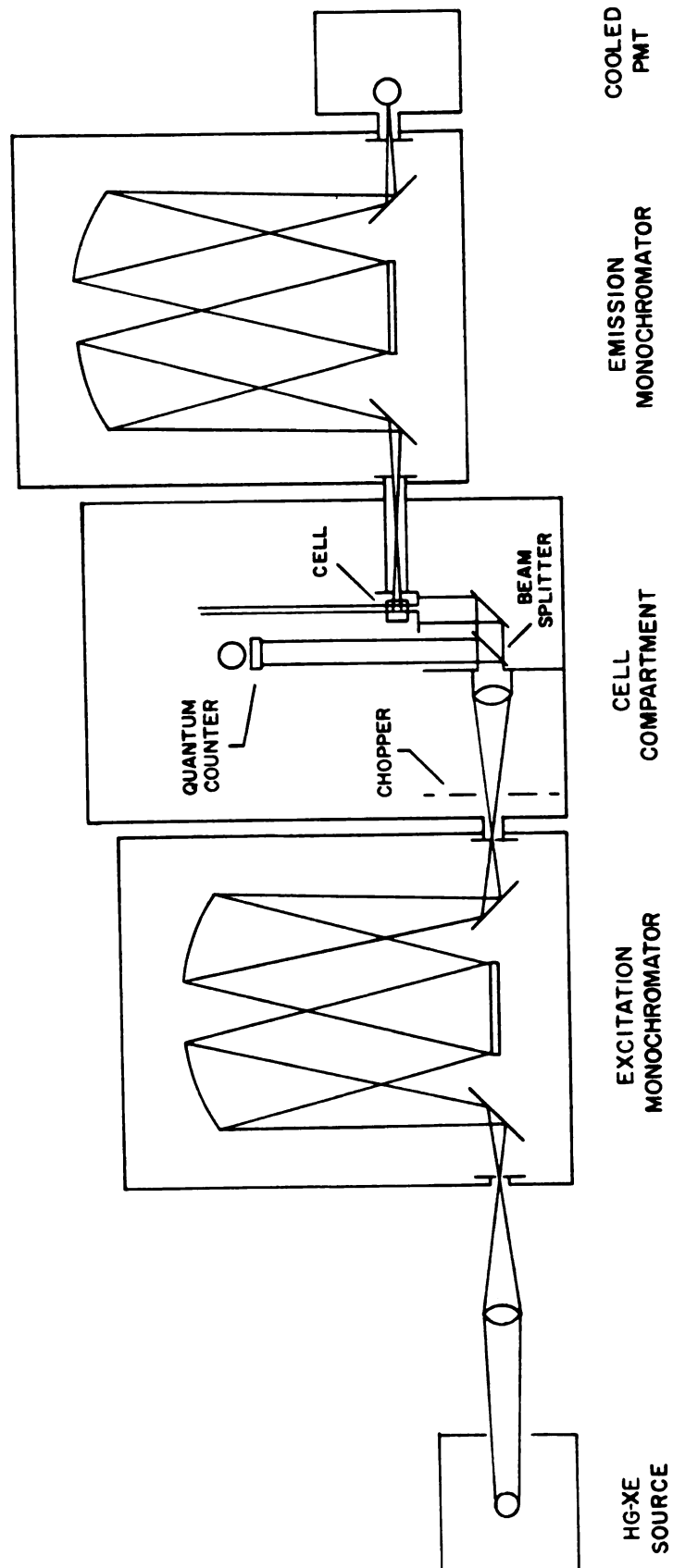


Figure 7. Instrument components and their arrangement.

and a slit arrangement like that shown in Figure 6. The excitation and emission slits are each 5.0 mm tall and 2.4 and 2.0 mm wide, respectively. The rather small dimensions chosen for the slits are necessary to maintain a high degree of beam collimation, even though this severely limits the sensitivity of the instrument. The emission slit and the entrance slit of the emission monochromator define the emission beam. These two slits are separated by a distance of 11.0 cm. With this arrangement, a lens is not needed to collimate the emission beam. The fluorescence detector is a Hamamatsu R666 photomultiplier that is bathed in cold N_2 (74) to reduce the dark current shot noise.

Movement of the fluorescence cell to the positions shown in Figure 6 is controlled by a microcomputer with the aid of an x-y positioner constructed in our laboratories. For all work described in this chapter, the displacement between cell positions 1 and 2 and positions 2 and 3 was 0.650 cm. The window parameters for each cell position were those given later in Table 4.

2. The Microcomputer

The computer interface of the instrument is shown schematically in Figure 8. Data acquisition, cell position, and the monochromator wavelength drives are under direct program control of an Intersil IM6100 12-bit microprocessor. The IM6100 CPU, 8K of RAM, memory extender, and two serial ports were purchased in kit form from Pacific Cyber/Metrix (San Ramon, CA). One serial port is used to communicate with the serial port of a PDP 8/e minicomputer and the

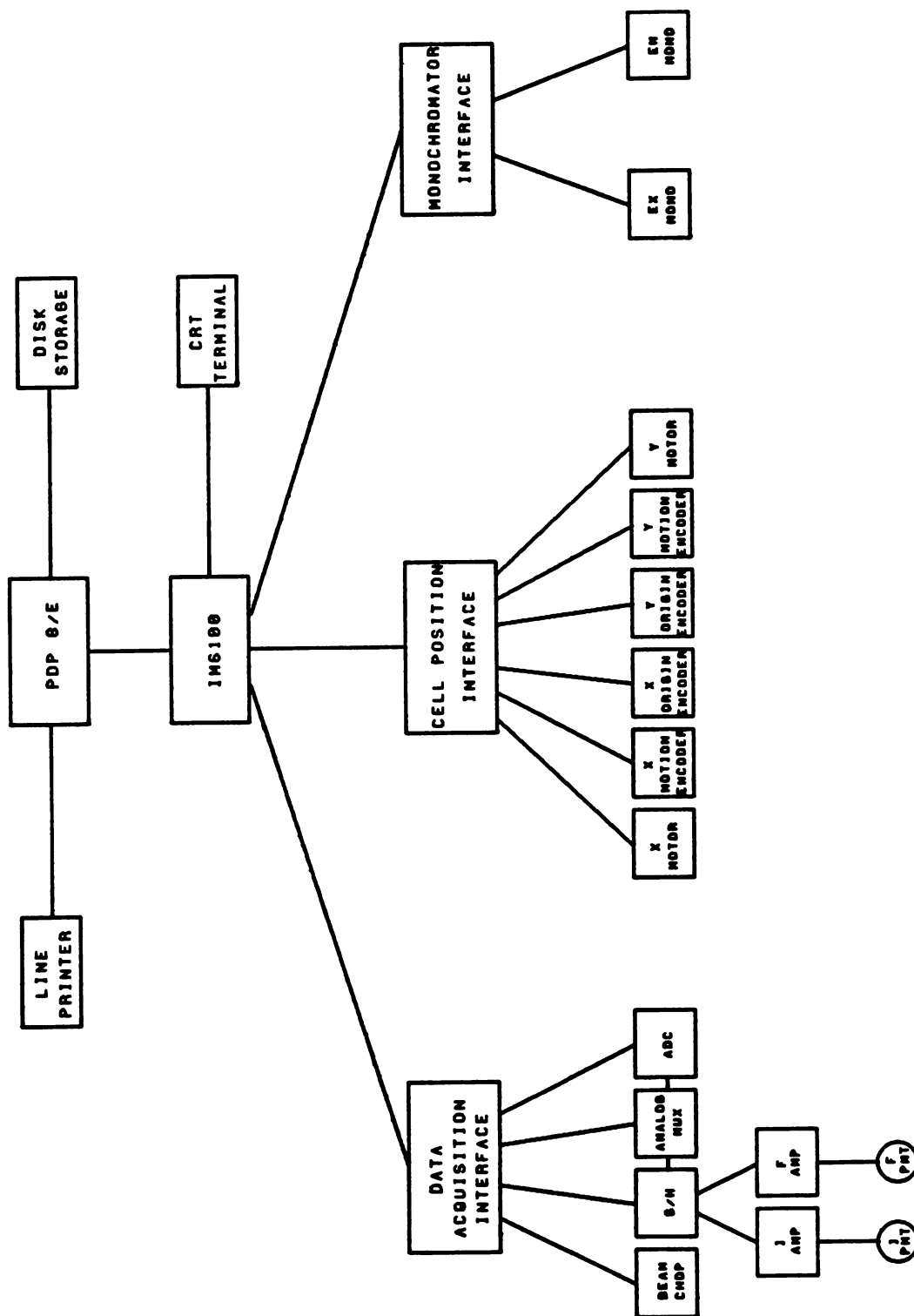


Figure 8. Block diagram of computer network.

other to communicate locally with a CRT terminal. All interfaces for the fluorimeter and a 2K PROM monitor board essential to the microcomputer operation are described in detail in Appendices A and B.

Programming of the IM6100 is accomplished through a mini-micro-computer network developed by Joseph (75). When power to the IM6100 is turned on, the PROM monitor immediately enters a transparent mode that enables the instrument operator to communicate with the OS/8 operating system of the PDP 8/e. Programs for the microcomputer are created on the 8/e in PAL8 assembly language or OS/8 Fortran II-SABR, compiled to binary format, and stored on floppy disc. The binary programs are loaded into the microcomputer memory by activating a modified OS/8 paper tape punch handler. The leader/trailer characters from the 8/e activate a binary loader section of the IM6100 PROM monitor that performs the loading function. When program loading is complete, the monitor enters a local mode which enables the memory contents to be examined and altered, and the program to be executed from the CRT terminal.

3. Data Acquisition

a. General Operation - Photocurrents from the fluorescence and reference detectors are converted to voltages, amplified, filtered, and sampled simultaneously by dual synchronously gated sample-and-hold circuits. The acquired signals are then multiplexed to a 12-bit analog-to-digital converter. By monitoring the radiation source modulation at the chopper wheel, the microcomputer controls data acquisition

so that signal plus background and background are alternately measured during each modulation cycle in each signal channel. The difference between these measurements, the net signal, is computed and integrated. In this way, the microcomputer functions as a dual-channel boxcar integrator. Typically, 4096 measurements of the net signal are averaged in each signal channel as one result.

Fixed wavelength or scanning measurements are made at cell positions 1, 2, and 3 sequentially before the cell is returned to the origin. The data are stored temporarily in the microcomputer memory until the measurement sequence is completed. The stored results are then transmitted to the minicomputer where corrections are made for variations of the source intensity, detector response, absorption effects, and fluorescence background.

b. Noise Characteristics - The noise characteristics of the fluorescence data acquisition system under typical measurement conditions are illustrated in Figure 9. The fluorescence signal-to-noise ratio (S/N) is plotted against the fluorescence photoanodic current on a log-log scale for photomultiplier temperatures of 22 and -30° C. The slope of the plot of the low temperature data is very near 0.5 which indicates that the fluorescence signal shot noise is the predominant factor limiting measurement precision. At room temperature, the S/N is significantly smaller over the lower range of signal magnitude and the slope is larger due to an increase in the photomultiplier dark current shot noise. This effect is illustrated more clearly in Figure 10 where the PMT rms dark current noise is plotted

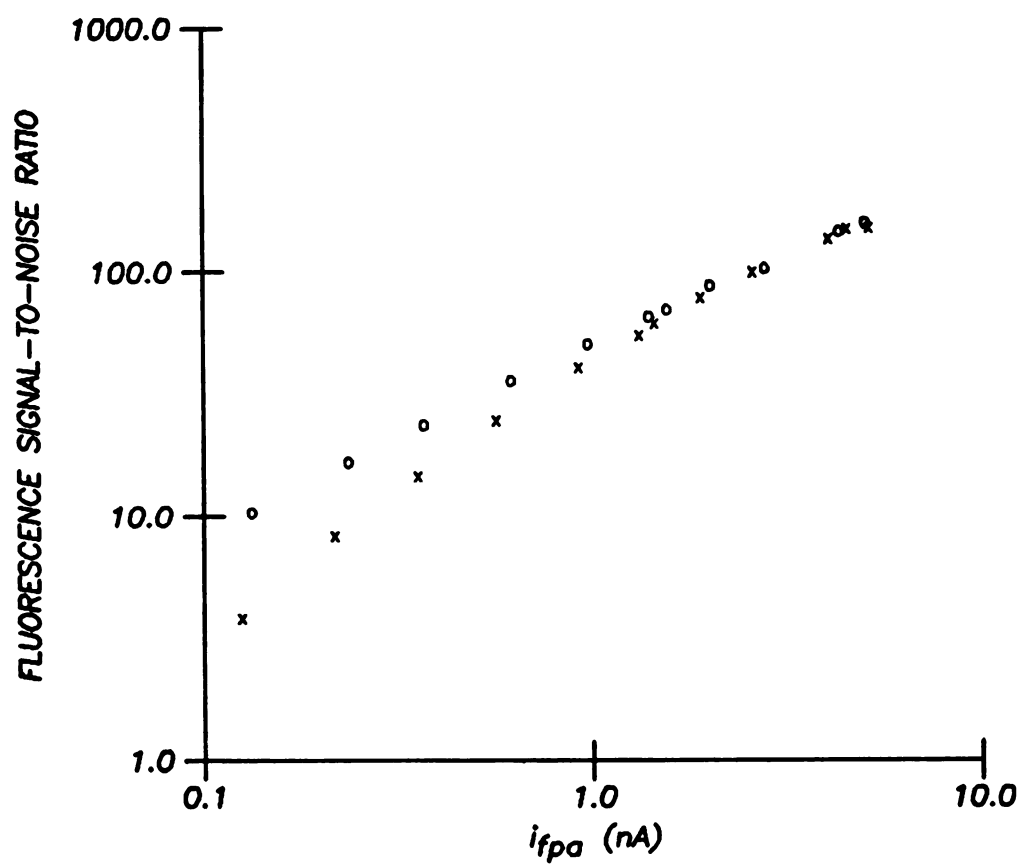


Figure 9. Fluorescence S/N vs. Fluorescence photoanodic current.
(x) + 22° C, (o) -30° C.

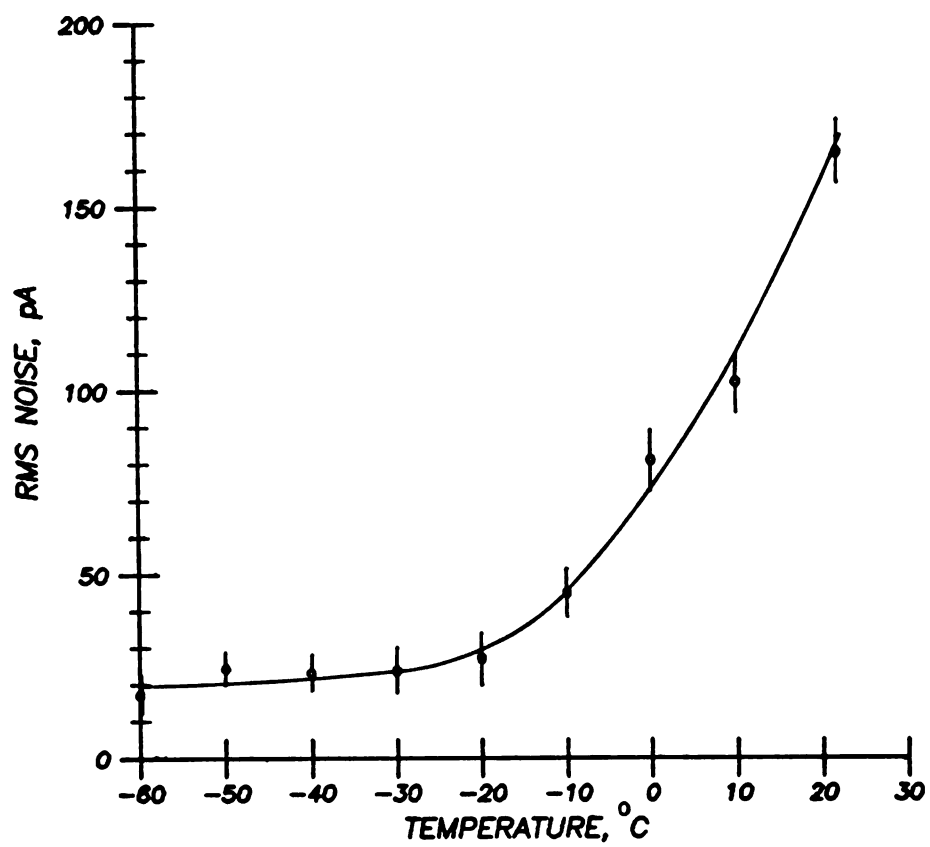


Figure 10. RMS dark current noise vs. temperature for Hamamatsu R666 PMT at 600 V.

as a function of the PMT temperature as measured with an iron-constantan thermocouple. From Figure 10 a standard operating PMT temperature of -20°C (an N_2 flow rate of 5 l/min) was selected and used throughout this work.

4. The Cell Positioner

The cell positioner, shown in Figures 11 and 12, was designed to allow flexible, multidirectional movement of the cell and to enable simple and accurate calibration of the cell movement and window parameters (see Alignment and Calibration below). The positioner consists of two dovetail slides arranged one on top of the other so that the track of the upper slide rides on the lower slide and the two tracks are perpendicular. Each slide has about a 3.5 cm range of movement. An aluminum block is mounted on the upper dovetail slide, and the fluorescence cell is mounted on top of a round post that slides vertically into this block. Four nylon screws hold the cell in a square depression in the top of the post. A single set screw holds the post in place. This arrangement facilitates vertical positioning and alignment of the cell with the optical axes of the fluorimeter.

Each slide is driven by a 12 V permanent magnet DC motor through a 0.5 mm pitch lead screw. A symmetric, five-bladed encoder wheel is coupled to each lead screw. An opto-interrupter (GE H13B1) associated with each encoder wheel allows the microcomputer to monitor the angular motion of the motor shaft and, therefore, the linear motion of the fluorescence cell. The microcomputer is programmed

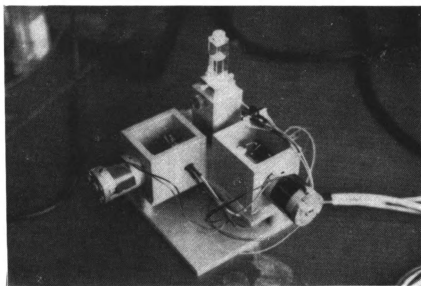


Figure 11. Photograph of the cell positioner.

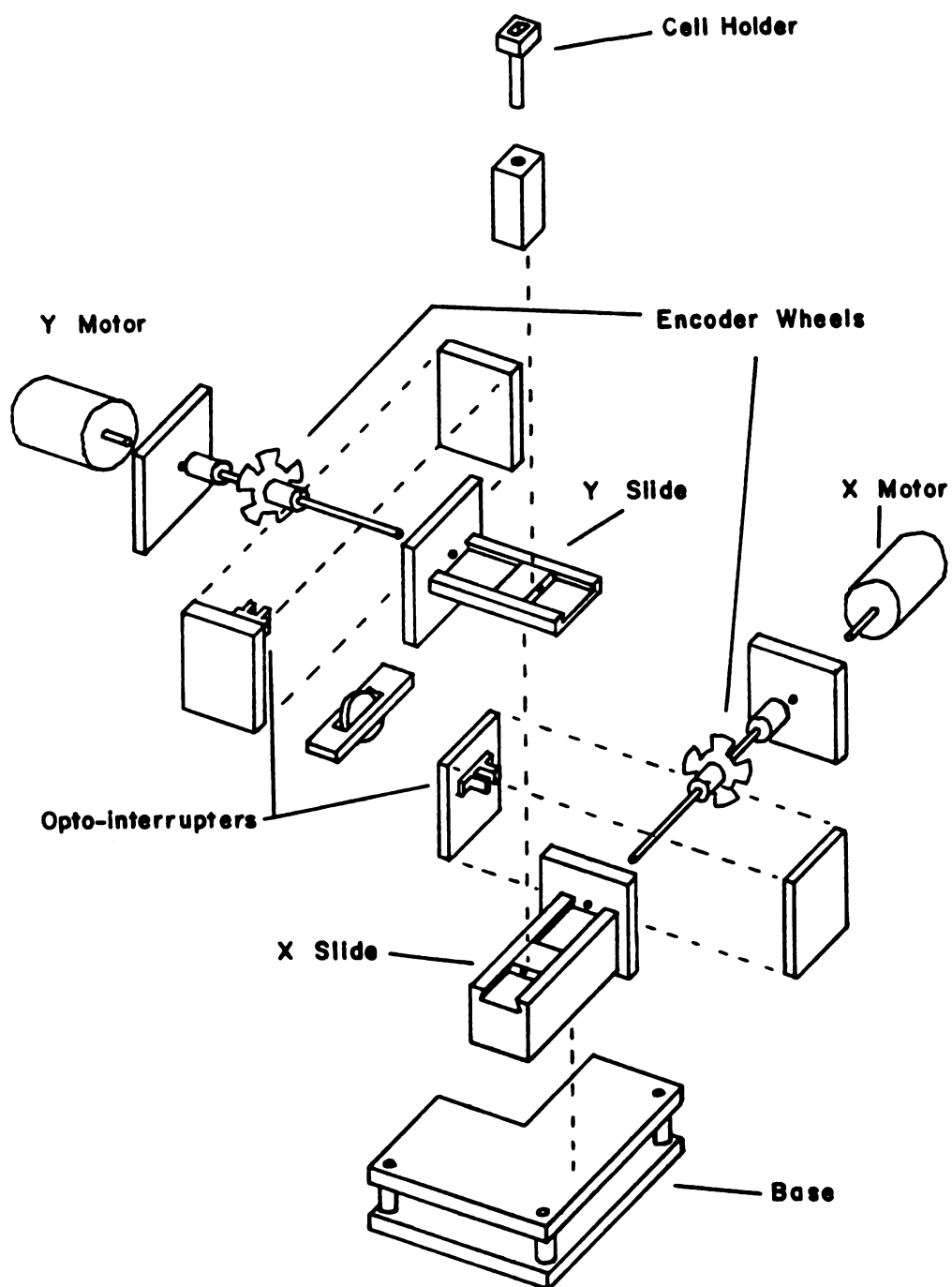


Figure 12. Components of the cell positioner.

to detect the change in logic level as the edge of an encoder wheel blade passes so that an angular resolution of 18° and a linear resolution of 0.005 cm in each dimension are achieved. Two additional opto-interrupters (not shown in Figure 12) are mounted on stationary parts of the positioner to define an x-y origin. Small blades attached to the cell holder and to the track of the upper slide, block the detector beams at the appropriate point in space to signal the microcomputer that the cell is at the origin.

Simple DC motors were used in the design of the cell positioner because of their low cost and simplicity of control. Although these motors have little holding torque and tend to coast when the power is removed, accurate and precise lead screw rotation and cell displacement are achieved by applying pulsed DC current to the motors. The pulse frequency is gradually reduced to slow the motors to a stop at the correct point. Errors due to mechanical play in the positioner are minimized by moving the cell to all positions, including the origin, from the same x and y directions.

Figure 13 illustrates the linearity and accuracy of the positioner. The cell displacement in the y-dimension from a stationary part of the positioner, as measured with a micrometer, is plotted against the angular motion of the lead screw. The regression line for these data has a slope of 0.04972 ± 0.00004 cm/revolution which agrees well with the designed value of 0.05 cm/revolution. The correlation coefficient is 0.99999. The linearity and accuracy in the x-dimension are similar. (The x movement was calibrated at 0.04964 ± 0.00004 cm/revolution.) Corrections are made for the small deviations from the designed value.

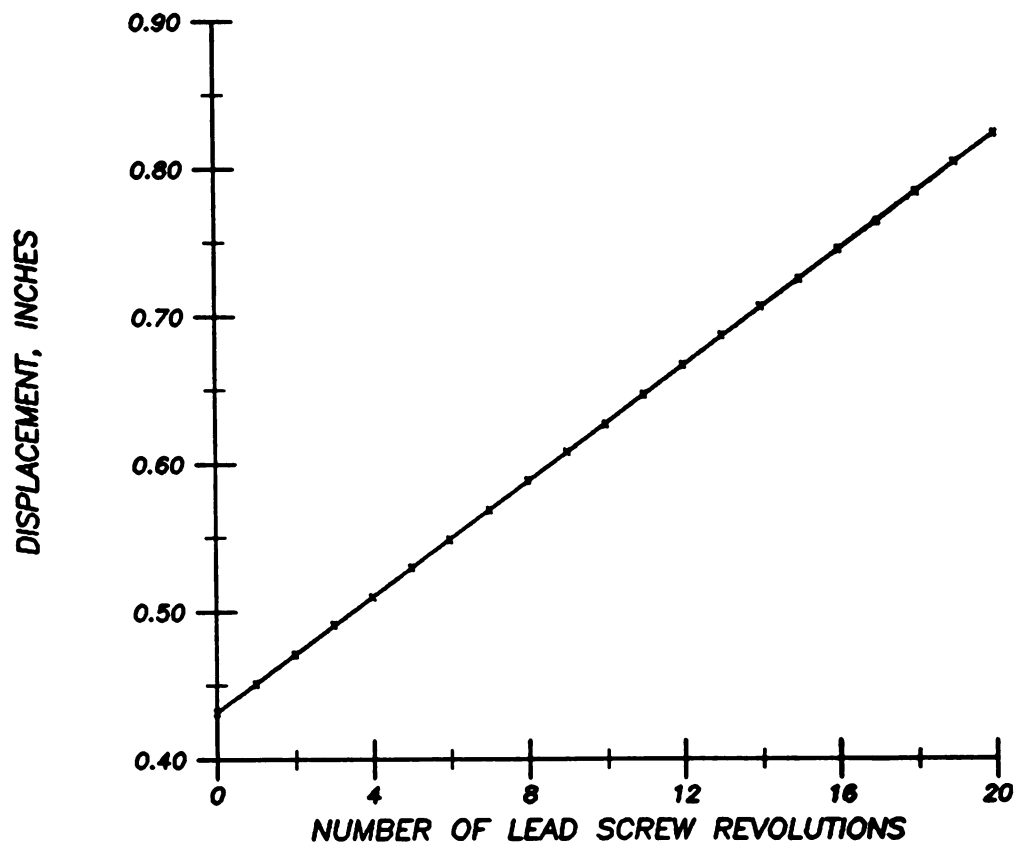


Figure 13. Cell displacement in y-dimension as a function of lead screw rotation.

The precision of the positioner is illustrated in Table 4. The average fluorescence intensities and relative standard deviations based on ten measurements in each cell position are shown for a 2×10^{-4} M solution of quinine sulfate in 0.1 N H_2SO_4 for the cases in which the cell is and is not repositioned between measurements. Due to strong absorption of the exciting radiation by this sample, the fluorescence intensity varies greatly with the x-coordinate of the cell as illustrated by the data for positions 1 and 2. The increase in the relative standard deviation of fluorescence caused by repositioning is clearly negligible. The imprecision of the cell position is estimated from these data to be less than ± 0.001 cm in each dimension which is a significant improvement compared to manual positioning.

5. Alignment and Calibration

When the cell is removed from the fluorimeter for cleaning and is then replaced, alignment and window calibration are necessary. The alignment of the cell with the optical axes of the fluorimeter is verified by placing a 2×10^{-5} M solution of quinine sulfate in 0.1 N H_2SO_4 in the cell and recording a fluorescence profile of the cell in the y-dimension as shown in Figure 14. Fluorescence is excited at 365 nm and monitored at 450 nm. As the cell is moved away from the origin, it moves into the excitation beam, and the fluorescence intensity increases until the beam is entirely in the cell. Since there is no absorption of the emission beam by this sample, the measured fluorescence intensity should be independent of

Table 4. Cell Position Reproducibility.^a

Position	<u>Cell Repositioned</u>		<u>Cell Not Repositioned</u>	
	Fl. Intensity	RSD, %	Fl. Intensity	RSD, %
1	32.4 ± 0.3	0.97	32.8 ± 0.4	1.09
2	672.1 ± 1.3	0.19	673.0 ± 1.1	0.16
3	671.5 ± 1.2	0.17	673.0 ± 0.7	0.11

$$^a \theta_{\alpha 1} = \theta_{\alpha 2} = \omega_{\alpha 2} = \omega_{\alpha 3} = 0.050, \omega_{\alpha 1} = \omega_{\alpha 3} = 0.700$$

$$\theta_{\beta 1} = \theta_{\beta 2} = 0.290, \omega_{\beta 3} = \omega_{\beta 2} = 0.265, \theta_{\beta 3} = 0.940, \omega_{\beta 1} = 0.915$$

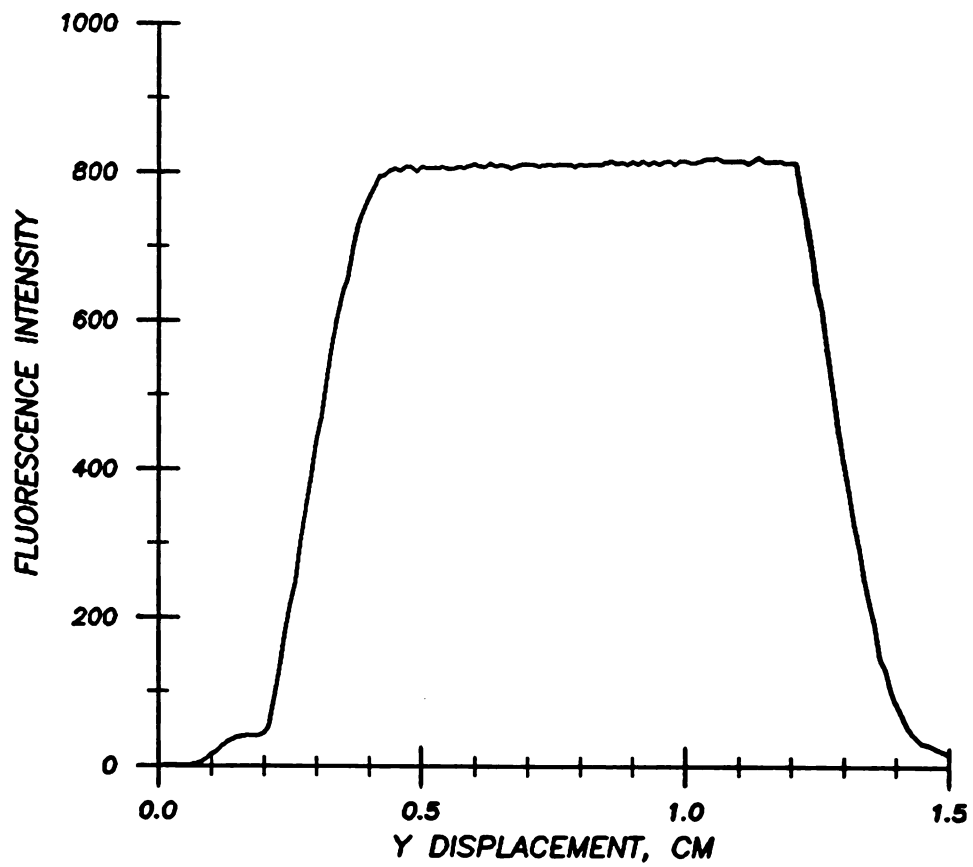


Figure 14. Fluorescence profile of the cell in the y-dimension.

further y-displacement until the beam begins to pass out of the cell. This condition is established by simply rotating the post which holds the cell on the positioner.

Rather than using the curve fitting procedures described previously (68), the information in Figure 14 can be used to calibrate the excitation window parameters for each cell position. The length of the flat portion of the profile is equal to the difference between the cell width and the width of the excitation beam. From the known cell width (1 cm) the excitation beam width was determined to be 0.240 ± 0.005 cm, in good agreement with the width of the excitation slit. The flat portion of the profile begins at the position at which the excitation beam lies just within the cell. The displacement past this point to any cell position is equal to the parameter $\Theta_{\alpha n}$ for that position. The other parameter $\Theta_{\beta n}$ is simply the sum of $\Theta_{\alpha n}$ and the beam width. In a similar manner, the emission window width was determined from a fluorescence profile of the cell in the x-dimension, like that in Figure 15, to be 0.215 ± 0.005 cm. This value is larger than the emission slit width because of a slight divergence of the emission beam. The x-profile is not flat because of the effect of absorption of the exciting radiation. The points at which the emission beam lies just within the cell are still evident, however, and the emission window parameters for each cell position can be determined in the same manner as the excitation window parameters.

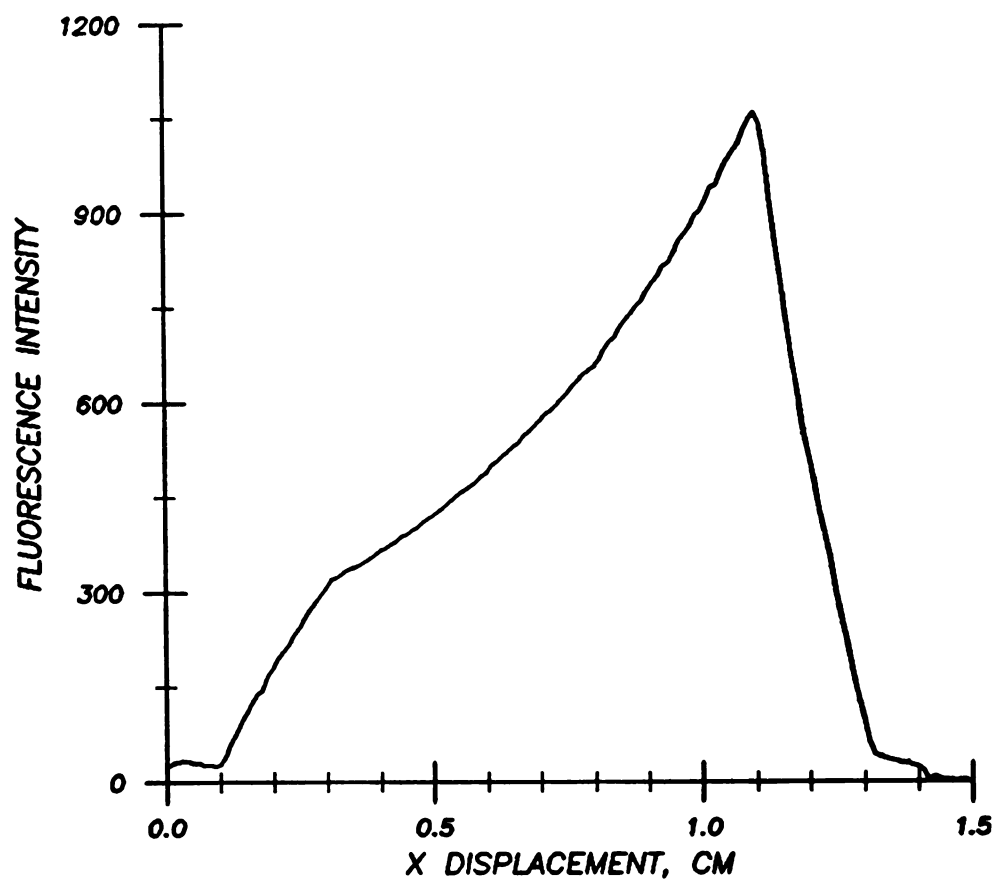


Figure 15. Fluorescence profile of the cell in the x-dimension.

D. Results and Discussion

1. Determination of the Sample Transmittance

One measure of the performance of the absorption-corrected spectrofluorimeter is the accuracy with which sample absorbance or transmittance values can be determined from the fluorescence measurements F_1 , F_2 , and F_3 . This is illustrated in Figure 16. Values of T_λ at 365 nm, computed from Equation (5.4) for a series of quinine sulfate solutions in 0.1 N H_2SO_4 , are converted to absorbances and plotted against the quinine sulfate concentration. Fluorescence was measured at 450 nm. The solid line is a regression line computed from spectrophotometric absorbance measurements made on the solutions with the same radiation source, monochromator, and 4 nm bandwidth used to excite the fluorescence. The absorbance results from the fluorescence data deviate from the regression line by less than 0.005 absorbance units over the absorbance range 0.05 to 2.70. Similar results were obtained for $T_{\lambda'}$, calculated from Equation (5.5), with other chemical systems.

Attempts to compute T_λ from Equation (5.3) and $T_{\lambda'}$ from Equation (5.6),

$$T_{\lambda'} = (F_3/F_2)^{1/\delta\theta} \quad (5.6)$$

which are low reflectance limiting forms of Equations (5.4) and (5.5), consistently resulted in erroneously low absorbance and high transmittance values. An example of this is shown in Table 5.

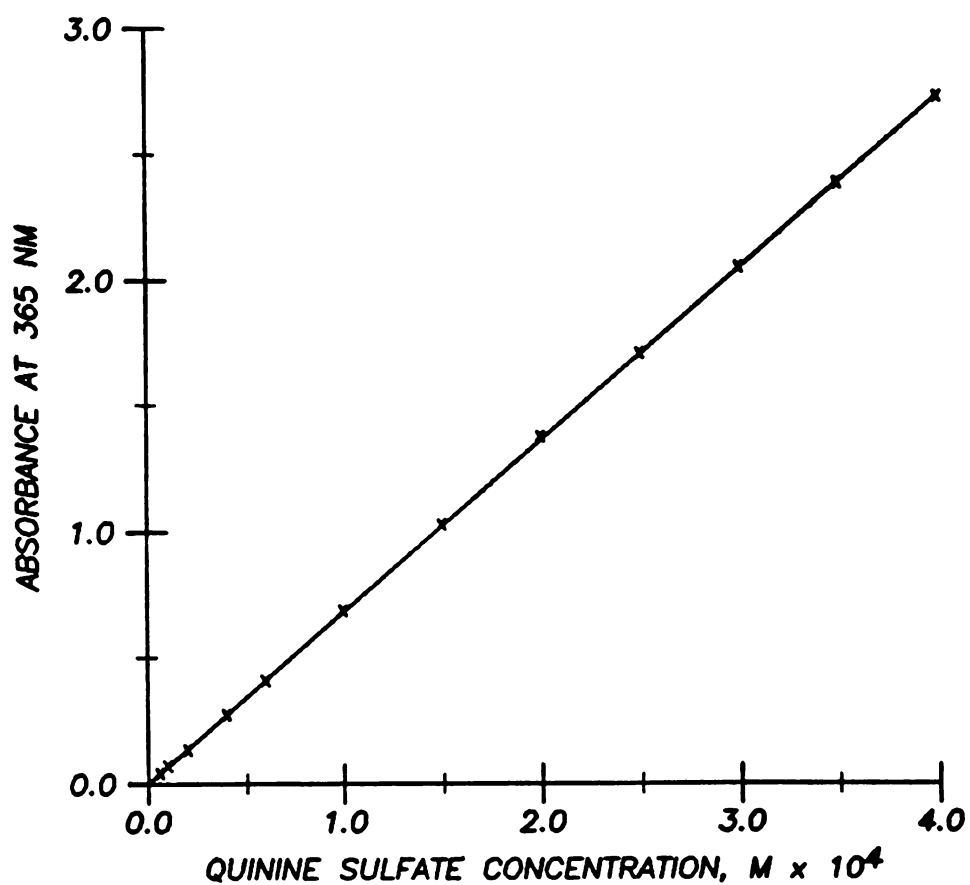


Figure 16. Absorbance at excitation wavelength vs. fluorophore concentration. (x) calculated from F_1 and F_2 , (-) regression line calculated from spectrophotometric data.

Table 5. Comparison of Sample Absorbance Estimates.^a

Equation 5.4	Equation 5.5	Spectrophotometric
0.168 ± .009	0.177 ± .009	0.1798 ± .0006
0.347 ± .004	0.356 ± .004	0.3531 ± .0005
0.521 ± .006	0.534 ± .006	0.5364 ± .0019
0.712 ± .002	0.724 ± .002	0.7205 ± .0006
0.876 ± .025	0.888 ± .025	0.8980 ± .0015
1.042 ± .020	1.052 ± .020	1.0609 ± .0020
1.246 ± .030	1.254 ± .030	1.2611 ± .0008

^aAverage of three measurements ± std. dev.

Absorbance values at 365 nm for solutions of quinine sulfate in 0.1 N H_2SO_4 computed from Equation (5.3) are compared to values determined spectrophotometrically and from Equation (5.4). For these solutions ρ_r was determined to be 0.041. Although the differences between the absorbance estimates are small, for each sample better agreement with the spectrophotometric result was obtained from Equation (5.4) than from Equation (5.3).

2. Fluorimetric Determination of Aluminum

In a recent report, Milham et al. (76) have shown that iron interferes in the fluorimetric determination of aluminum with oxine (8-hydroxyquinoline) by forming a tris-oxinate that absorbs both the exciting radiation and the fluorescence of the aluminum oxinate. Titanium and vanadium also interfere in this manner (77). Controlled potential electrolysis and cation exchange resins (78) have been used successfully to remove iron and other metal ions to avoid these interferences, but at the expense of complicating the experimental procedure, increasing cost, and increasing the analysis time.

To test the effectiveness of the absorption-corrected spectrofluorimeter to reduce this interference a simple experiment was performed. Six 100 ml aqueous solutions, each containing 10 μg of Al(III) and amounts of Fe(III) from 0 to 500 μg , were treated with oxine and extracted with chloroform as outlined by Goon, et al. (77). The chloroform extracts were excited at 365 nm and the fluorescence was measured at 515 nm. Five measurements were obtained by the

cell shift method and five by the conventional fluorimetric method with the cell stationary at position 2. The average aluminum recoveries by each method and the standard deviations are listed in Table 6. Even at cell position 2, at which the absorption interference is reduced by the short radiation paths through the sample, the fluorescence decrease in the presence of 500 μg of Fe(III) corresponded to a 34% loss of aluminum. The absorbances were 0.65 at 365 nm and 0.42 at 515 nm for this sample. For the absorption-corrected cell shift results, however, the interference due to iron oxinate was eliminated. The results for up to 500 μg of Fe(III) are not statistically different at the 95% confidence level from the result when no iron was present.

In addition to an increase in accuracy, the use of this instrument in the aluminum analysis enabled the sample treatment to be kept to a minimum and the analysis time to be reduced compared to the other corrective procedures mentioned above. The time required for a single measurement cycle and computation of the absorption-corrected result is about 40 seconds.

Performing the aluminum analysis also revealed the disadvantage that the instrument is several orders of magnitude less sensitive than most commercial spectrofluorimeters. The detection limit for quinine sulfate, at the 95% confidence level, is about 1×10^{-8} M. This is due not only to the excitation source, the low light throughput, and the narrow bandwidth of the monochromators used, but also to the significant quantity of radiation that is discarded to ensure that the excitation and emission beams are collimated. Although the

Table 6. Recovery of Aluminum in the Presence of Iron.

$\mu\text{g Fe}$	$\mu\text{g Al Recovered}$	
	Cell Shift Method	Normal Fluorimetry ^a
0	10.0 ± 0.4	10.0 ± 0.2
100	10.1 ± 0.4	9.2 ± 0.2
200	10.1 ± 0.3	8.3 ± 0.1
300	10.0 ± 0.4	7.5 ± 0.2
400	10.1 ± 0.3	7.2 ± 0.2
500	10.5 ± 0.3	6.6 ± 0.1

^aCell stationary at position 2.

sensitivity could probably be increased by an order of magnitude or more with a more intense excitation source and faster monochromators, little improvement could probably be achieved by compromising beam collimation before correction accuracy would be degraded. For this reason it is doubtful that an instrument of this type could ever be as sensitive as a conventional spectrofluorimeter. This will obviously limit the usefulness of the instrument for trace analyses for which fluorescence methods have been most useful in the past. At the same time the usefulness of the instrument will be greater than that of a conventional spectrofluorimeter for concentrated samples for which the raw fluorescence intensity is not a linear function of the fluorophore concentration.

The poor sensitivity of the instrument is reflected in the moderate measurement precision shown in Table 6. For the absorption-corrected results the precision is even poorer. This effect has been predicted by Novak (69) and is discussed more completely in the next chapter.

3. Correction of Fluorescence Emission Spectra

The use of the instrument to correct fluorescence emission spectra for absorption interferences is illustrated in Figures 17, 18, and 19. Figure 17 shows the emission spectra recorded at cell positions 1, 2, and 3 in 2 nm intervals for a 10^{-6} M solution of rhodamine B in ethanol excited at 313 nm. Because the sample was very weakly absorbing at all wavelengths, the three emission spectra coincide within experimental error. In Figure 18 emission spectra from a

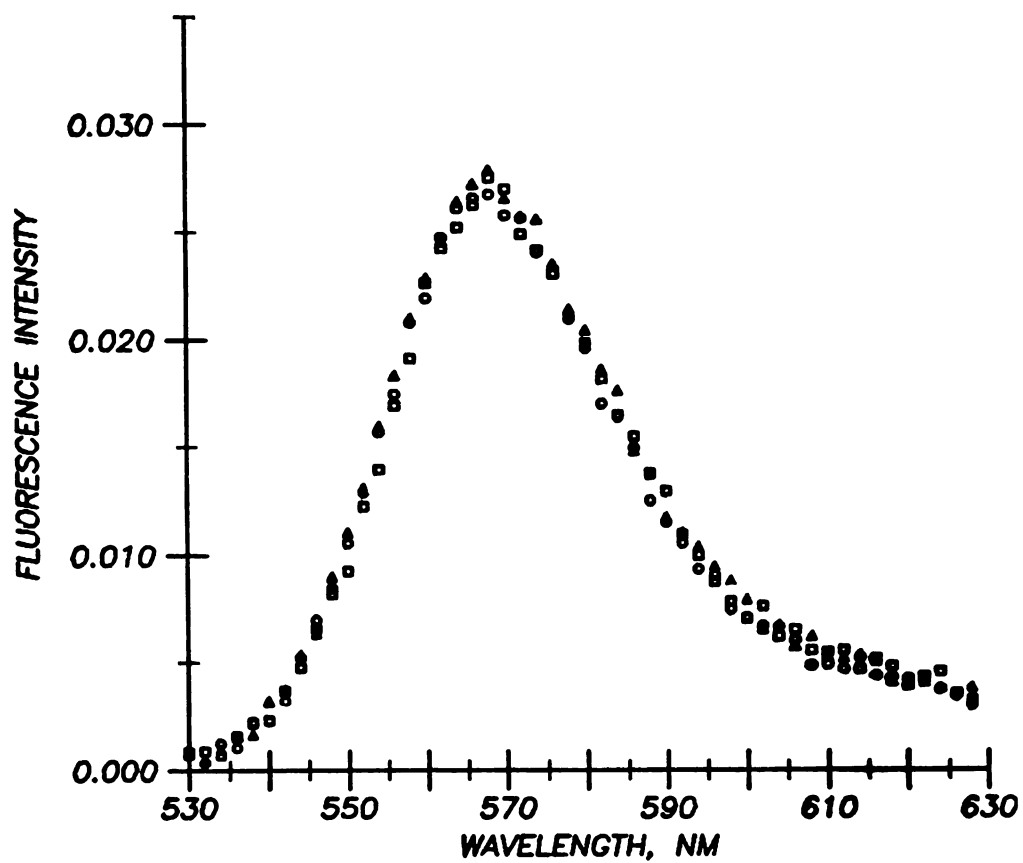


Figure 17. Uncorrected fluorescence emission spectra of 10^{-6} M rhodamine B in ethanol. (o) cell position 1, (Δ) cell position 2, (\square) cell position 3.

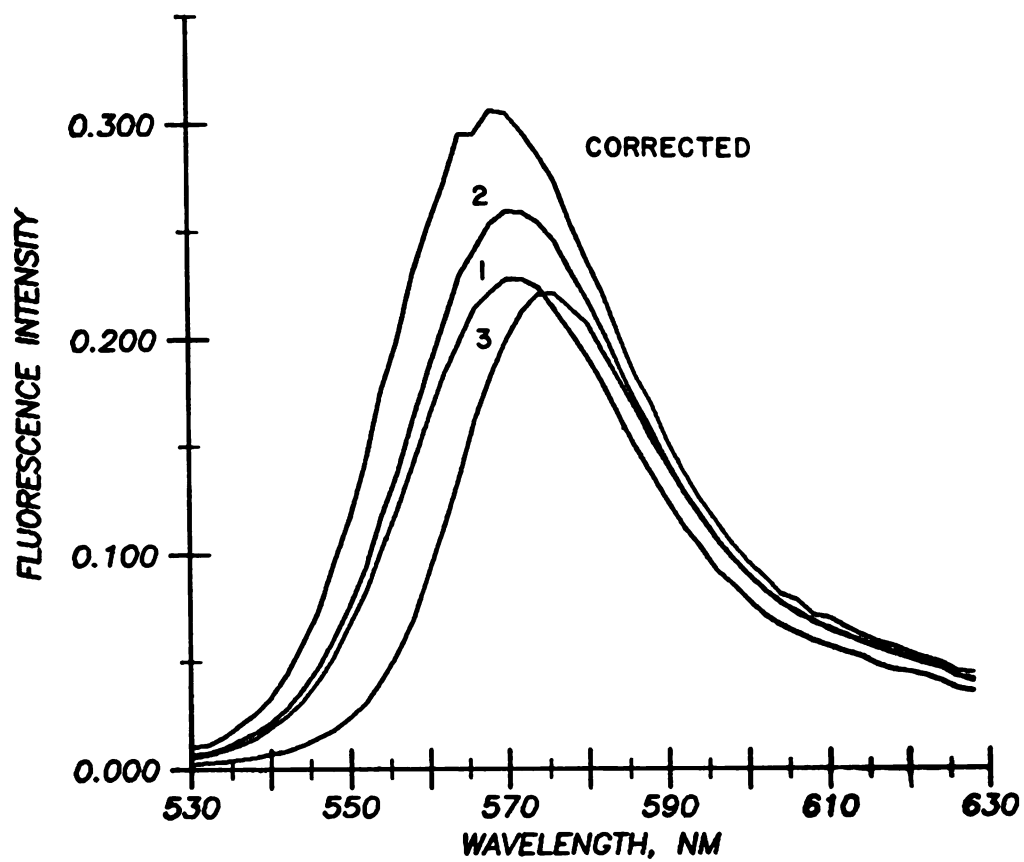


Figure 18. Uncorrected and absorption-corrected fluorescence emission spectra of 10^{-5} M rhodamine B in ethanol, (1) Response from cell position 1. (2) Response from cell position 2. (3) Response from cell position 3.

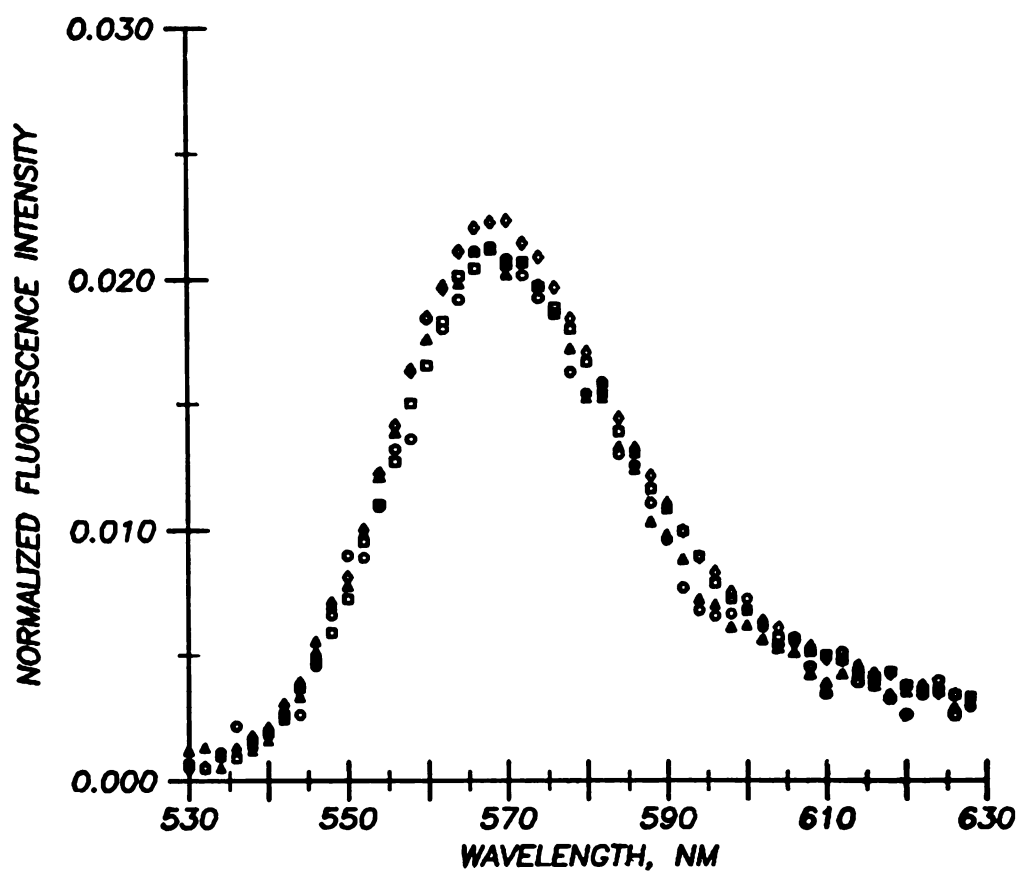


Figure 19. Normalized absorption-corrected fluorescence emission spectra of rhodamine B in ethanol. (o) 10^{-6} M, (Δ) 2×10^{-6} M, (\square) 6×10^{-6} M, (\diamond) 10^{-5} M.

10^{-5} M solution of rhodamine B are shown. The responses from cell positions 1, 2, and 3 differ significantly due to the effects of primary and secondary absorption by the more concentrated fluorophore solution. The absorption processes clearly cause the location and magnitude of the fluorescence maximum and the band shape to vary with the cell position and to differ from that predicted from Figure 17. The absorption-corrected emission spectrum, however, agrees very well in each of these respects with the low absorbance data of Figure 17. Figure 19 illustrates this more clearly. Absorption-corrected emission spectra of solutions of 10^{-6} , 2×10^{-6} , 6×10^{-6} , and 10^{-5} M rhodamine B in ethanol are shown normalized for the fluorophore concentration. Within experimental error, the four spectra coincide, although the 10^{-5} M spectrum is slightly more intense than the others. The reason for this discrepancy is considered in Chapter VI.

CHAPTER VI

PRECISION AND ACCURACY OF ABSORPTION-CORRECTED MOLECULAR FLUORESCENCE MEASUREMENTS BY THE CELL SHIFT METHOD

A. Introduction

The cell shift method considered in Chapter V offers several advantages over other absorption correction procedures described in the literature (66,73). First, direct measurement of the sample absorbance at the excitation and emission wavelengths is not required. A spectrofluorimeter is, therefore, the only measurement device that is needed, and errors arising from the use of a spectrophotometer are avoided (69,72). Commercial fluorescence instruments are suitable for the method with only minor modifications (72). The method has also been easily automated, resulting in a simpler calibration procedure, reduced measurement time, and the elimination of cell positioning as a source of error.

The cell shift method has been used to correct for self-absorption and to improve the accuracy of solvent fluorescence subtraction in fluorescence emission spectra (69). In the previous chapter it was demonstrated that matrix absorption interferences in a fluorimetric assay for aluminum can be corrected with the technique. Although these applications have been successful, several factors that may

affect the accuracy of the corrected fluorescence have been thoroughly studied and are reported in this chapter. These factors include the reemission of absorbed fluorescence by the sample, light scattering by the sample, and the spectral bandwidths of excitation and emission. Knowledge of these effects is valuable so that errors in the cell shift correction procedure can be minimized. Also of importance is the effect of the correction procedure on analytical precision. The factors affecting the precision of the absorption-corrected fluorescence intensity and the relationship between the measurement precision and the precision of the corrected result are considered in detail.

B. Experimental

1. Instrumentation

All fluorescence measurements were performed with the micro-computer-controlled spectrofluorimeter described in Chapter V. The instrumental parameters and the measurement procedure were the same as given previously. Spectrophotometric measurements of the sample absorbance were obtained with this same instrument by the procedure outlined in Chapter IV. These measurements should be distinguished from values of the apparent sample absorbance calculated from the fluorescence measurements.

2. Reagents

All reagents were of analytical grade and were used without further purification. Solutions were prepared in volumetric glassware with house distilled water. Quinine sulfate solutions were stored in hard polyethylene bottles to minimize adsorption losses. All solutions were stored in the dark until use to prevent photo-decomposition.

C. Results and Discussion

1. Correction Accuracy When Reemission is Negligible

In the theory of the cell shift method (50,69) and in other absorption correction procedures (66,73), the least discussed and, perhaps, most important assumption is that reemission of absorbed fluorescence by the sample is negligible. Several tests of absorption correction accuracy in which this condition is satisfied have been described previously (2,73). These tests were repeated in this study to illustrate the potential accuracy of the cell shift method under ideal conditions. The results are shown in Figures 20, 21, and 22.

Figure 20A illustrates the accuracy of the correction for absorption of exciting radiation by the fluorophore itself. For 10^{-7} to 4×10^{-4} M solutions of quinine sulfate in 0.1 N H_2SO_4 , absorption-corrected fluorescence intensities and uncorrected fluorescence intensities from the three cell positions are plotted against the solution absorbance at the excitation wavelength. Curvature of the

Figure 20. Correction for absorption of exciting radiation by the fluorophore. A - Fluorescence of quinine sulfate vs. absorbance at the exciting wavelength, (■) corrected fluorescence; (▲) measured fluorescence for cell positions 2 and 3; (●) measured fluorescence for cell position 1. B - RSD of corrected fluorescence vs. absorbance.

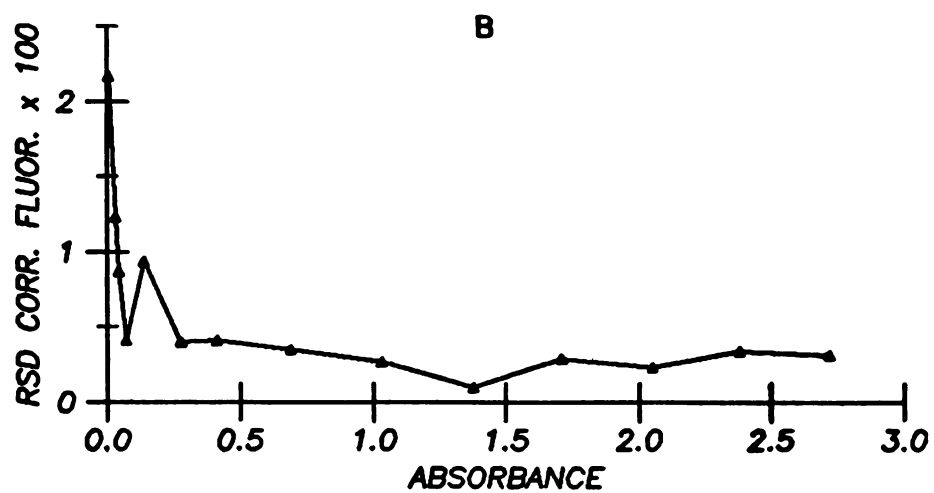
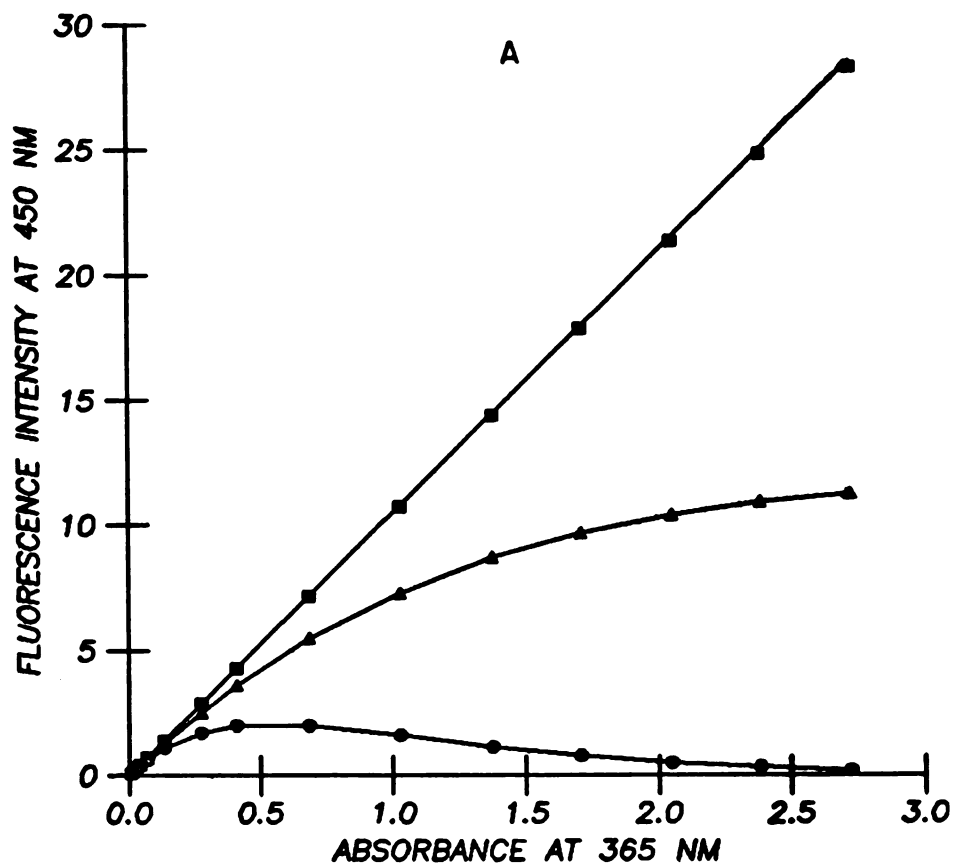


Figure 20

Figure 21. Correction for absorption of exciting radiation by the sample matrix. A - Fluorescence of a constant amount of quinine sulfate in the presence of increasing amounts of gentisic acid, (▲) corrected fluorescence; (■) measured fluorescence for cell positions 2 and 3; (●) measured fluorescence for cell position 1. B - RSD of corrected fluorescence vs absorbance.

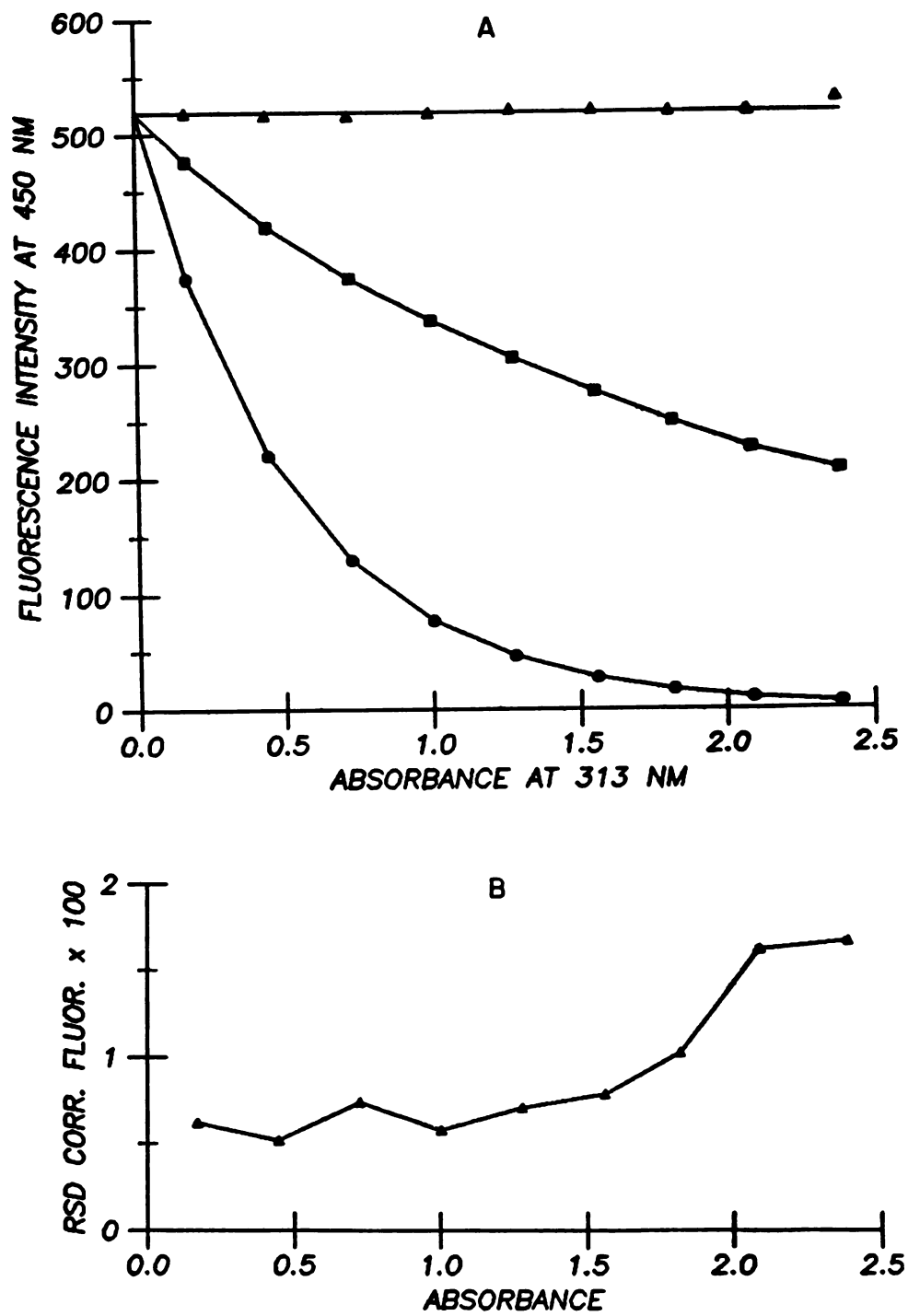


Figure 21

Figure 22. Correction for absorption of exciting and fluorescence radiation. A - Fluorescence of a constant amount of quinine sulfate in the presence of increasing amounts of fluorescein; (●) corrected fluorescence; (▲) measured fluorescence for cell position 1; (■) measured fluorescence for cell position 2; (◆) measured fluorescence for cell position 3. B - RSD of corrected fluorescence vs. absorbance.

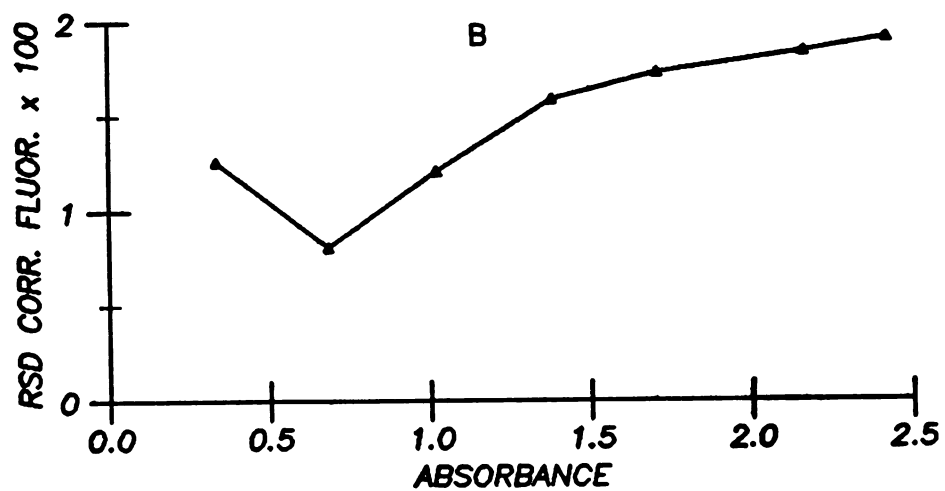
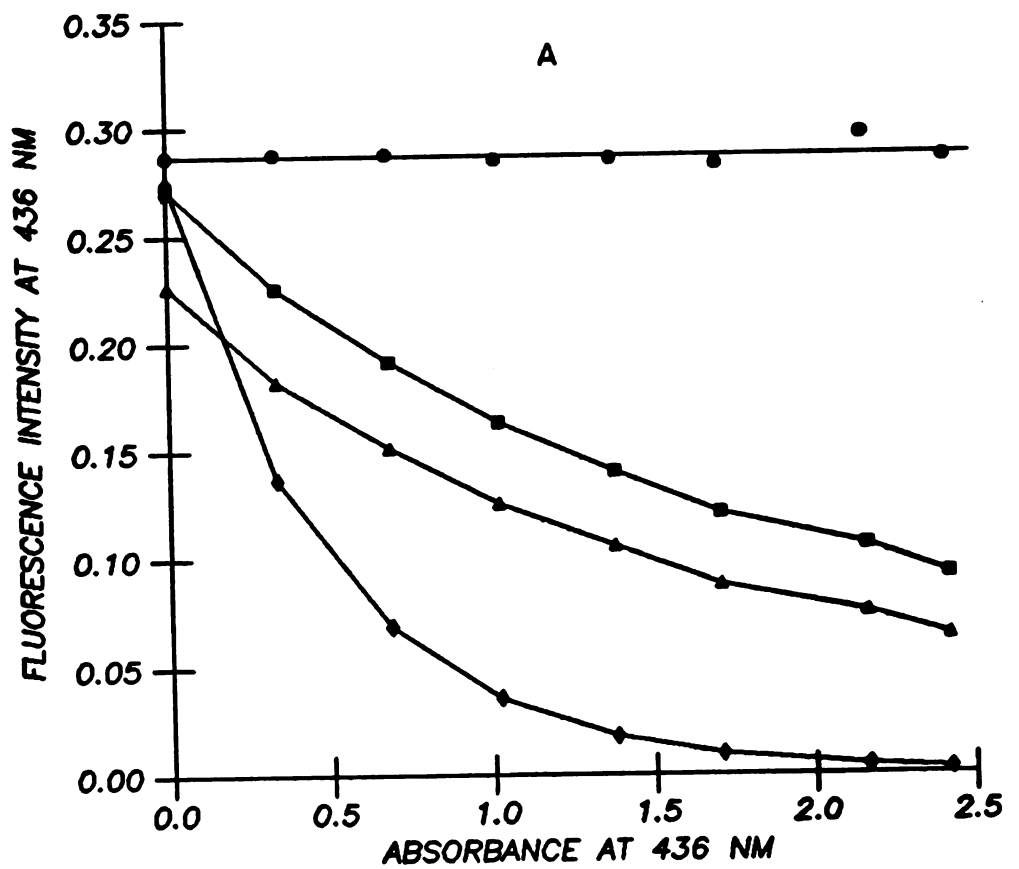


Figure 22

measured fluorescence response due to absorption of the exciting light is evident. Figure 21A illustrates the accuracy of the correction for absorption of exciting radiation by sample components other than the fluorophore. Corrected and uncorrected fluorescence intensities for a series of solutions of 2×10^{-5} M quinine sulfate and 0 to 4×10^{-4} M gentisic acid in 0.1 N H_2SO_4 are plotted against the solution absorbance at the exciting wavelength. In Figure 22A, raw and corrected fluorescence intensities for solutions of 2×10^{-5} M quinine sulfate and 0 to 6.5×10^{-5} M fluorescein in 0.1 N H_2SO_4 are plotted as a function of the solution absorbance at the emission wavelength. The uncorrected data in Figure 22A reflect the effects of absorption of exciting radiation by both the fluorophore and the sample matrix and the effect of absorption of the fluorescence emission by the sample matrix. The straight line in part A of each figure represents the theoretical absorption-free fluorescence response which was determined by extrapolating from the corrected data at low absorbance (≤ 0.01). Part B of each figure shows the precision of the corrected results, as the relative standard deviation (RSD), as a function of the sample absorbance.

In each of these tests, the cell shift corrected results do not differ significantly ($\alpha = 0.05$) from the theoretical lines up to an absorbance of 2.0. In Figure 20A, the corrected results are in error by less than two percent up to an absorbance of 2.7. The decrease in accuracy at higher absorbances is most likely due to inaccuracies in the extrapolation of the theoretical fluorescence response and in the values of the instrument window parameters used in the correction

calculations. No fundamental limitation of the accuracy of the cell shift method is indicated under the conditions of these experiments.

As shown, the relative standard deviation of the corrected fluorescence results was very good in each test, ranging from 0.2 to about 2.0 percent. Increases in the RSD occurred as the magnitude of the measured fluorescence intensities and the fluorescence signal-to-noise ratio decreased. This behavior is discussed in more detail later.

2. Effect of Reemission

To investigate the accuracy of the cell shift method under conditions in which the reemission of absorbed fluorescence is not negligible, solutions of 10^{-7} to 5×10^{-6} M fluorescein in 0.1 N NaOH were prepared and excited at 313 nm. Fluorescein has a relatively small Stokes shift of 1100 cm^{-1} (79) and, therefore, a large degree of overlap between its absorption and fluorescence emission bands. Fluorescence emission was monitored at 510 nm (in the overlap region) and also at 540 nm (outside the overlap region). In Figures 23 and 24, the corrected fluorescence intensities at each emission wavelength are plotted against the fluorescein concentration. Also plotted are values of the apparent solution absorbance calculated by the cell shift method and used to compute the absorption correction factors. The straight lines in each figure are absorbance analytical curves determined from spectrophotometric data and extrapolated fluorescence analytical curves. The data show that at concentrations greater than about 10^{-5} M there is a definite decrease in the accuracy of the

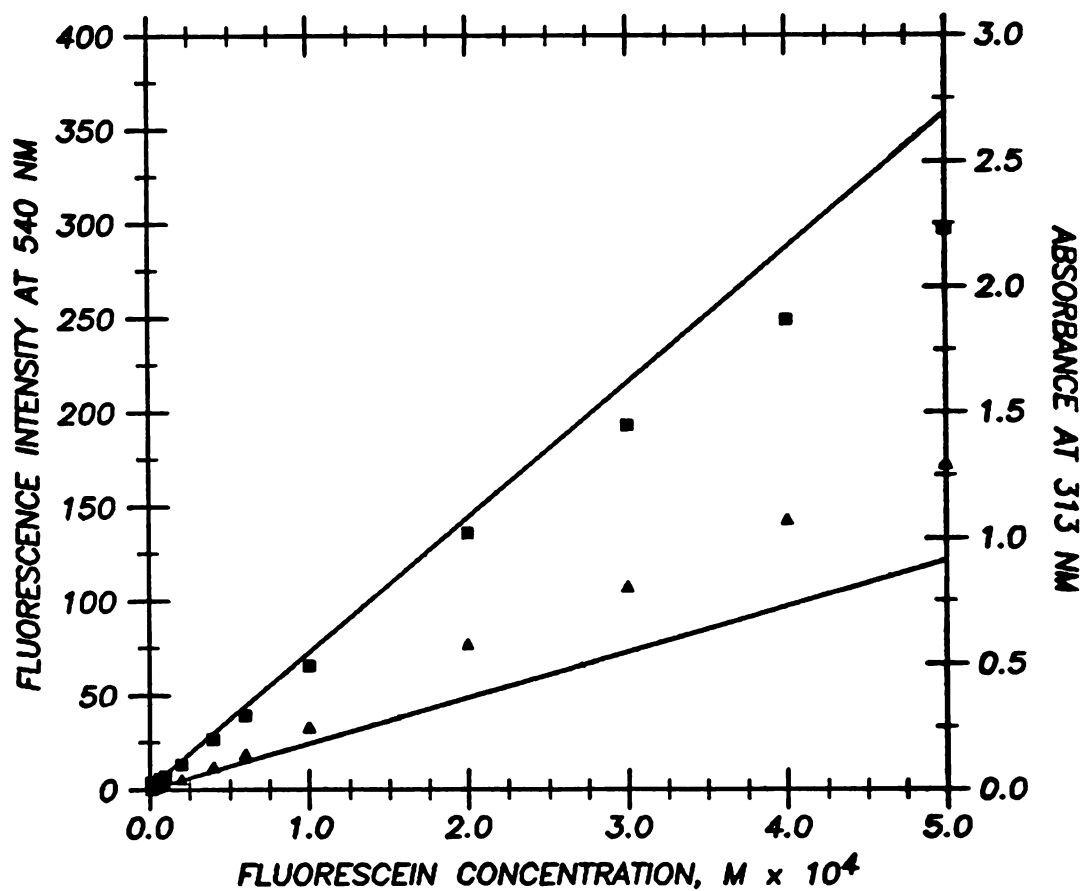


Figure 23. Effect of reemission on the corrected fluorescence (▲) and apparent sample absorbance at the excitation wavelength (■) when fluorescence is monitored outside the overlap region.

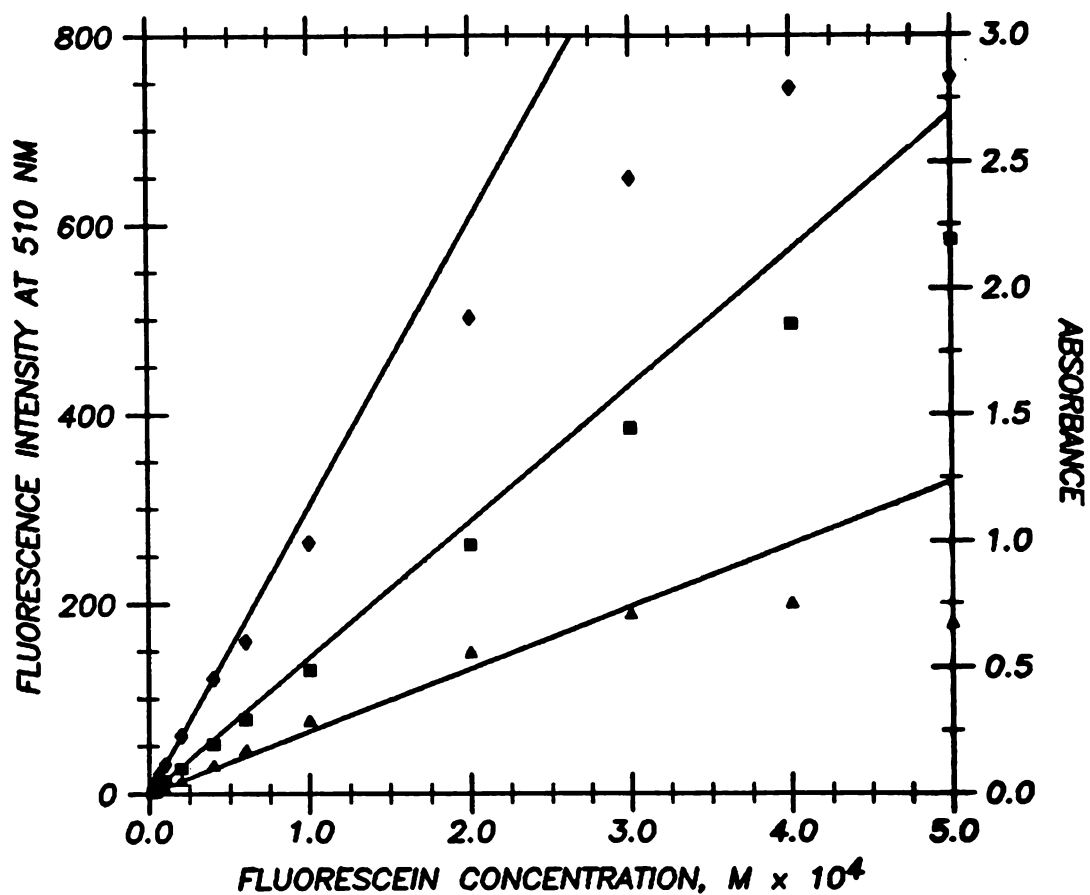


Figure 24. Effect of reemission on the corrected fluorescence (\blacktriangle) and apparent sample absorbance at the excitation (\blacksquare) and emission (\blacklozenge) wavelengths when fluorescence is monitored in the overlap region.

absorption-corrected fluorescence. Two effects are apparent from Figures 23 and 24. First, the presence of a small reemission component in the measured fluorescence signals causes a negative error in the sample absorbance calculated by the cell shift method. This is similar to the effect of stray light on a spectrophotometric absorbance measurement. The absorbance error tends to cause a negative error in the corrected fluorescence. Opposing this effect, however, is the reemission component in the measured signal which tends to make the corrected fluorescence larger than the theoretical value. The nature of the net error due to reemission depends on the emission wavelength chosen. Away from the region of overlap (Figure 23), where corrections for absorption of fluorescence radiation are minor, the absorption-corrected fluorescence shows a positive error. The error increases in magnitude as the fluorophore concentration is increased. If fluorescence is monitored in the region of overlap (Figure 24) where the correction for absorption of fluorescence radiation can be significant, however, the error in the corrected fluorescence is first positive, but eventually decreases and becomes negative as the fluorophore concentration is increased. Evidently, the combined negative errors in the apparent sample absorbances at the excitation and emission wavelengths become large enough to dominate the effect of the extra component of fluorescence due to reemission. Further evidence of this is given in Figure 25. Absorption-corrected fluorescence emission spectra for 5×10^{-6} , 10^{-5} , and 3×10^{-5} M solutions of rhodamine B in ethanol, normalized for concentration, are shown. Clearly, as the fluorophore concentration is increased, a decrease in

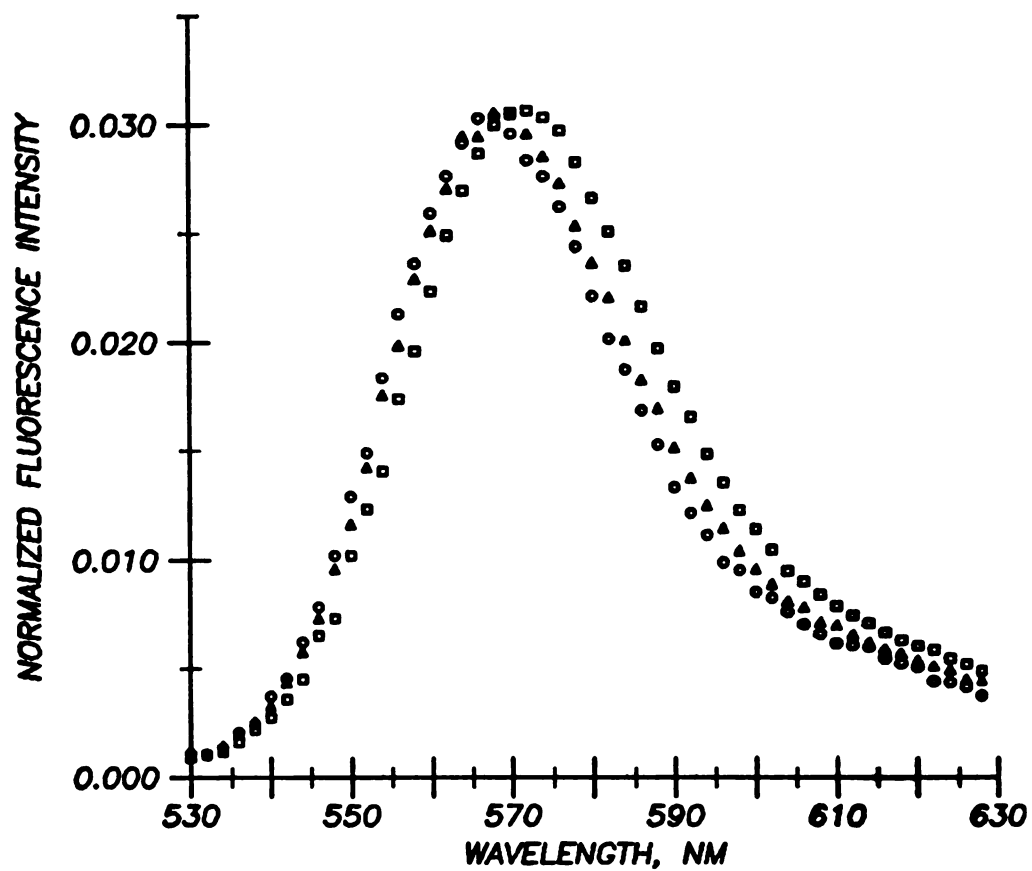


Figure 25. Absorption-corrected fluorescence emission spectra of rhodamine B in ethanol. (o) 5×10^{-6} M, (Δ) 10^{-5} M, (\square) 3×10^{-5} M.

fluorescence intensity on the low wavelength side of the emission band and an increase in intensity on the high wavelength side occur which are statistically significant. This is exactly the effect predicted from the data of Figures 23 and 24.

Regardless of the emission wavelength chosen, the accuracy of the cell shift method can be poor when the absorption and emission bands of the fluorophore overlap. The data of Figures 23 and 24 and of Figure 19 in Chapter V indicate, however, that errors due to reemission are insignificant below a concentration of about 10^{-5} M. Because the examples used here approach the worst case for degree of absorption-emission overlap, it is expected that, in general, re-emission errors will not be significant below this concentration limit and below a much higher concentration limit for many fluorophores.

3. Effect of Light Scattering

Scattering of the exciting and fluorescence radiations by the sample matrix is a potential problem common to all fluorimetric methods. To determine the effect of matrix scattering on cell shift corrected fluorescence measurements, a series of solutions of 4×10^{-5} M quinine sulfate in 0.1 N H_2SO_4 containing increasing amounts of soluble starch were prepared. The solutions were excited at 365 nm and fluorescence was monitored at 450 nm. In Figure 26 the corrected fluorescence intensities and solution absorbances, normalized to the values in the absence of the scattering agent, are plotted as a function of the scattering agent concentration. Clearly, the effect

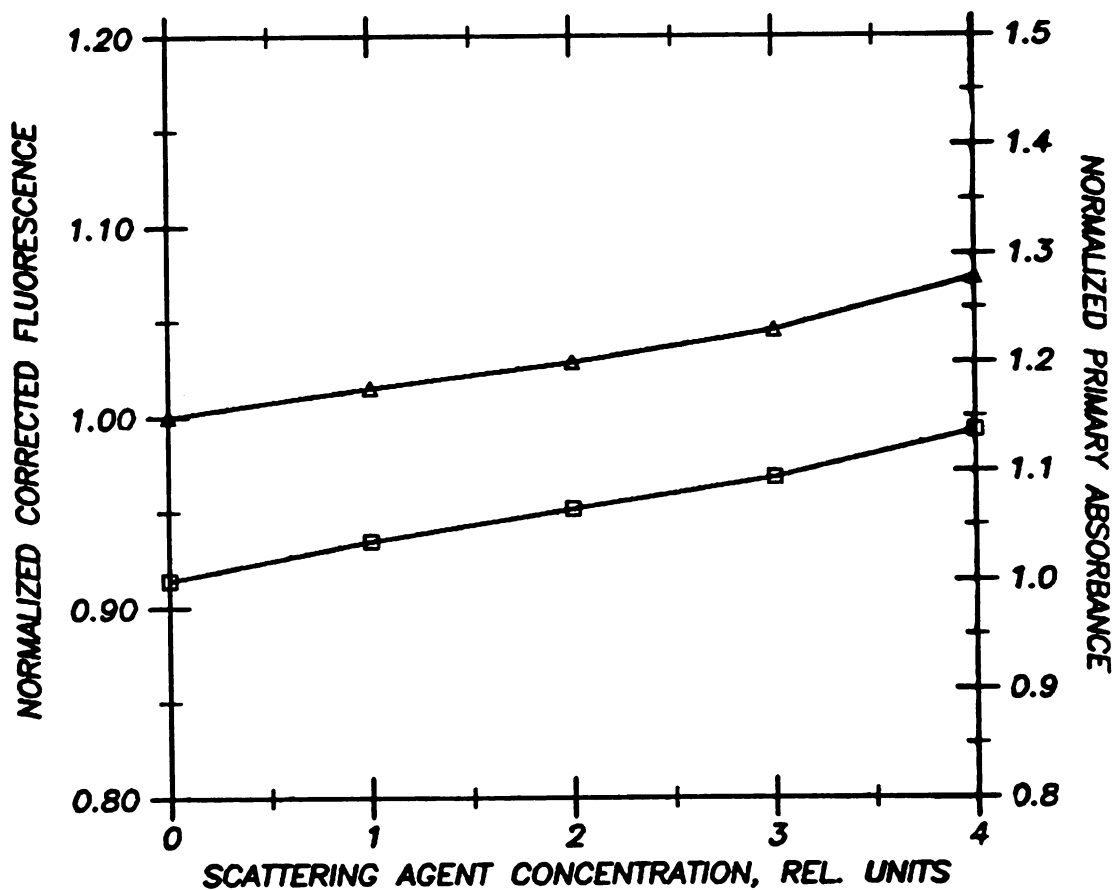


Figure 26. Corrected fluorescence (Δ) and apparent absorbance (\square), normalized to zero scattering agent, of a constant concentration of quinine sulfate as a function of increasing amounts of soluble starch.

of light scattering by the sample matrix is a positive error in both the apparent sample absorbance and the corrected fluorescence. The magnitude of the error increases as the scattering agent concentration is increased.

4. Effect of Spectral Bandwidth

Because the spectral bandwidths of excitation and emission have been shown to affect the accuracy of other absorption correction procedures (66), the effect of this measurement parameter on cell shift corrected fluorescence measurements was investigated. The excitation monochromator of the spectrofluorimeter, which has a maximum bandwidth of 4 nm, was replaced with a Corning 7-60 band filter which has a bandwidth at half height of approximately 40 nm. Quinine sulfate standards from 10^{-7} to 4×10^{-4} M were excited with a 200 W Xe-Hg arc lamp, and their fluorescence emission was measured at 450 nm. In Figure 27 the corrected fluorescence intensities and solution absorbances determined by the cell shift method are plotted against the quinine sulfate concentration. The extrapolated fluorescence response from low concentration and the absorbance analytical curve determined by spectrophotometry are also shown. Clearly, the increased excitation bandwidth resulted in negative deviations of both the sample absorbance and the corrected fluorescence from their theoretical values at concentrations above 1.5×10^{-4} M. The effect is similar to that which polychromatic radiation has on spectrophotometric measurements. Although the effect on the corrected fluorescence in this example is not very severe, it would be expected to

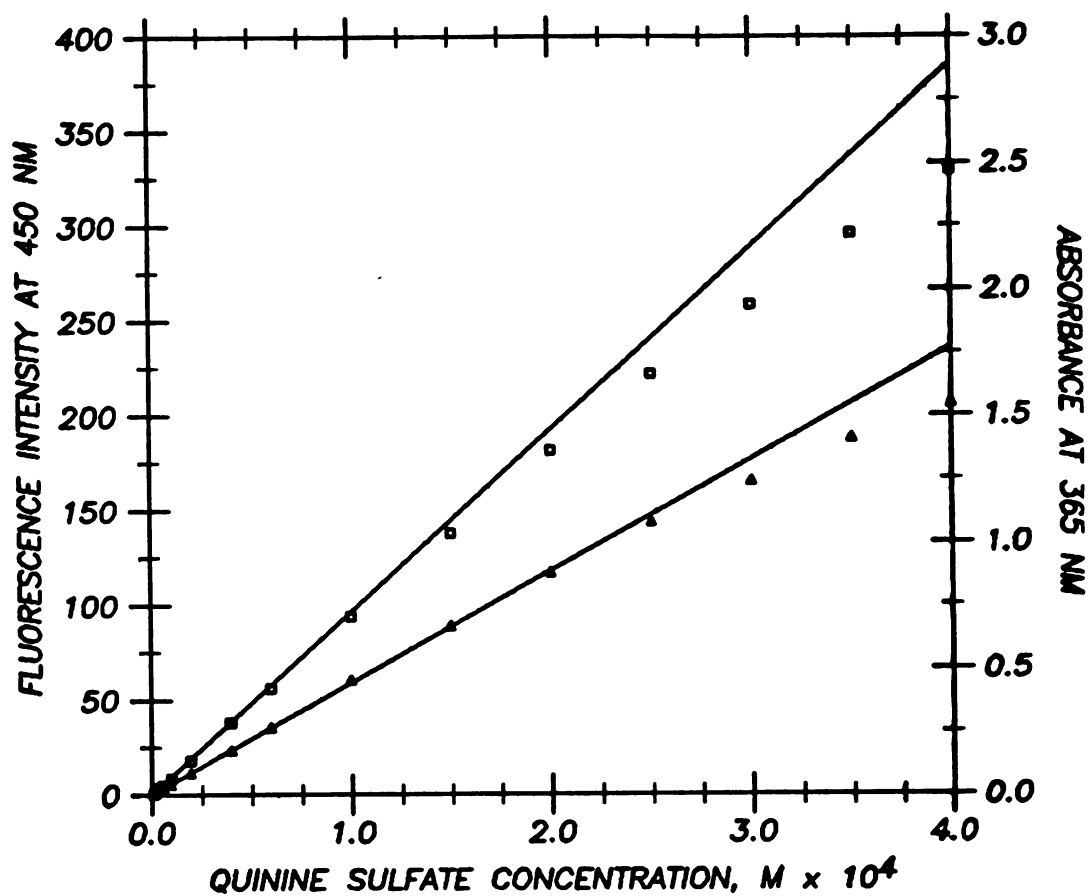


Figure 27. Corrected fluorescence (Δ) and apparent absorbance at the exciting wavelength (\square) vs. concentration for quinine sulfate excited with a Xe-Hg arc lamp and Corning 7-60 filter.

be worse if a continuum radiation source had been used or if the emission monochromator had also been replaced with a band filter. By using interference filters rather than band filters the errors would probably be less severe.

5. Correction Precision

Although Novak (69) has discussed the effect of the instrument window parameters on the precision of the absorption correction factors, the results shown in Figures 20B, 21B, and 22B are better understood through a simple extension of his discussion. Ignoring the corrections for reflections within the sample cell, the corrected fluorescence intensity from the cell shift method F_c is given, to a good approximation, by

$$F_c = F_1^x F_2^y F_3^z \quad (6.1)$$

where F_1 , F_2 , and F_3 are the measured fluorescence intensities at the three cell positions, and the exponents x , y , and z are given by

$$x = -(\omega_{\beta 2} + \omega_{\alpha 2})/2\delta\omega \quad (6.2)$$

$$y = 1 + (\omega_{\beta 2} + \omega_{\alpha 2})/2\delta\omega + (\theta_{\beta 2} + \theta_{\alpha 2})/2\delta\theta \quad (6.3)$$

$$z = -(\theta_{\beta 2} + \theta_{\alpha 2})/2\delta\theta \quad (6.4)$$

The window parameters $\omega_{\beta 2}$, $\omega_{\alpha 2}$, $\delta\omega$, $\theta_{\beta 2}$, $\theta_{\alpha 2}$, and $\delta\theta$ were defined in

Chapters III and V. Since F_1 , F_2 , and F_3 are not measured simultaneously, the random errors in these measurements will not be correlated, and the relative uncertainty of the corrected result will be given by

$$\frac{\sigma_{F_c}}{F_c} = \left(x^2 \frac{\sigma_{F_1}^2}{F_1^2} + y^2 \frac{\sigma_{F_2}^2}{F_2^2} + z^2 \frac{\sigma_{F_3}^2}{F_3^2} \right)^{1/2} \quad (6.5)$$

Making use of the relationships: $F_1 = F_2 10^{-A\delta\omega}$, $F_3 = F_2 10^{-A'\delta\theta}$, and that σ_{F_n}/F_n is proportional to $F_n^{-\xi}$ where $n = 1, 2$, or 3 , Equation (6.5) can be reduced to

$$\frac{\sigma_{F_c}}{F_c} = \frac{\sigma_{F_2}}{F_2} \left(x^2 10^{2A\xi\delta\omega} + y^2 + z^2 10^{2A'\xi\delta\theta} \right)^{1/2} \quad (6.6)$$

where A is the sample absorbance at the exciting wavelength and A' is the sample absorbance at the emission wavelength. The parameter ξ is the slope of the log-log plot of fluorescence signal-to-noise ratio versus fluorescence signal. It can assume values from 0 to 1 depending on the noise characteristics of the spectrofluorimeter and will be 0.5 if the instrument is signal shot noise limited.

Equation (6.6) predicts that the RSD of the cell shift corrected fluorescence depends directly on the RSD of the measured fluorescence signal from cell position 2 and will be greater by a factor that is a function of the instrument window parameters, the sample

absorbances at both the excitation and emission wavelengths, and of the noise parameter ξ . The data in Figures 20B, 21B, and 22B confirm that the relative precision of the measured fluorescence intensity is the major factor affecting the relative precision of the corrected result. In each experiment, the RSD of the corrected fluorescence increased as the RSD of the raw measurements increased, i.e., as the measured signal magnitude decreased. The effect of all other parameters on the precision of the corrected fluorescence is illustrated in Figure 28. The experiment for which results are shown in Figure 20 was repeated five times and values of the RSD of the corrected fluorescence were divided by the RSD of the measured signal from cell position 2. The average values of the normalized relative standard deviation are plotted against the solution absorbance at the excitation wavelength along with a theoretical curve calculated from Equation (6.6). Figure 28 shows clearly that the cell shift correction process reduces the experimental precision, but also that the effect is small (a factor of two or less in this example). The effect of the correction process on the experimental precision becomes greater as the sample absorbance increases. This is predicted by Equation (6.6) (broken curve). The effect also becomes greater at low sample absorbances, contrary to what Equation (6.6) predicts. The reason for this behavior is not presently understood. It is clear, however, that the effect will not generally be important because the order of magnitude of the precision of the corrected fluorescence is determined by the measurement precision.

The imprecision introduced by the absorption correction process

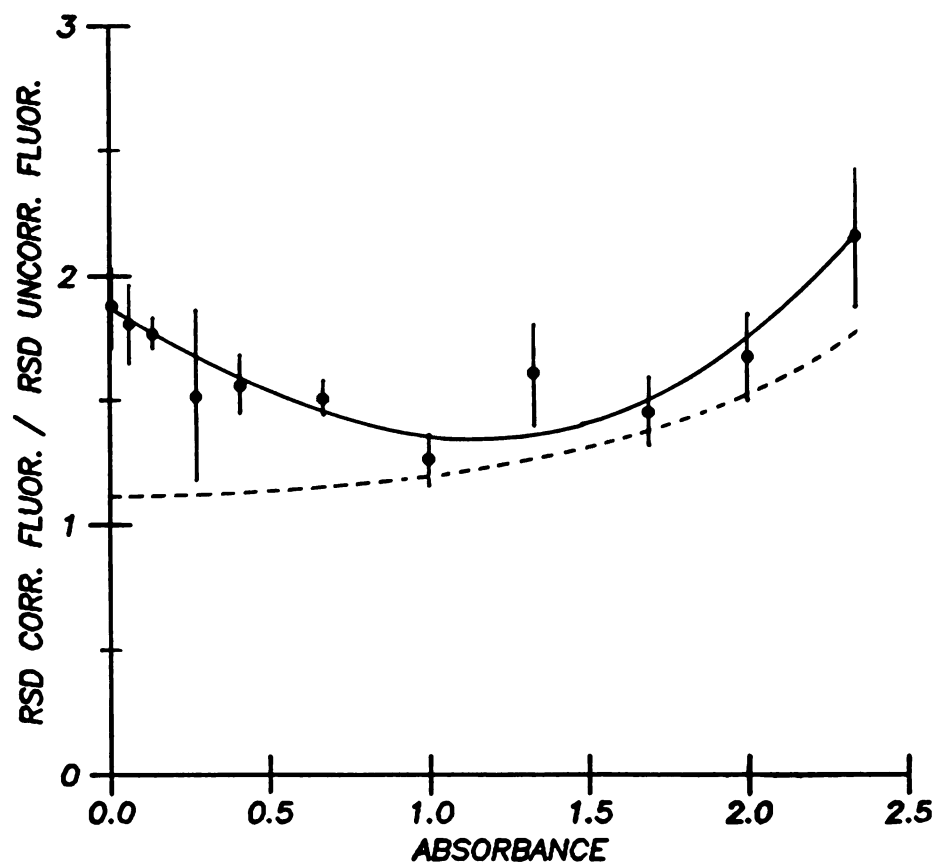


Figure 28. Normalized RSD of corrected fluorescence as a function of absorbance. (●) $(\sigma_{F_C}/F_C)/(\sigma_{F_2}/F_2)$, (---) theoretical result from Equation (6.6) for $\xi = 1/2$

can be minimized by making the window parameters for cell position 2 as small as possible as Novak (69) has stated. Maximizing the distance between cell positions, i.e., the parameters $\delta\omega$ and $\delta\theta$, will also reduce the imprecision at low sample absorbance. Although the precision at high sample absorbance will suffer from this, it may often not be a disadvantage because of limitations of the accuracy of the cell shift method at higher absorbances due to the factors discussed previously.

CHAPTER VII

CONCLUSIONS

A. Summary

A correction factor has been developed for interferences due to absorption of fluorescence radiation in a dispersive right-angle fluorimeter. This expression is a function of the sample transmittance at the emission wavelength and of the geometric window parameters of the instrument. When applied along with a correction factor for interferences due to absorption of exciting radiation developed by previous workers, this procedure enables absorption errors greater than 90 percent to be reduced to three percent or less, making an accurate estimate of the absorption-free fluorescence intensity of a sample possible.

It has been shown that the accuracy of this absorption correction procedure can be further improved to one percent or better by including explicit corrections for the effects of reflections within the sample cell at the excitation and emission wavelengths. The natural reflection properties of a typical glass or quartz fluorescence cell can cause errors as great as eight percent in the absorption-corrected fluorescence if the sample is highly absorbing at both the excitation and emission wavelengths. The errors due

to reflection can be reduced by using a curve fitting procedure to determine the best window parameters for the absorption correction factors, but better accuracy can be achieved by applying explicit corrections for the reflection effects. Although additional knowledge of the reflectance values of the cell at the excitation and emission wavelengths is required for this process, these quantities can be easily determined from a simple algebraic formula and transmittance measurements of the solvent filled cell at the appropriate wavelengths. For many typical solvent systems, dilute aqueous acids and bases or ethanol, for example, the cell reflectance varies by one percent or less over the visible spectrum and can, therefore, be taken as a constant without seriously reducing the accuracy of the correction procedure.

For the absorption and reflection corrections to be valid, it is necessary that the beams of exciting and fluorescence radiation be highly collimated and of narrow spectral bandwidth with respect to the sample absorption bands. Stray light, scattering phenomena, and reemission of absorbed fluorescence must also be negligible. Of the instrumental requirements, the stray light and bandwidth limitations are probably the most severe and will preclude the use of the equations presented here to correct filter fluorimetric data for absorption errors. Reemission phenomena have been shown to cause serious positive errors in the absorption-corrected fluorescence for fluorophores with highly overlapping absorption and fluorescence emission bands, but only at concentrations greater than about 10^{-5} M in the worst case. Although this problem will obviously limit the

usefulness of absorption-corrected fluorescence for concentrated solutions of some fluorophores, the absorption corrections developed in this work will be a valuable aid to the analytical chemist. Substantial absorption errors can occur at fluorophore concentrations below 10^{-5} M for which the correction procedure is highly accurate.

A significant practical limitation of the absorption correction procedure is the necessity of measuring the sample transmittances at both the excitation and emission wavelengths along with the fluorescence intensity. Employing a spectrophotometer for this purpose can be satisfactory, but requires more time for the analysis, introduces the added cost of a second instrument, and can introduce errors related to wavelength calibration and spectral bandwidth differences between the instruments.

A new procedure called the "cell shift method" has been investigated to reduce these problems. It has been shown that the required sample transmittance values can be accurately computed from only three fluorescence measurements obtained with the sample cell in different positions with respect to the excitation and emission windows of the fluorimeter. Because manual positioning of the sample cell for these measurements can be time consuming and a significant source of error, an instrument has been constructed in which the cell positioning and data acquisition are performed automatically under microcomputer control. The instrument is linked to a mini-computer to which the collected fluorescence data are transmitted for permanent storage and where data processing can be more efficiently done. This approach to the cell shift method has eliminated

cell positioning as a source of error, reduced the analysis time, and increased the accuracy and simplicity of the window parameter calibration.

Using this new instrument, the precision and accuracy of the cell shift method of absorption correction have been investigated. For samples that are nonscattering and do not exhibit reemission phenomena, the cell shift method has been found to correct for primary and secondary absorption errors very accurately. An accuracy of better than two percent can be achieved when the sample absorbance at the excitation wavelength is as great as 2.7 and could probably be improved by a more accurate knowledge of the instrument window parameters.

Under less ideal conditions, the cell shift method has been found to be less accurate. For samples that are turbid it has been shown that the cell shift method gives erroneously high results and that the magnitude of the error increases with the turbidity. This susceptibility to scattering errors is expected to limit the use of absorption-corrected fluorescence measurements with real samples, but no more than for normal fluorimetric measurements. The usual precautions against scattering errors in right-angle fluorimetry should be observed.

Because of reemission phenomena, it is also expected that the cell shift method will be of limited use with samples in which the fluorophore is present at concentrations higher than 10^{-5} M. It has been shown that the accuracy of the method can be poor above this concentration limit for fluorophores with highly overlapping absorption and emission bands. Unlike the correction procedure based

on spectrophotometric transmittance measurements, reemission can cause both positive and negative errors in the cell shift corrected fluorescence depending on the emission wavelength chosen. The implications that reemission errors have on the usefulness of the two correction approaches are the same, however.

To ensure the accuracy of the cell shift method, it has been shown that the spectral bandwidths of excitation and emission must be narrow compared to the sample absorption bands. The best general accuracy could be expected by following the rules of molecular absorption spectrophotometry when selecting the spectral bandwidth. Because the accuracy is degraded most for highly absorbing solutions, however, it might be possible to use a wider monochromator bandwidth, or even interference filters, when only more dilute samples are involved and the added sensitivity would be an advantage. Results indicate that the accuracy of the cell shift method would probably be poor with glass cutoff and band filters used in filter fluorimetry due to the very large excitation and emission bandwidths.

Although a fundamental loss of precision has been found to result from the use of the cell shift correction procedure, through proper selection of the instrument window parameters, the magnitude of the loss can be kept small and usually insignificant, a factor of about two. The major factor that determines the precision of the absorption-corrected fluorescence result is the measurement precision of the spectrofluorimeter. Generally, the measurement precision of fluorescence instrumentation is very good due to its superior sensitivity. However, to maintain the high degree of collimation of the exciting and fluorescence beams required for the cell shift

method, a large fraction of the normally available fluorescence radiation must be discarded. The reduction in measurement precision and sensitivity that results is probably the greatest practical limitation of the cell shift method.

B. Suggestions for Further Work

Because of the poor sensitivity of the absorption-corrected spectrofluorimeter constructed for this work, applications of the absorption corrections to some common fluorimetric assays have been limited. If the sensitivity of the instrument could be improved, it is probable that the absorption correction procedures would prove invaluable for improving the accuracy of many fluorimetric analytical methods. Further work in the immediate future should, therefore, be directed toward this goal.

Several steps could be taken to improve the sensitivity of the absorption-corrected spectrofluorimeter. Most obviously, a set of monochromators with a greater spectral throughput would increase the intensity of excitation and, therefore, of the fluorescence radiation. New monochromators might allow wider spectral bandwidths to be used, within limits, for excitation and emission which would further increase the intensity of excitation and also allow more fluorescence radiation to be collected. A more intense excitation source, possibly a laser, and excitation optics more efficient than a simple collimator would help further. From the combined effects of all of these improvements it is estimated that an increase in sensitivity by a factor of between one and two orders of magnitude could

reasonably be expected. More improvement might be attained with the addition of a photon counting detection system. The collimation of the excitation and emission optical beams might also be compromised to some extent to gain sensitivity, although this would certainly reduce the absorption correction accuracy.

In the process of increasing the instrument sensitivity, several other improvements in the instrument could be made. If sufficient sensitivity could be achieved through the changes outlined above, the addition of a solid state array detector to the instrument could greatly reduce the time required to obtain a fluorescence spectrum. Although the low fluorescence light levels characteristic of the instrument suggest that an excessively long integration time would have to be used with this type of detector, spectral data might still be obtained more quickly than with a scanning monochromator system. Currently, the fluorescence signals must be integrated for at least eight seconds at each wavelength to obtain a reasonable S/N. A diode array could be allowed to integrate for 800 seconds and still acquire a spectral record of several hundred nanometers more quickly than the current system. The use of an intensified array would be even more feasible.

Another improvement would be to miniaturize the cell compartment and the other components of the instrument so that it requires less laboratory space. As part of this development, a miniaturized quantum counter reference detector would have to be constructed. Some work has been done with a quantum counter design based on a silicon photodiode which indicates that a significant size reduction is feasible.

If the instrumental limitations discussed above can be overcome, the analytical problems to which absorption-corrected fluorescence could be applied are too numerous to be described in this short space. Two things of particular interest deserve mention, however. First, fluorescence quantum efficiency and partial quantum efficiency measurements can both be seriously distorted by absorption interferences, especially when other chemical species are present in the sample with the fluorophore of interest. Studies of these quantities derived from absorption-corrected fluorescence measurements can easily be conducted with the spectrofluorimeter developed in this work. Suitable data processing programs will, of course, have to be written. Secondly, it has not been previously possible to determine several components with overlapping emission bands in a single fluorescence sample accurately by the method of simultaneous linear equations. Absorption interferences cause the fluorescence signals to be nonadditive, and the method therefore fails. With absorption-corrected fluorescence measurements, however, the fluorescence signals should be additive making the method valid. An interesting system to which this procedure could be applied is the binary mixture of aluminum and gallium oxinates.

A final possibility for future work in the area of absorption-corrected fluorimetry is the problem of interferences due to re-emission phenomena. This type of error has only been identified in this work, and no solution can currently be offered. It is obvious, however, that a correction for reemission errors would be a significant improvement in the absorption correction procedure.

REFERENCES

REFERENCES

1. Wehry, E. L., Anal. Chem. 1980, 52, 75R-90R and previous biennial reviews.
2. Holland, J. F.; Teets, R. E.; Kelly, P. M.; Timnick, A., Anal. Chem. 1977, 49, 706-10.
3. Parker, C. A., "Photoluminescence of Solutions"; Elsevier: Amsterdam, 1968; pp. 220-34.
4. Guilbault, G. G., "Practical Fluorescence, Theory, Methods, and Techniques"; Dekker: New York, 1973; pp. 17-19.
5. Skoog, D. A.; West, D. M., "Principles of Instrumental Analysis"; Holt, Rinehart, and Winston: New York, 1971; p. 233.
6. Willard, H. H.; Merritt, L. L.; Dean, J. A., "Instrumental Methods of Analysis", 5th ed.; D. Van Nostrand: New York, 1974; p. 141.
7. Lam, R. B.; Leary, J. J., Appl. Spectrosc. 1979, 33, 17-19.
8. Winefordner, J. D.; Schulman, S. G.; O'Haver, T. C., "Luminescence Spectrometry in Analytical Chemistry"; John Wiley and Sons: New York, 1972; pp. 293-4.
9. Holland, J. F., Ph.D. Thesis, Michigan State University, 1971; pp. 97-105.
10. Ohnesorge, W. E., Anal. Chim. Acta 1964, 31, 484-7.
11. Henderson, G., J. Chem. Educ. 1977, 54, 57-9.
12. Lamola, A. A.; Joselow, M.; Yamane, T., Clin. Chem. 1975, 21, 93-7.
13. Griebel, R. J.; Knoblock, E. C.; Koch, T. R., Clin. Chem. 1979, 25, 1983-4.
14. Parker, C. A.; Rees, W. T., Analyst 1962, 87, 83-111.
15. Parker, C. A., Nature 1958, 182, 1002-4.
16. Parker, C. A., Anal. Chem. 1962, 34, 502-5.

17. White, C. E.; Ho, M.; Weimer, E. Q., Anal. Chem. 1960, 32, 438-40.
18. Rosen, P.; Edelman, G. M., Rev. Sci. Instr. 1965, 36, 809-15.
19. Argauer, R.; White, C. E., Anal. Chem. 1964, 36, 368-71.
20. Witholt, B.; Brand, L., Rev. Sci. Instr. 1968, 39, 1271-8.
21. Parker, C. A.; Rees, W. T., Analyst 1960, 85, 587-600.
22. Gill, J. E., Photochem. Photobiol. 1969, 9, 313-22.
23. Parker, C. A.; Barnes, W. J., Analyst 1957, 82, 606-20.
24. Demas, J. N.; Crosby, G. A., J. Phys. Chem. 1971, 75, 991-1024.
25. Lloyd, J. B. F., Nature, Phys. Sci. 1971, 231, 64-5.
26. John, P.; Soutar, I., Anal. Chem. 1976, 48, 520-4.
27. Lloyd, J. B. F., Analyst 1975, 100, 82-95.
28. Lloyd, J. B. F., J. Forensic Sci. Soc. 1971, 11, 235.
29. Lloyd, J. B. F., J. Forensic Sci. Soc. 1971, 11, 531.
30. Lloyd, J. B. F., J. Forensic Sci. Soc. 1972, 12, 83.
31. Vo Dinh, T., Anal. Chem. 1978, 50, 396-401.
32. Lloyd, J. B. F.; Evett, I. W., Anal. Chem. 1977, 49, 1710-15.
33. Latz, H. W.; Ullman, A. H.; Winefordner, J. D., Anal. Chem. 1978, 50, 2148-9.
34. Lloyd, J. B. F., Anal. Chem. 1980, 52, 189-91.
35. Latz, H. W.; Ullman, A. H.; Winefordner, J. D., Anal. Chem. 1980, 52, 191.
36. White, J. U., Anal. Chem. 1976, 48, 2089-92.
37. Ellis, D. W., J. Chem. Educ. 1966, 43, 259-61.
38. Birks, J. B., J. Res. Natl. Bur. Stand. Sect. A 1976, 80, 389-99.
39. McDonald, R. J.; Selinger, B. K., Photochem. Photobiol. 1971, 14, 753-7.
40. Berlman, I. B. "Handbook of Fluorescence Spectra of Aromatic Molecules"; Academic Press: New York, 1971; p. 35.

41. Melhuish, W. H., J. Phys. Chem. 1961, 65, 229-35.
42. Budo, A.; Dombi, J.; Szollosy, L., Acta Phys. et. Chem. Szeged. 1956, 2, 18.
43. Chen, R. F.; Hayes, J. E., Jr., Anal. Biochem. 1965, 13, 523-9.
44. Mitchell, D. G.; Garden, J. S.; Aldous, K. M., Anal. Chem. 1976, 48, 2275-7.
45. Wirth, M. J.; Lytle, F. E., Anal. Chem. 1977, 49, 2054-7.
46. Weber, K., Z. Elektrochem. 1930, 36, 26-36.
47. Sen-Gupta, S. B., J. Indian Chem. Soc. 1938, 15, 263-73.
48. Ghosh, I. C.; Sen-Gupta, S. B., Z. Phys. Chem. 1938, B41, 117-41.
49. Rollefson, G. K.; Dodgen, H. W., J. Chem. Phys. 1944, 12, 107-11.
50. van Slageren, R.; den Boef, G.; van der Linden, W. E., Talanta 1973, 20, 501-12.
51. Förster, T., "Fluoreszenz Organischer Verbindungen"; Vandenhoeck-Ruprecht: Göttingen, Germany, 1951.
52. Budo, A.; Ketskemety, I., J. Chem. Phys. 1956, 25, 595-6.
53. Budo, A.; Ketskemety, I., Acta Phys. 1957, 7, 207-23.
54. Budo, A.; Dombi, J.; Horvai, R., Acta Phys. et. Chem. Szeged. 1957, 3, 3-15.
55. Dombi, J.; Hevesi, J.; Horvai, R. Acta Phys. et. Chem. Szeged. 1959, 5, 20.
56. Melhuish, W. H., J. Res. Natl. Bur. Stand. Sect. A 1972, 76, 547-60.
57. Birks, J. B., Phys. Rev. 1954, 94, 1567-73.
58. Rohatgi, K. K.; Singhal, G. S., Anal. Chem. 1962, 34, 1702-6.
59. Rohatgi, K. K.; Singhal, G. S., Photochem. Photobiol. 1968, 7, 361-7.
60. Alan Mode, V.; Sisson, D. H., Anal. Chem. 1974, 46, 200-3.
61. Braunsberg, H.; Osborn, S. B., Anal. Chim. Acta 1952, 6, 84-95.
62. Lauer, J. L., J. Opt. Soc. Amer. 1951, 41, 482-3.

63. Thomas, J. F.; Mukai, M.; Tebbens, D. B., Natl. Cancer Inst. Monogr. 1962, 9, 127-33.
64. St. John, P. A.; McCarthy, W. J.; Winefordner, J. D., Anal. Chem. 1966, 38, 1828-35.
65. Kolb, A. C.; Streed, E. R., J. Chem. Phys. 1952, 20, 1872-8.
66. Leese, R. A.; Wehry, E. L., Anal. Chem. 1978, 50, 1193-7.
67. Gill, J. E., Appl. Spectrosc. 1970, 24, 588-90.
68. Kelly, P. M., Ph.D. Thesis, Michigan State University, 1976; pp. 20-46.
69. Novak, A. Coll. Czech. Chem. Comm. 1978, 43, 2869-78.
70. Reference 8, pp. 324-7.
71. Holland, J. F.; Teets, R. E.; Timnick, A., Anal. Chem. 1973, 45, 145-53.
72. Britten, A.; Archer-Hall, Jr.; Lockwood, G., Analyst 1978, 103, 928-36.
73. Christmann, D. R.; Crouch, S. R.; Holland, J. F.; Timnick, A. Anal. Chem. 1980, 52, 291-5.
74. Hoyt, S. D.; Ingle, J. D., Jr., Anal. Chem. 1976, 48, 232-4.
75. Joseph, M., Ph. D. Thesis, Michigan State University, 1979; pp. 46-60.
76. Milham, P. J.; Hudson, A. W.; Maquire, M. J.; Haddad, K. S.; Short, C. C., Appl. Spectrosc. 1979, 33, 298-300.
77. Goon, E.; Petley, J. E.; McMullen, W. H.; Wiberly, S. E., Anal. Chem. 1953, 25, 608-10.
78. Noll, C. A.; Stefanelli, L. J., Anal. Chem. 1963, 35, 1914-16.
79. Reference 40, p. 410.

APPENDICES

APPENDIX A

THE IM6100 PROM MONITOR

A. Introduction

The IM6100 PROM monitor is a simple software operating system developed at Michigan State University for the PCM-12 microcomputer when it is configured in the mini-microcomputer network described in Chapter V. The system program consists of three parts: a transparent mode, a binary loader, and a simple keyboard monitor routine. The function and operation of each of these programs has been described previously in Chapter V and by Joseph (75).

In its original development, the IM6100 PROM monitor was designed to fit into 256 12-bit words of programmable read-only-memory (PROM) and to support the operation of a microcomputer equipped with 4096 words (4K) of random-access-memory (RAM). However, for the work described in this dissertation it was necessary to add another 4K of RAM to the microcomputer to supply temporary storage for the large amount of data collected in a spectral record. This introduced the necessity of setting the microcomputer instruction and data fields with keyboard commands, an operation beyond the capability of the original monitor. To overcome this problem, the system program was expanded to a length of 324 instructions to

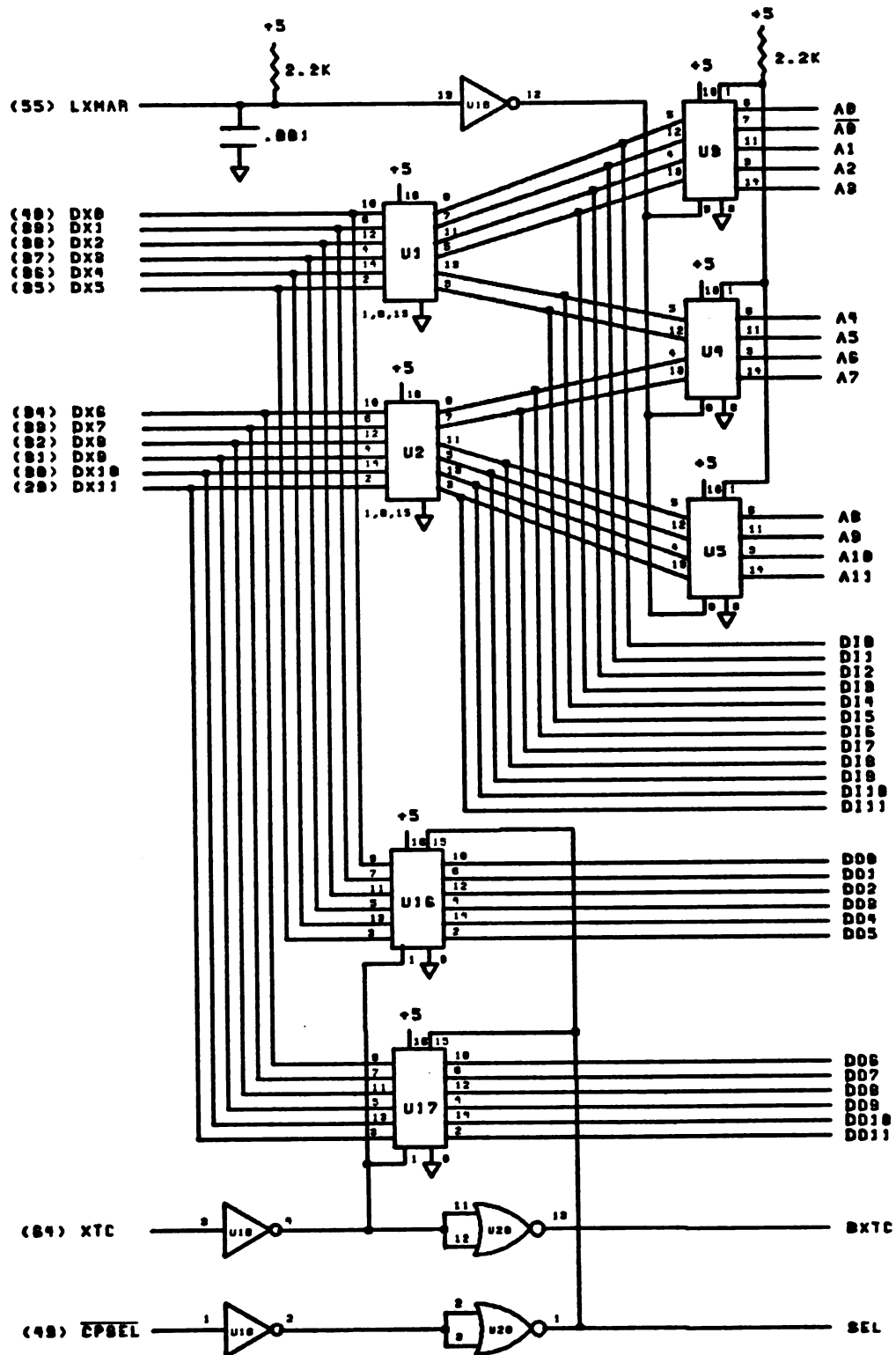
include field setting capability and several other features. The PROM monitor hardware was redesigned to accommodate the expanded system program and any future expansions up to a length of 2048 instructions. In this Appendix, both the hardware and software design of the new IM6100 PROM monitor are documented. For a better understanding of this discussion, the reader is referred to the PCM-12 System Operating Manual published by Pacific Cyber/Metrix, Inc., San Ramon, CA.

B. Hardware Design and Operation

The hardware required to support the expanded IM6100 PROM monitor is contained on a single printed circuit (PC) board. Detailed diagrams of the circuitry are shown in Figures A1, A2, and A3. The identity of the circuit components and their location on the PC board are given in Table A1 and Figure A4, respectively.

1. Memory and Decoding Circuitry

The IM6100 PROM monitor board contains three 1K x 8-bit arrays of erasable programmable read-only-memory (EPROM), devices U8-U10. Because of the action of decoding devices U6, U19, and U20 the EPROMs occupy the octal memory space 4000-7777. Device U8 contains the least significant eight bits of the memory locations 4000-5777, and device U10 contains the least significant eight bits of the memory locations 6000-7777. The most significant four bits of each of these memory sectors are contained in device U9. EPROM U9 is



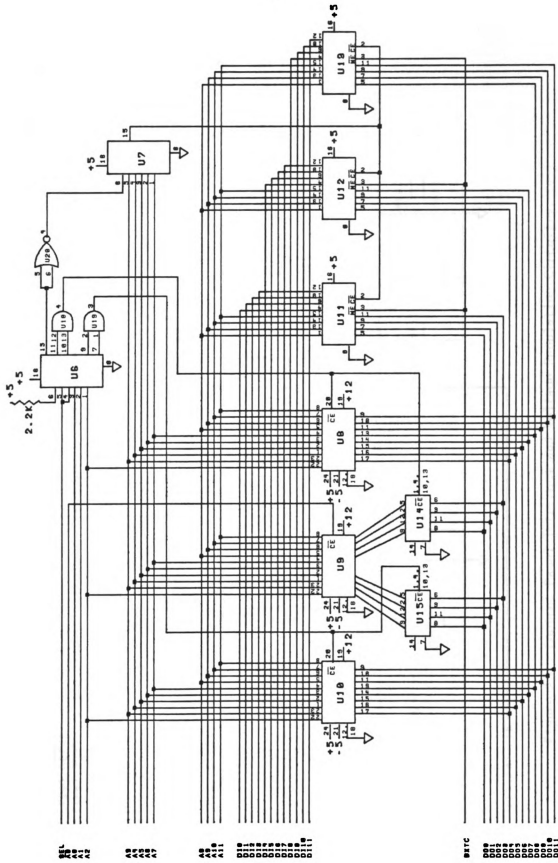


Figure A2. PROM Board Memory and Decoding Circuitry

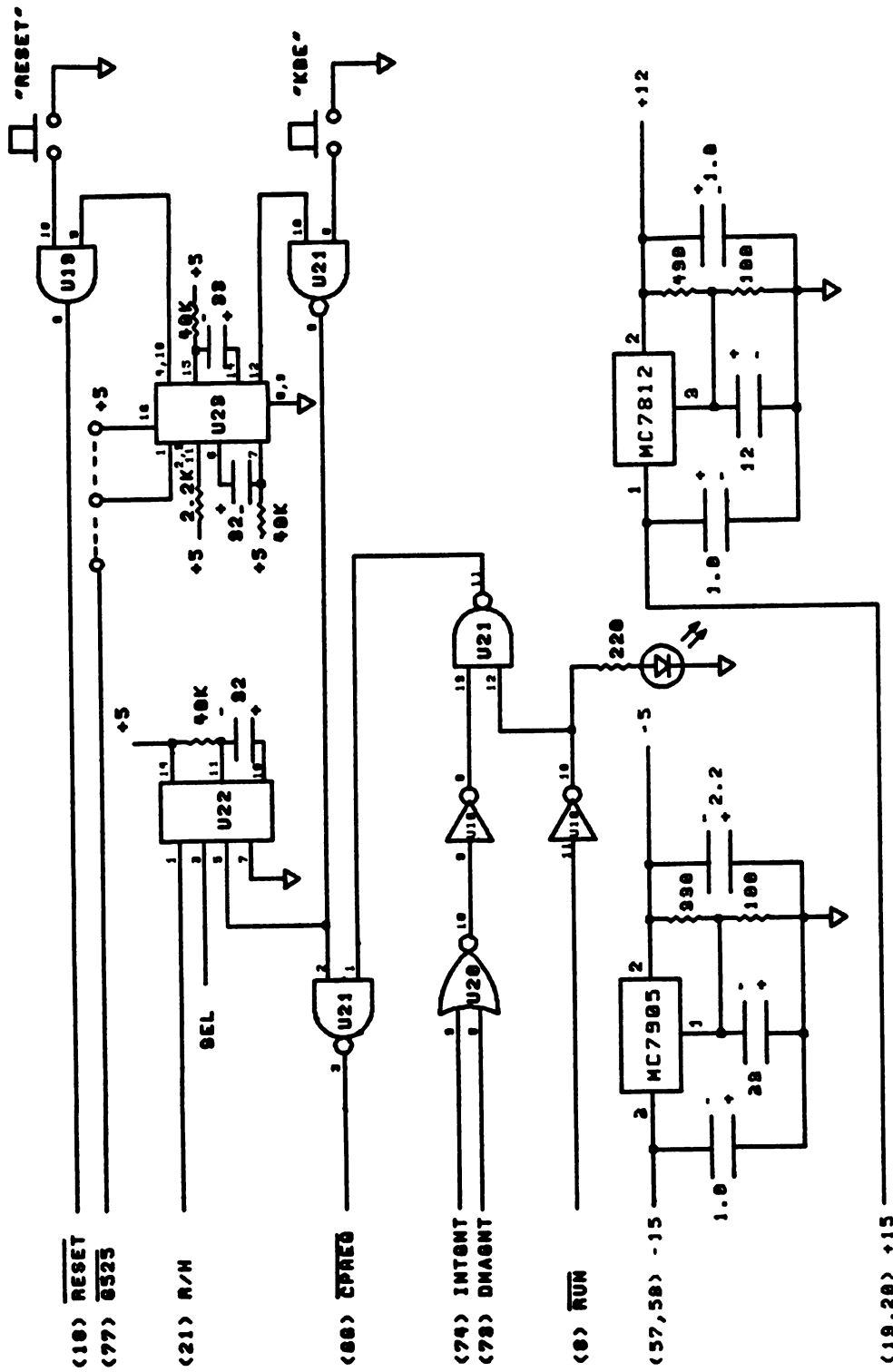


Figure A3. Control Panel Interrupt and Voltage Regulation Circuitry.

Table A1. Identity of Circuit Components in Figures A1-A4.

Circuit Symbol	Device Identity	
U1, U2	74LS366	Tri-state Hex Buffers
U3, U4, U5	74175	Tri-state Quad D Flip-Flops
U6, U7	74LS138	Decoder
U8, U9, U10	2708	Erasable Programmable Read-Only-Memory
U11, U12, U13	7489	64-Bit Read/Write Memory
U14, U15	74125	Tri-state Quad Buffer
U16, U17	74365	Tri-state Hex Buffer
U18	7404	Hex Inverter
U19	7408	Quad 2-Input AND Gate
U20	7402	Quad 2-Input NOR Gate
U21	7403	Quad 2-Input NAND Gate
U22	74121	Monostable Multivibrator
U23	74123	Dual Monostable Multivibrator

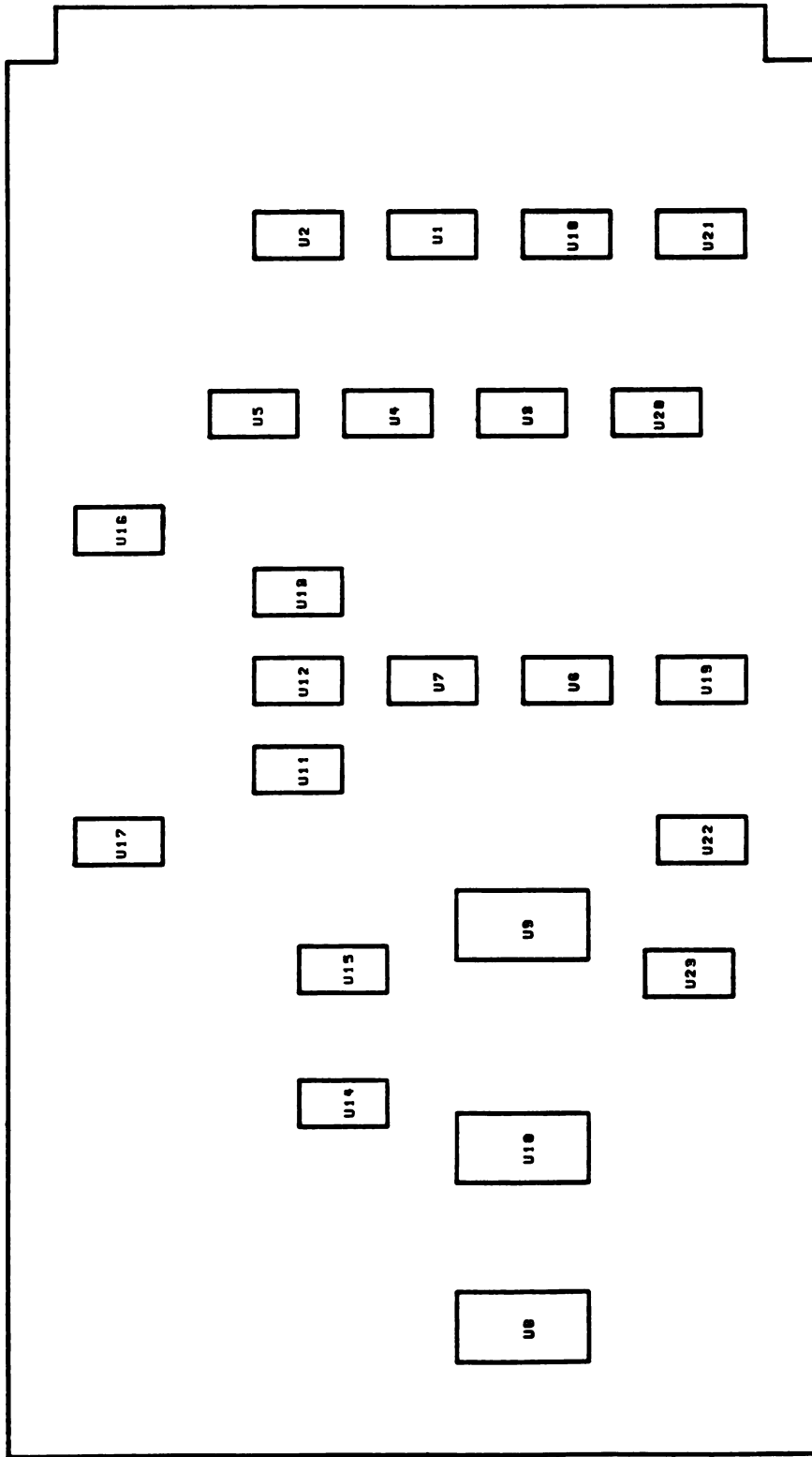


Figure A4. PROM Board Component Layout

enabled by address line $\overline{A0}$, and therefore by any address in the octal memory space 4000-7777. Only four bits of its memory contents are accessed at one time, however, because of the action of tri-state buffers U14 and U15. When addresses of the form 4XXX and 5XXX are decoded, EPROMs U9 and U10 and buffer U15 are enabled. When addresses of the form 6XXX and 7XXX are decoded, EPROMs U8 and U9 and buffer U14 are enabled. In this manner, 2048 12-bit words of EPROM are obtained from only three memory devices.

The PROM monitor board also contains 16 words of RAM for scratch pad operations by the monitor. This memory is arranged in three 16 x 4-bit arrays, devices U11-U13. Device U11 contains the most significant four bits of memory. Device U13 contains the least significant four bits. Devices U6, U20, and U7 enable the RAM for read and write operations when addresses 0000-0017 are decoded.

2. Read and Write Operation

The manner in which the IM6100 CPU reads from and writes into the memory on the PROM board can be understood by referring to Figures A1 and A2. When power to the microcomputer is on, tri-state buffers U1 and U2 continuously drive the contents of data bus lines DX0-DX11 onto the PROM board where they become data input lines DI0-DI11.. Early in each instruction cycle, a 12-bit memory address is placed on these lines by the IM6100 CPU. At the same time, a pulse is generated on the LXMAR control line. The trailing edge of this pulse latches the address into the D flip-flops U3-U5. If the PROM board memory is to be accessed, a short time later the CPSEL

line is pulsed L0 by the CPU. This causes devices U6, U7, U19, and U20 to decode the address and to enable the appropriate memory devices so that their contents appear on the data output lines D00-D011. During the first half of the instruction cycle the control line XTC is exerted HI. This prevents data from being written into the RAM devices U11-U13 and in combination with CPSEL being L0 enables tri-state buffers U16 and U17 to drive the memory contents onto the DX lines where they are read by the CPU.

If a write operation into the scratch pad RAM is to be carried out, the read sequence described above is first executed but is irrelevant. After the read operation, the CPU exerts the XTC line L0 which write enables the RAM devices U11-U13. A short time later, the data to be stored in memory are placed on the DX lines and CPSEL is exerted L0. If the appropriate memory space is decoded, the chip enable pins of U11-U13 are exerted L0 by U7. The combination of chip enable and write enable signals causes the contents of the DI lines to be transferred into the RAMs.

3. Control Panel Interrupt Circuitry

Memory on the PROM monitor board is selected by the IM6100 CPU over the microcomputer mainframe memory when the CPU exerts the CPSEL line L0 rather than the MEMSEL control line. To enter the PROM monitor the CPSEL line must be activated by issuing a control panel interrupt request to the CPU. This action is carried out by the circuitry shown in Figure A3. When power to the microcomputer is turned on, monostable U23 automatically pulses the RESET control

line L0 for two seconds. This forces the CPU into the HALT state, clears the accumulator, and sets the program counter to 7777. The trailing edge of this pulse triggers another two second logic L0 pulse to the CPREQ line to request the control panel interrupt. The second logic pulse also triggers device U22 to apply a logic L0 pulse to the Run/Halt control line. This forces the CPU into the RUN state beginning at memory location 7777.

If the IM6100 CPU is in the RUN state and is executing instructions from mainframe memory, the PROM monitor can be entered by initiating the sequence described above manually or from program control. The sequence can be initiated manually by pressing the momentary action switches "RESET" and then "KBE" on the PROM board. If pin 1 of device U23 is connected to bus line 77 by a jumper, the PROM monitor entry sequence can also be started by executing a device input/output instruction that is decoded onto line 77 by another interface. A 6525 instruction was used for this purpose in this work. If a device interrupt or direct memory access request is being serviced by the CPU, both of these modes of PROM monitor entry are inhibited.

C. Software Description

The expanded IM6100 PROM monitor software closely resembles the original monitor program developed by Joseph (75). The reader is referred to the original work for a detailed description of the program operation. Features which have been added to the monitor include: 1) the ability to set the microcomputer instruction and

data fields by typing the keyboard command "FN" where N is the octal field number; 2) the ability to open and examine successive and preceeding locations of mainframe memory with the keyboard commands "<" and ">"; and 3) the ability to return to the transparent mode from the local mode by typing the keyboard command "control-T".

A further description of these commands and how they were incorporated into the monitor program is given in the program assembly listing on the following pages.

The monitor software was written in PAL8 assembly language and stored in the file MON.PA. After compiling the program to binary format, it was written into the EPROM devices with the aid of the C. G. Enke 2708 PROM programmer and the RSX-11 version of the program PROM. Since the expanded monitor software required less than 1K of EPROM memory, it was necessary to program only two EPROM chips. Because the program entry point is at location 7777, the program was written into devices U9 and U10 at chip addresses 1000-1777.

```

////////////////////////////////////
/
/      PROM MONITOR FOR IM6100 MICROPROCESSORS      /
/
/      FILE:  MON.PA                                /
/
////////////////////////////////////

7000  ORG=      7000
6136  PDPIN=   6136
6131  PDPISF=  6131
6146  PDPOUT=  6146
6141  PDPOSF=  6141
0000  TEMP=    0
0002  FLDSW=   2
0004  PC=      4
0005  FLDFLG=  5
0006  SUBR=    6
0007  PCSAVE=  7
0010  CHKSN=   10
0011  WORD1=   11
0012  WORD2=   12
0013  BEGSW=   13
0014  RUBCT=   14
0015  BYTSW=   15
0016  FLG=     16
0017  CHAR=    17
/
/TRANSPARENT MODE
/
/SPECIAL CHARACTERS:
/
/      TTY:  CONTROL-A  -> CHAIN TO MONITOR
/
/      MAIN COMPUTER: 200(8)  -> CHAIN TO BINARY LOADER
/

07000 7000  *ORG
07001 7300  MODE1,  CLA CLL          /START OF MODE ONE
07002 1235          TAD K5401        /SET UP FIELD CHANGE SUBROUTINE
07003 3003          DCA FLDSW+1
07004 6031  TTY,    KSF              /TTY HIT?
07005 5216          JMP PDP          /NO; CHECK PDP
07006 6036          KRB              /YES; READ IN
07007 1377          TAD (-201        /CHECK FOR CONTROL-A AT TTY
07008 7450          SNA              /CONTROL-A ?
07009 5633          JMP I XMON        /YES; GO TO MONITOR
07010 1376          TAD (201         /NO; RESTORE CHARACTER
07011 6146          PDPOUT          /SEND TO PDP
07012 6141          PDPOSF          /WAIT PDPOUT FLAG
07013 5213          JMP .-1
07014 5200          JMP MODE1        /LOOK FOR MORE
07015 6131  PDP,    PDPISF          /PDP CHAR?
07016 5203          JMP TTY          /NO; CHECK TTY
07017 6136          PDPIN           /YES; READ IN
07018 1231          TAD M200         /SUBTR 200(8)
07019 7450          SNA              /LEADER-TRAILER?
07020 5634          JMP I XMODE2      /YES; GO TO BIN LOADER
07021 1232          TAD K200         /NO, RESTORE
07022 6046          TLS              /TO TTY
07023 6041          TSF
07024 5226          JMP .-1
07025 5200          JMP MODE1        /LOOK FOR MORE
07026 7600  M200,   -200
07027 0200  K200,   200
07028 7200  XMON,   MON1TR
07029 7600  XMODE2, MODE2
07030 5401  K5401,  5401
07176 0201

```

```

07177 7577
7600
      *7600
      /
      /BINARY LOADER SECTION
      /CHAINS TO MONITOR IF CHECKSUM = 0
      /
07600 7300 MODE2, CLA CLL /FALL THRU TO BIN LOADER
07601 3003 DCA FLDFLG /ENABLE INITIAL FIELD CHANGE
07602 6132 START, 6132 /INITIALIZE READER
07603 6214 RDF /GET CURRENT DATA FIELD
07604 1321 TAD K6201
07605 3002 DCA FLDSW /SET UP FIELD CHANGE SUBROUTINE
07606 7040 CMA /FORM -1
07607 3013 DCA BEGSW /SET BEGINNING-END FLAG
07610 7040 MSBYTE, CMA
07611 3015 DCA BYTSW /SET BYTE FLAG
07612 6131 LSBYTE, PDPISF /WAIT FOR PDP FLAG
07613 5212 JMP LSBYTE
07614 6136 PDPIN /GET A CHARACTER
07615 3000 DCA TEMP /SAVE IT TEMPORARILY
07616 1000 TAD TEMP
07617 2015 ISZ BYTSW
07620 5232 JMP LSSAVE
07621 0324 AND M0300
07622 1300 TAD K7600 /SUBTRACT 200
07623 7510 SPA /2 OR 300 ?
07624 5242 JMP DAORG /NO, MUST BE AN ADDRESS OR AN
      INSTRUCTION
07625 7750 SPA SNA CLA /LT ?
07626 5237 JMP LT /YES
07627 1000 FLDSET, TAD TEMP /NO, MUST BE A FIELD SETTING
07630 0323 AND M0070
07631 1321 TAD K6201
07632 3002 DCA FLDSW
07633 1005 TAD FLDFLG
07634 7650 SNA CLA /HOLD UP ON FIELD CHANGE AT THIS
      POINT
07635 4001 JMS FLDSW-1
07636 5210 JMP MSBYTE
07637 2013 LT, ISZ BEGSW
07640 5311 JMP END
07641 5206 JMP MSBYTE-2
07642 7200 DAORG, CLA
07643 2013 ISZ BEGSW
07644 5236 JMP DEPOST
07645 3010 GO, DCA CHKSM /ADD TO CHECKSUM REGISTER
07646 1000 TAD TEMP
07647 3011 DCA WORD1 /SAVE IT AS WORD1
07650 3015 DCA BYTSW
07651 5212 JMP LSBYTE
07652 3012 LSSAVE, DCA WORD2 /SAVE IT AS WORD2
07653 1011 TAD WORD1
07654 7006 RTL
07655 7006 RTL
07656 7006 RTL
07657 7430 SZL
07660 5263 JMP OVER
07661 7240 STA
07662 3003 DCA FLDFLG
07663 7300 OVER, CLA CLL
07664 3013 DCA BEGSW
07665 5210 JMP MSBYTE
07666 1011 DEPOST, TAD WORD1
07667 7106 CLL RTL
07670 7006 RTL
07671 7006 RTL
07672 1012 TAD WORD2

```



```

07673 7430          SZL
07674 5302          JMP ORIGIN
07675 3404          DCA I PC
07676 4001          JMS FLDSW-1      /EXECUTE FIELD CHANGE
07677 2004          ISZ PC
07700 7600  K7600, 7600      /CLA
07701 5305          JMP CHEX
07702 3004  ORIGIN, DCA PC      /SAVE THE ORIGIN
07703 1004          TAD PC
07704 3007          DCA PCSAVE      /SAVE THE NEW ORIGIN
07705 1011  CHEX,  TAD WORD1
07706 1012          TAD WORD2
07707 1010          TAD CHKSM
07710 5245          JMP GO
07711 1011  END,  TAD WORD1
07712 7002          BSW
07713 1012          TAD WORD2
07714 7041          CIA
07715 1010          TAD CHKSM
07716 7450          SNA      /CHECKSUM ZERO?
07717 5722          JMP I XMN      /YES; CHAIN TO MONITOR
07720 7402  K7402, HLT      /NO; ERROR HALT
07721 6201  K6201,
07722 7200  XMN,  MONITR
07723 0070  M0070, 0070
07724 0300  M0300, 300
/KEYBOARD MONITOR SECTION
/
/THIS SECTION OF THE PROM ROUTINE IS CHAINED TO
/AFTER THE USER TYPES CONTROL-A WHILE IN THE TRANSPARENT
MODE
/OR WHEN A ZERO CHECKSUM IS ENCOUNTERED AFTER DOWNLOADING
/AN ABSOLUTE BINARY PROGRAM FROM THE MAIN COMPUTER.
/
/KEYBOARD MONITOR TYPES A "S" WHEN READY FOR INPUT
/
/INPUT IS OF THE FORM
/
/      NNNNX
/
/WHERE NNNN IS A FOUR DIGIT OCTAL NUMBER
/AND X IS ONE OF THE FOLLOWING CONTROL CHARACTERS
/
/      X = "/" MEANS OPEN LOCATION NNNN AND
/          DISPLAY ITS CONTENTS
/
/      X = "D" MEANS DEPOSIT THE DATA NNNN
/          IN THE LOCATION WHICH IS CURRENTLY
/          OPEN
/
/      X = "G" MEANS BEGIN EXECUTION AT THE
/          ADDRESS NNNN
/
/ONCE A LOCATION HAS BEEN OPENED IN THIS MANNER
/THE FOLLOWING COMMANDS MAY BE USED
/
/      "/" = DISPLAY CONTENTS OF LOCATION WHICH
/          IS CURRENTLY OPEN
/
/      "<" = OPEN PRECEDING LOCATION AND DISPLAY
/          ITS CONTENTS
/
/      ">" = OPEN SUCCEEDING LOCATION AND DISPLAY
/          ITS CONTENTS
/
/      "CONTROL-T" = RETURN TO TRANSPARENT MODE
/

```

/IN ADDITION, THE INSTRUCTION AND DATA FIELDS MAY BE
/SET BY TYPING

/

FN

/WHERE N IS THE OCTAL FIELD NUMBER.

/

/IF ANY COMMAND SEQUENCE OTHER THAN THOSE LISTED ABOVE
/IS TYPED, THE MONITOR RESPONDS WITH A "?" AND IGNORES
/THE COMMAND.

/

07200	7200	*7200	
07200	7300	MONITR, CLA CLL	/START OF THE MONITOR
07201	1326	TAD C7205	/SET UP FOR "JMS"
07202	3006	DCA SUBR	
07203	1330	TAD C7215	/OUTPUT A CR
07204	5750	JMP I XTYPE	
07205	1327	TAD C7211	
07206	3006	DCA SUBR	
07207	1331	TAD LF	/AND A LINE FEED
07210	5750	JMP I XTYPE	
07211	1330	TAD C7215	
07212	3006	DCA SUBR	
07213	1332	TAD DOLLAR	/DOLLAR SIGN
07214	5750	JMP I XTYPE	
07215	3016	DCA FLC	
07216	1325	TAD C7221	
07217	3006	DCA SUBR	
07220	5746	JMP I XREAD	/INPUT AN OCTAL NUMBER
07221	7012	RTR	
07222	7012	RTR	
07223	3000	DCA TEMP	/BITS 0-2
07224	1331	TAD LF	
07225	3016	DCA FLC	
07226	1333	TAD C7231	
07227	3006	DCA SUBR	
07230	5746	JMP I XREAD	/INPUT
07231	7002	BSW	/BITS 3-5
07232	1000	TAD TEMP	/COMBINE
07233	3000	DCA TEMP	
07234	1334	TAD C7237	
07235	3006	DCA SUBR	
07236	5746	JMP I XREAD	
07237	7006	RTL	
07240	7004	RAL	/BITS 6-8
07241	1000	TAD TEMP	
07242	3000	DCA TEMP	
07243	1335	TAD C7246	
07244	3006	DCA SUBR	
07245	5746	JMP I XREAD	/BITS 9-11
07246	1000	TAD TEMP	
07247	3000	DCA TEMP	
07250	6031	KSF	
07251	5250	JMP .-1	
07252	6036	KRB	/NOW GET CONTROL CHAR
07253	6046	TLS	
07254	6041	TSF	
07255	5254	JMP .-1	
07256	1337	TAD MD	/SUBTRACT "D"
07257	7450	SNA	/ "D" ?
07260	5751	JMP I XSTORE	/YES; DEPOSIT
07261	1340	TAD M3	/NO, "C"?
07262	7450	SNA	
07263	5752	JMP I XEXEC	/YES; BEGIN EXECUTION
07264	1342	TAD C30	/NO, "/"?
07265	7650	SNA CLA	
07266	5274	JMP .+6	

07267	1341	QM,	TAD C277	/NO, TYPE "?" AND RESTART
07270	6046		TLS	
07271	6041		TSF	
07272	5271		JMP .-1	
07273	5200		JMP MONITR	
07274	1000		TAD TEMP	/YES, DISPLAY CONTENTS
07275	3007		DCA PCSAVE	/FROM MAINFRAME MEMORY
07276	1336	DSPLAY,	TAD C7304	
07277	3006		DCA SUBR	
07300	1407		TAD I PCSAVE	
07301	7006		RTL	
07302	7006		RTL	
07303	5747		JMP I XOUT	/DISPLAY BITS 0-2
07304	1343		TAD C7311	
07305	3006		DCA SUBR	
07306	1407		TAD I PCSAVE	
07307	7002		BSW	
07310	5747		JMP I XOUT	/DISPLAY BITS 3-5
07311	1344		TAD C7317	
07312	3006		DCA SUBR	
07313	1407		TAD I PCSAVE	
07314	7012		RTR	
07315	7010		RAR	
07316	5747		JMP I XOUT	/DISPLAY BITS 6-8
07317	1345		TAD C7323	
07320	3006		DCA SUBR	
07321	1407		TAD I PCSAVE	
07322	5747		JMP I XOUT	/DISPLAY BITS 9-11
07323	5200		JMP MONITR	
07324	7477	XFLDCHG,	FLDCHG	
07325	7221		C7221, 7221	
07326	7205		C7205, 7205	
07327	7211		C7211, 7211	
07330	7215		C7215, 7215	
07331	0212		LF, 212	
07332	0244	DOLLAR,	244	
07333	7231		C7231, 7231	
07334	7237		C7237, 7237	
07335	7246		C7246, 7246	
07336	7304		C7304, 7304	
07337	7474	MD,	-304	
07340	7775	M3,	-3	
07341	0277		C277, 277	
07342	0030		C30, 30	
07343	7311		C7311, 7311	
07344	7317		C7317, 7317	
07345	7323		C7323, 7323	
07346	7407	XREAD,	READ	
07347	7400	XOUT,	OUT	
07350	7472	XTYPE,	TYPE	
07351	7515	XSTORE,	STORE	
07352	7520	XEXEC,	EXEC	
	7400		*7400	
07400	0325	OUT,	AND C0007	/BITS 9-11 ONLY
07401	1327		TAD C260	/MAKE IT ASCII
07402	6046		TLS	
07403	6041		TSF	
07404	5203		JMP .-1	
07405	7300		CLA CLL	
07406	5406		JMP I SUBR	/RETURN
07407	6031	READ,	KSF	
07410	5207		JMP .-1	
07411	6036		KRB	/INPUT A CHARACTER
07412	6046		TLS	/ECHO
07413	6041		TSF	
07414	5213		JMP .-1	
07415	3017		DCA CHAR	

07416	1017	TAD CHAR	
07417	0330	AND C177	/JUST 7 BITS
07420	1331	TAD M60	/LOWEST OCTAL NUMBER
07421	7510	SPA	
07422	5230	JMP .+6	/NOT AN OCTAL NUMBER, IS IT A VALID
	COMMAND?		
07423	1332	TAD M10	
07424	7500	SMA	
07425	5230	JMP .+3	/NOT AN OCTAL NUMBER, IS IT A VALID
	COMMAND?		
07426	1333	TAD C10	/RESTORE
07427	5406	JMP I SUBR	/RETURN
07430	7200	CLA	
07431	1016	TAD FLG	/ONE OCTAL NUMBER MUST BE FOLLOWED
			/BY THREE MORE
07432	7440	SZA	
07433	5736	JMP I XQM	
07434	1017	TAD CHAR	
07435	1322	TAD M257	/IS IT A "/"?
07436	7450	SNA	
07437	5735	JMP I XDSPLAY	/YES, DISPLAY CONTENTS
07440	1323	TAD M15	/NO, IS IT A "<"?
07441	7440	SZA	
07442	5247	JMP .+5	
07443	7240	STA	/YES, OPEN PRECEDING LOCATION
07444	1037	TAD PCSAVE	
07445	3007	DCA PCSAVE	
07446	5735	JMP I XDSPLAY	/DISPLAY CONTENTS
07447	1324	TAD M2	/NO, IS IT A ">"?
07450	7440	SZA	
07451	5256	JMP .+5	
07452	2007	ISZ PCSAVE	/YES, OPEN NEXT LOCATION
07453	7000	NOP	
07454	7200	CLA	
07455	5735	JMP I XDSPLAY	/DISPLAY CONTENTS
07456	1332	TAD M10	/NO, IS IT AN "F"?
07457	7450	SNA	
07460	5277	JMP FLDCHG	/YES, CHANGE FIELDS
07461	7200	CLA	/NO, IS IT CONTROL-T?
07462	1017	TAD CHAR	
07463	1340	TAD M224	
07464	7450	SNA	
07465	5270	JMP .+3	/YES, RETURN TO TRANSPARENT MODE
07466	7200	CLA	/NO, TYPE QUESTION MARK AND IGNORE
	COMMAND		
07467	5736	JMP I XQM	
07470	1341	TAD C215	/PROMPT TO OS/8 MONITOR
07471	5737	JMP I XMODE1	
07472	6046	TYPE, TLS	/OUTPUT A CHARACTER
07473	6041	TSF	
07474	5273	JMP .-1	
07475	7300	CLA CLL	
07476	5406	JMP I SUBR	
07477	6031	FLDCHG, KSF	
07500	5277	JMP .-1	
07501	6036	KRB	/GET FIELD NUMBER
07502	6046	TLS	/ECHO IT
07503	6041	TSF	
07504	5303	JMP .-1	
07505	0325	AND C0007	/BITS 9-11 ONLY
07506	7100	CLL	
07507	7004	RAL	
07510	7006	RTL	
07511	1326	TAD K6203	
07512	3002	DCA FLDSW	/FORM CDF CIF COMMAND
07513	4001	JMS FLDSW-1	/EXECUTE FIELD CHANGE
07514	5734	JMP I XMONITR	

```

07515 1090 STORE, TAD TEMP /GET THE DATA
07516 3407 DCA I PCSAVE /DEPOSIT INTO MAINFRAME MEMORY
07517 5734 JMP I XMONITR /RESTART
07520 6001 EXEC, ION /REQUIRED TO LEAVE CP MEMORY
07521 5400 JMP I TEMP /CHAIN TO MAINFRAME MEMORY
07522 7521 M257, -257
07523 7763 M15, -15
07524 7776 M2, -2
07525 0007 C0007, 7
07526 6203 K6203, 6203
07527 0260 C260, 260
07530 0177 C177, 177
07531 7720 M60, -60
07532 7770 M10, -10
07533 0010 C10, 10
07534 7200 XMONITR, MONITR
07535 7276 XDSPLAY, DSPLAY
07536 7267 XQM, QM
07537 7012 XMODE1, PDP-4
07540 7554 M224, -224
07541 0215 C215, 215
/
/ACTUAL CONTROL-PANEL INTERRUPT ENTRY POINT = 7777
/
7776 7776 *7776
07776 7000 STRT, MODE1
07777 5776 JMP I STRT
/
      S      S      S      S      S      S      S

```

APPENDIX B

MICROCOMPUTER CONTROL OF THE FLUORIMETER

A. Introduction

As discussed in Chapter V, the absorption-corrected spectrofluorimeter constructed in this work for study of the cell shift method is controlled by an Intersil IM6100 microcomputer. Control is accomplished through three distinct electronic interfaces: a data acquisition interface; a cell positioner control interface; and a monochromator control interface. Both the design and operation of these circuits are described on the following pages. The reader is again referred to the PCM-12 System Operation Manual (Pacific Cyber/Metrix, Inc., San Ramon, CA) for a deeper understanding of the diagrams and discussion presented. The hardware description is followed by a description of the microcomputer software developed to operate the interfaces and to transmit data to the minicomputer. A description of the minicomputer software developed to process the raw fluorescence data concludes this appendix.

B. Hardware Design and Operation

1. Circuit Layout

The microcomputer-fluorimeter interface circuits are constructed primarily on two printed circuit cards which plug into the IM6100 data and control bus plane. A third interface card is also used, but contains only the radiation chopper monitoring circuitry. To simplify the interface circuits and to reduce the number of electronic components required, all I/O instruction decoding is performed on the interface card that contains the analog-to-digital converter (ADC). The decoded device select signals for the cell positioner and monochromator control circuits are fed from this card onto unused lines of the IM6100 bus plane where they are picked up by the other interface cards.

2. Instruction Decoding

Figures B1 and B2 illustrate the decoding circuitry for the entire microcomputer-fluorimeter interface. The identities of the electronic components shown are given in Table B1. Data bus lines DX0-DX11 are continuously buffered onto the ADC card by tri-state drivers U1 and U2. Early in the device I/O instruction cycle, the IM6100 CPU places the 12-bit I/O instruction on these lines and pulses the LXMAR control line HI. The trailing edge of the LXMAR pulse latches the instruction into D flip-flops U7 and U8. A short time later, the DEVSEL line is pulsed LO enabling devices U9-U11 to decode the nine least significant bits of the instruction.

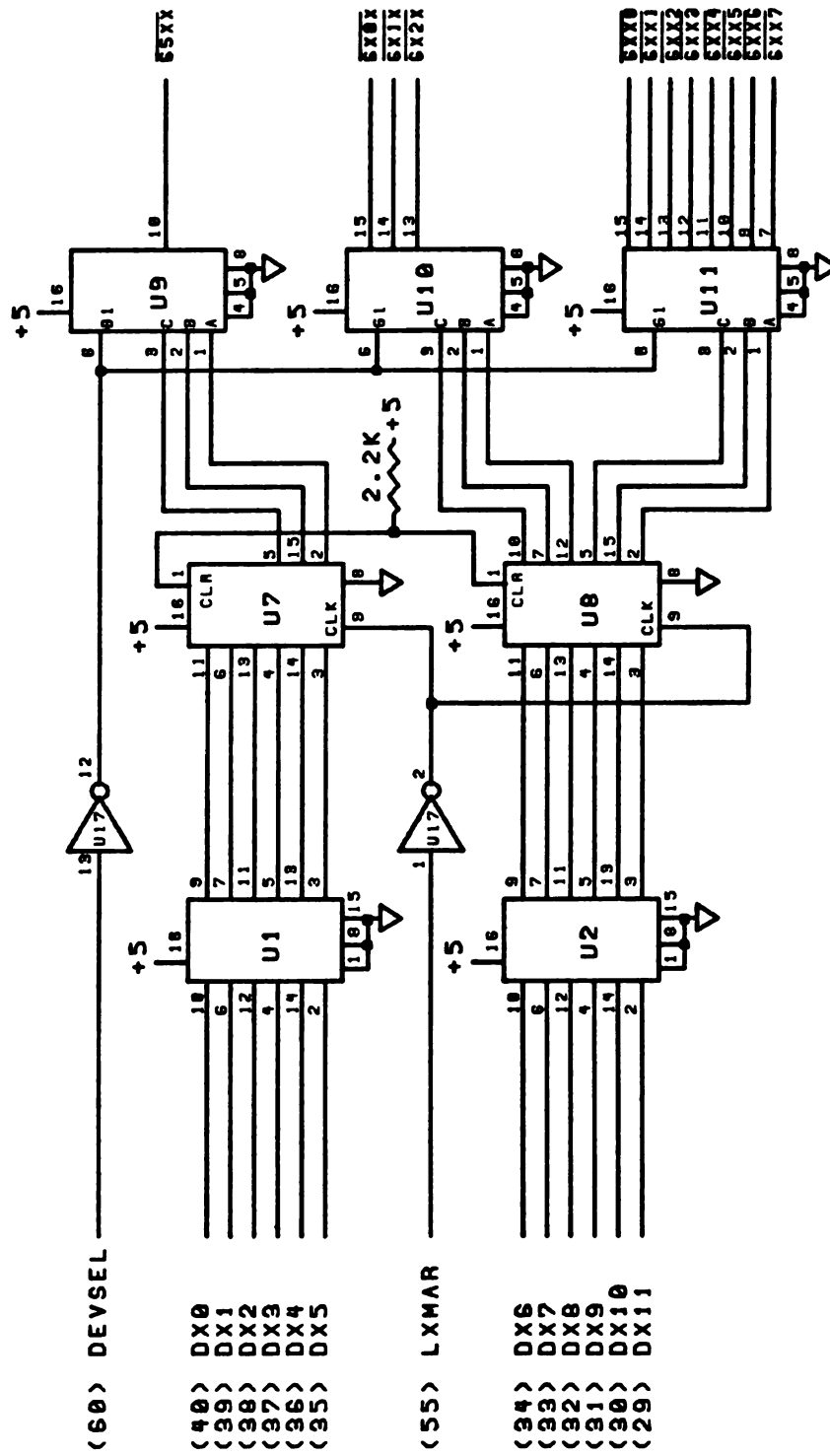


Figure B1. I/O Instruction Decoding Circuitry

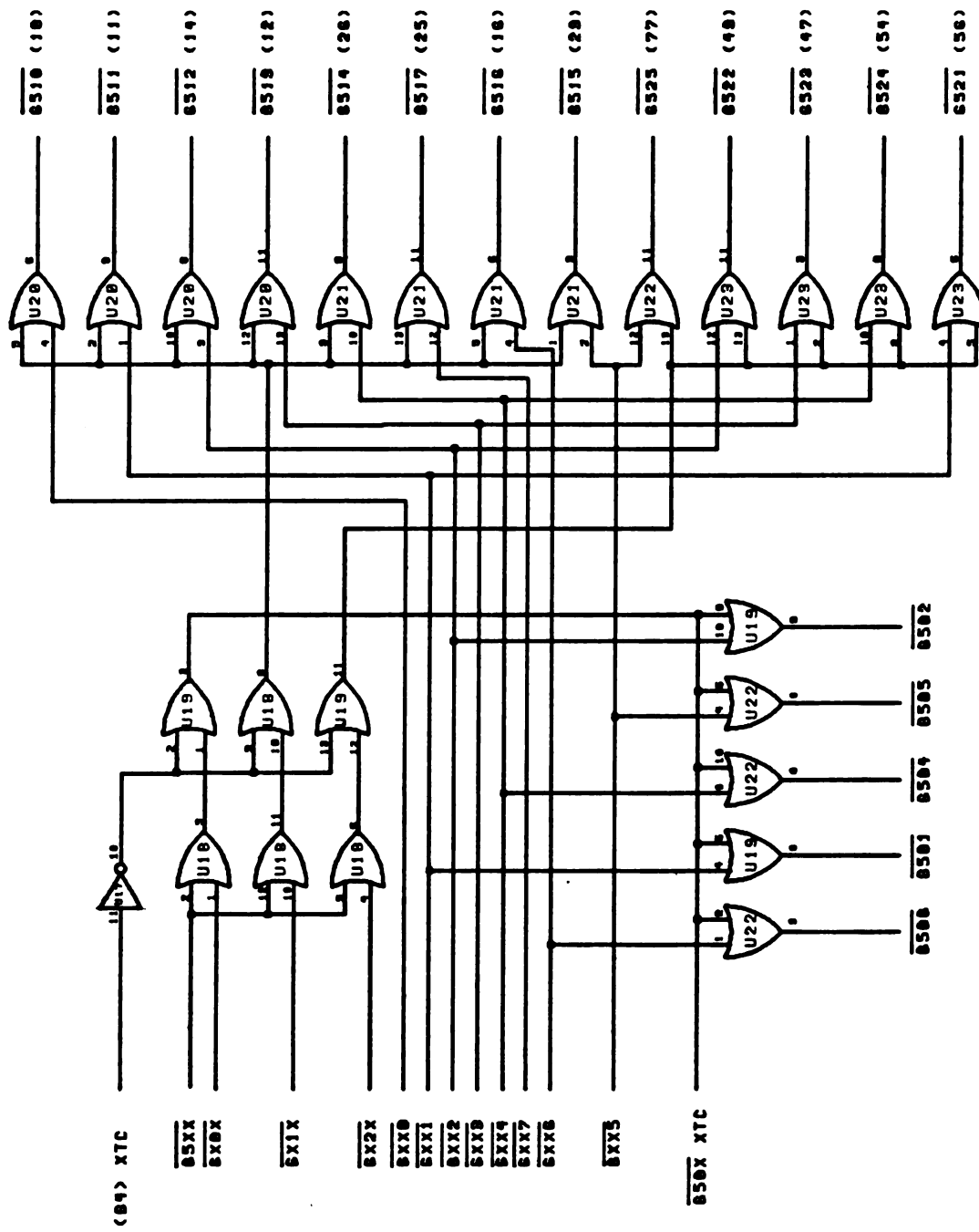


Figure B2. Device Select Circuitry

Table B1. Identity of Interface Circuit Components.

Circuit Symbol	Device Identity	
U1-U6, UE-UH, UK	74LS365	Hex Tri-state Buffer
U7, U8	74LS174	Hex D Flip-Flop
U9-U11	74LS138	Decoder
U12, U13	DG191 or IH5043	Dual SPDT FET SWITCH
U14	74123	Dual Monostable Multivibrator
U15	7474	Dual D Flip-Flop
U16	Burr Brown ADC80AG-12 12 Bit Analog-to-Digital Converter	
U17	74LS04	Hex Inverter
U18-U23	7432	Quad 2-Input OR Gate
UA-UD	7473	Dual J-K Flip-Flop
UI	7408	Quad 2-Input AND Gate
UJ	7417	Hex Open Collector Buffer
OA1-OA3, AM1-AM3	LF351 or CA3140	BiMOS Op Amp

The three most significant bits are decoded within the CPU and used to generate the DEVSEL pulse.

All I/O instructions that operate the fluorimeter interfaces are of the form 65NM where N = 0, 1 or 2 and M = 0, 1, ... 7. The instructions are fully decoded by the OR gates on the appropriate outputs of decoders U9-U11 as shown in Figure B2. Because the CPU executes the sequence described above twice during each I/O instruction cycle, first with XTC exerted HI and then with XTC exerted LO, the signal $\overline{\text{XTC}}$ is ORed with the decoded device select signals so that the interfaces will be activated only once by each I/O instruction that is executed. All decoded device select signals are active LO. The instructions that operate the fluorimeter interfaces and the actions they initiate are summarized in Table B2.

3. Data Acquisition

a. Signal Conditioning - Photocurrents from the fluorescence and reference detectors are converted to voltages, amplified, and filtered with the amplifier circuit shown in Figure B3. The circuit components are listed in Table B1. Identical amplifiers are used in each signal channel. The input stage of the amplifiers is a simple current-to-voltage converter with a transfer function of 10^6 V/A. The second stage is an inverting amplifier with variable gain in decades from 10^{-1} to 10^4 . The output stage is a unity gain inverting amplifier-first order active low pass filter with a variable time constant from 5 μ s to 150 ms. The overall transfer function of the amplifiers is variable from 10^5 to 10^{10} V/A in

Table B2. I/O Instructions for the Fluorimeter.

Octal Code	Action Initiated
6501	Set S/H to HOLD mode and start A-to-D conversion
6502	Skip on end of A-to-D conversion
6503	Jam transfer ADC result into the accumulator
6504	Set multiplexer to reference channel
6505	Set multiplexer to fluorescence channel
6506	Set S/H to SAMPLE mode
6510	Skip on Y position encoder L0
6511	Skip on X position encoder L0
6512	Reverse power to Y motor ON/OFF
6513	Forward power to Y motor ON/OFF
6514	Forward power to X motor ON/OFF
6515	Reverse power to X motor ON/OFF
6516	Skip on Y origin encoder L0
6517	Skip on X origin encoder L0
6521	Set/Clear scan flip-flop
6522	Enable/Disable emission scan
6523	Enable/Disable excitation scan
6524	Skip on radiation chopper encoder L0
6525	Initiate control panel interrupt to enter PROM monitor

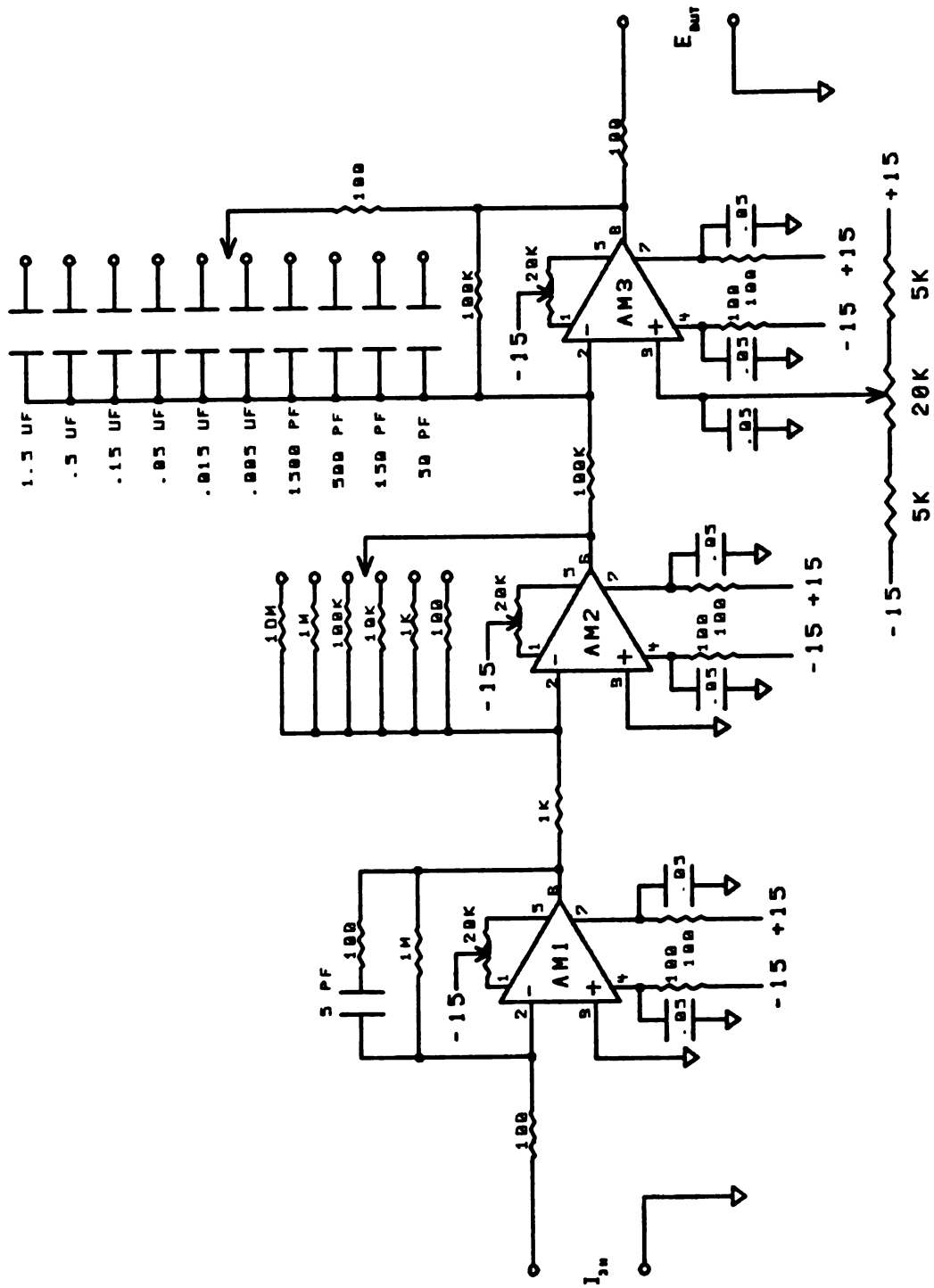


Figure B3. Photocurrent Amplifier Circuitry

decades and is typically set at 10^7 V/A for the reference channel and at 10^9 V/A for the fluorescence channel. The potentiometer in the output stage can be used to offset the amplifier outputs continuously from about -12 to +12 V to accommodate the input window of the analog-to-digital converter. Currently this window is -2.5 to +2.5 V. A time constant of 50 μ s is used in each signal channel to pass the 500 Hz modulated signals with a minimum of distortion.

b. Sample-and-Hold and Multiplexing Circuitry - After amplification and filtering, the reference and fluorescence signals are passed to dual synchronously gated sample-and-hold (S/H) circuits and a two channel multiplexer shown in Figure B4. Initially, when power to the microcomputer is turned on, outputs Q1 and Q2 of flip-flop U15 are cleared. This sets the multiplexer to the reference channel and the S/H to the HOLD mode. To sample the reference and fluorescence signals, a 6506 instruction is executed. This reverses the state of output Q1 and closes FET switches 1 and 2 of device U13. Execution of a 6501 instruction clears output Q1 of U15 to enter the HOLD mode. The 6501 instruction also triggers monostable U14 to issue a 700 ns logic HI pulse to the ADC to initiate analog-to-digital conversion. This pulse is issued after a 4 μ s delay to allow the S/H circuits to settle. The acquisition time of the S/H circuit is estimated to be about 1 μ s for a 5 V step signal to an accuracy of about one percent. Since the average device I/O instruction time of the IM6100 CPU is 8.5 μ s, the speed of these circuits is more than sufficient for use with the microcomputer.

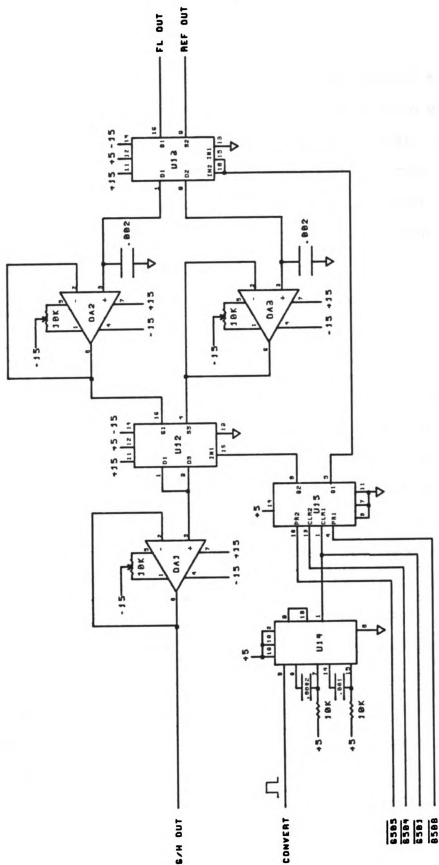


Figure B4. Sample-and-Hold and Multiplexer Circuitry

Multiplexing of the S/H outputs to the ADC is accomplished with FET switches 1 and 3 of device U12. Execution of a 6506 instruction forces output Q2 of flip-flop U15 HI which opens switch 3 and closes switch 1 to pass the fluorescence signal. Execution of a 6504 instruction clears output Q2 of U15 and reverses the states of the switches to pass the reference signal. Follower OA1 is necessary to prevent an IR voltage drop across the switches. The settling time of the multiplexer is about 1 μ s, and so, poses no problem for use with the microcomputer.

c. Analog-to-Digital Conversion - Figure B5 shows the circuit used for analog-to-digital conversion of the signals from the fluorimeter. After receiving the CONVERT pulse from monostable U14, the ADC (U16) requires 25 μ s to complete the digital conversion. At the end of the conversion, the EOC output is exerted L0. After starting the conversion, the microcomputer is programmed to execute 6502 instructions in a program loop to test for the end of conversion. The first 6502 instruction executed after EOC goes L0 enables tri-state buffer U6 to exert the SKP line L0 causing the CPU to exit from the end of conversion test loop. The result of the conversion is read by the CPU when a 6503 instruction is executed. Buffers U3 and U4 are enabled by this instruction to drive the contents of the ADC outputs into the DX lines, and buffer U5 exerts control lines C0 and C1 L0 and line C2 HI to cause the contents of the DX lines to be jam transferred into the IM6100 accumulator.

Because the reference and fluorescence signals from the

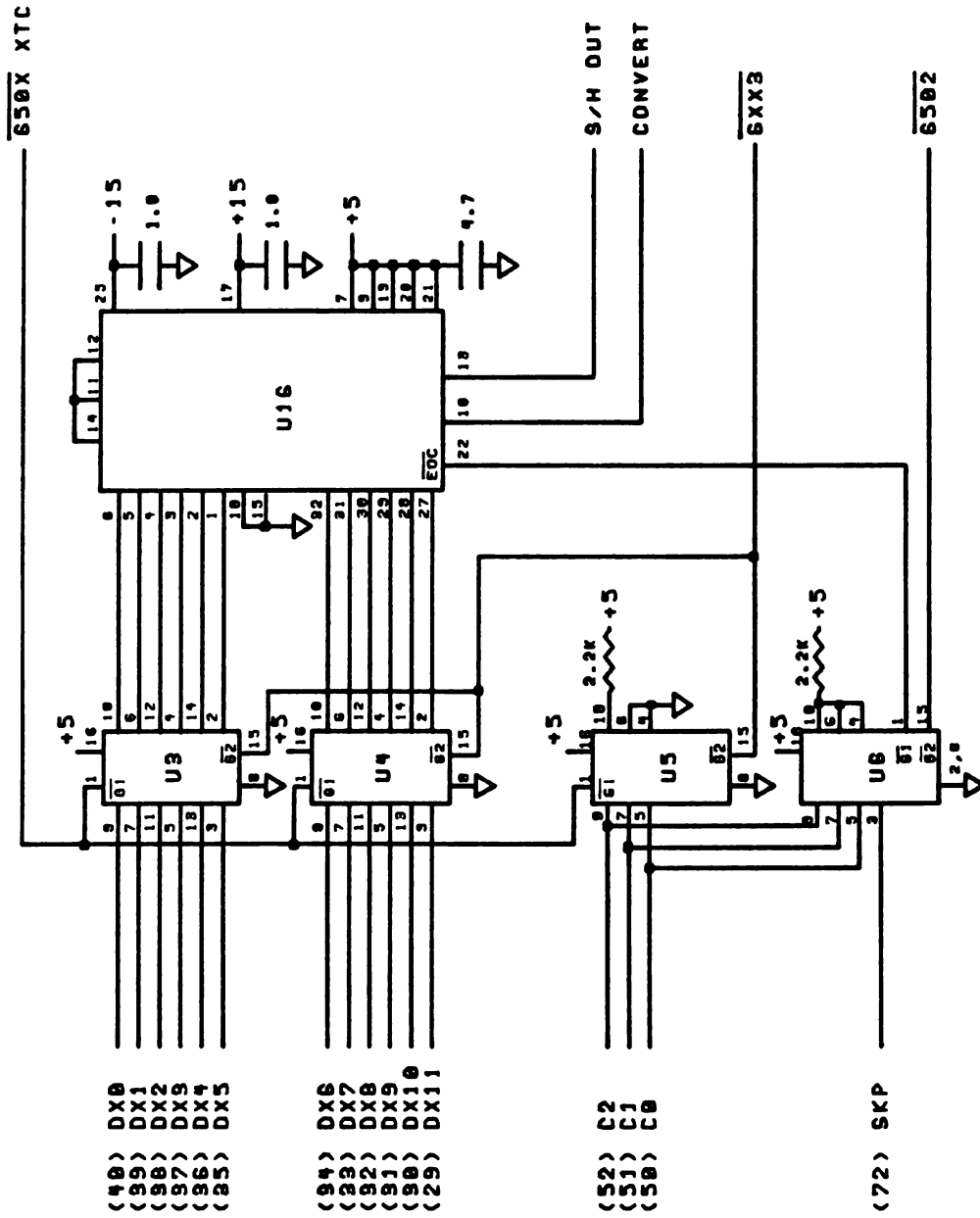


Figure B5. Analog-to-Digital Conversion Circuitry

fluorimeter are modulated, the microcomputer must synchronize the analog-to-digital conversions with the modulation cycle of the optical chopper. The circuit used to monitor the chopper wheel is shown in Figure B6. When the optical beam of the GEH13B1 detector is blocked by a blade of the chopper wheel, pin 1 of tri-state buffer UK is exerted L0. To test for this condition, the microcomputer is placed in a program loop repetitively executing 6524 instructions. The first 6524 instruction executed after the chopper detector is blocked enables UK to drive the SKP line L0 causing the microcomputer to exit from the test loop. Through an appropriate software routine, the same circuit is used to detect when the chopper detector is not blocked by a chopper wheel blade.

Because the signal from the chopper detector and the fluorescence and reference signals may not be exactly in phase due to the position of the chopper detector, a timing delay is employed between the change of state of the chopper signal and the initiation of data acquisition. A delay of about 300 μ s was found to be suitable in the present instrument and is accomplished by a software timing loop.

4. Cell Positioner Control Circuitry

a. Cell Position Monitoring - The circuitry used to monitor the position and movement of the fluorescence sample cell is also shown in Figure B6. The circuitry and its operation are identical to that associated with the radiation chopper wheel. Four GEH13B1 detectors are located on the cell positioner, two associated with encoder wheels on the motor shafts, and two located to define an origin

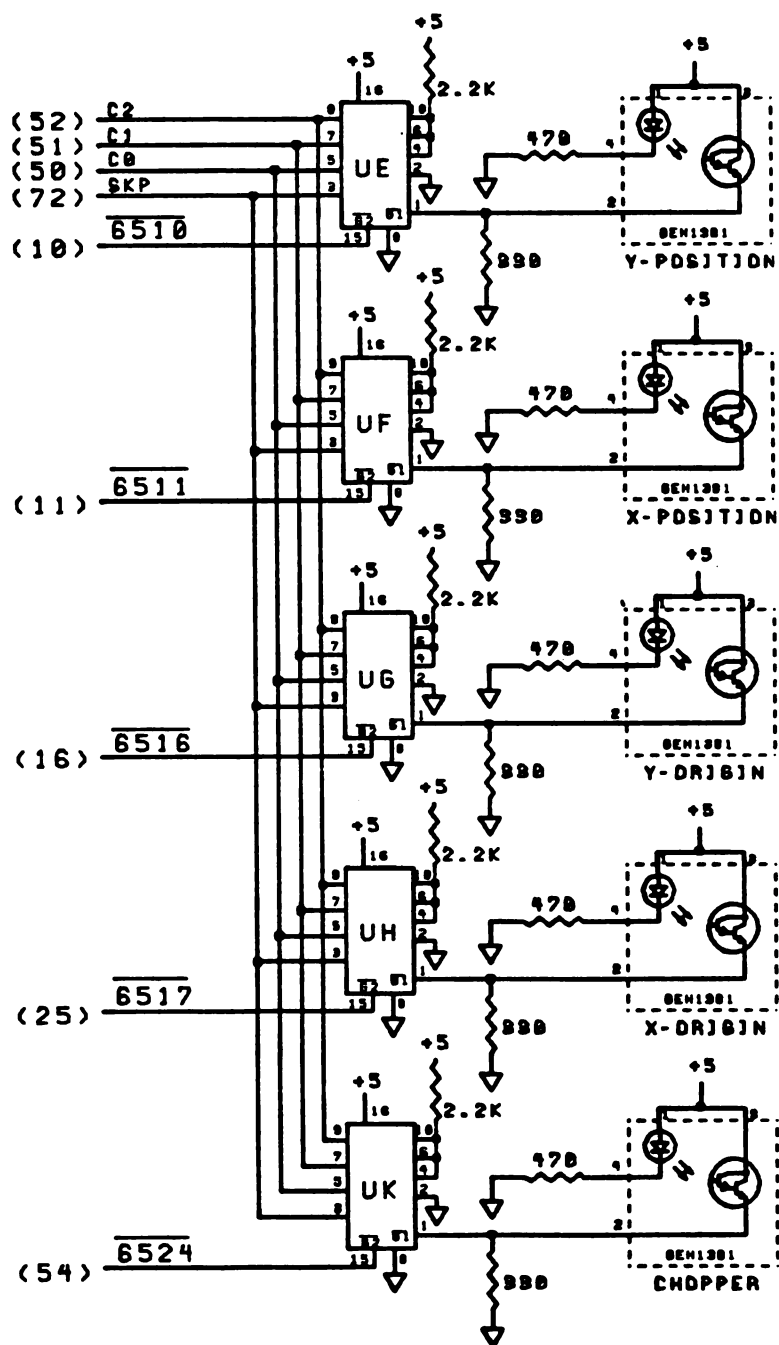


Figure B6. Cell Position and Chopper Wheel Monitoring Circuitry

in the x-y plane. When the optical beam of one of these detectors is blocked by an encoder wheel blade or by a vane on the positioner, the enable input $\overline{G1}$ of the corresponding tri-state buffer UE, UF, UG, or UH is exerted LO. The microcomputer checks for this condition by executing skip test instructions in a program loop. The 6510 and 6511 instructions test the states of the y and x encoder wheels respectively. The y and x origin encoders are tested by 6516 and 6517 instructions. When one of these instructions is executed, enable input $\overline{G2}$ of the corresponding buffer is exerted LO. If $\overline{G1}$ is LO at that time, the buffer drives the SKP line LO causing the microcomputer to jump out of the test loop. The displacement of the cell during a movement is determined simply by counting the number of LO-HI and HI-LO logic transitions from the position encoders.

b. Control of Power to the Cell Positioner - Power is supplied to the cell positioner from a separate 12 V DC power supply by the circuit shown in Figure B7. When the IM6100 is first turned on and the R/H bus line is pulsed LO by the PROM board circuitry, flip-flops UA and UB are cleared. This turns transistors Q1, Q3, Q5, and Q7 ON while Q2, Q4, Q6, and Q8 are turned OFF. Both sides of each motor on the positioner are at the same voltage (about 9.0 V) and, therefore, no current flows through the motors. To move the cell in the +y direction, a 6513 instruction is executed. This toggles flip-flop A1 and turns transistors Q1 OFF and Q2 ON. One side of the y motor is grounded causing current to flow through the motor. Execution of a second 6513 instruction reverses the state of flip-flop A1 and stops the current flow. Movement in the -y direction

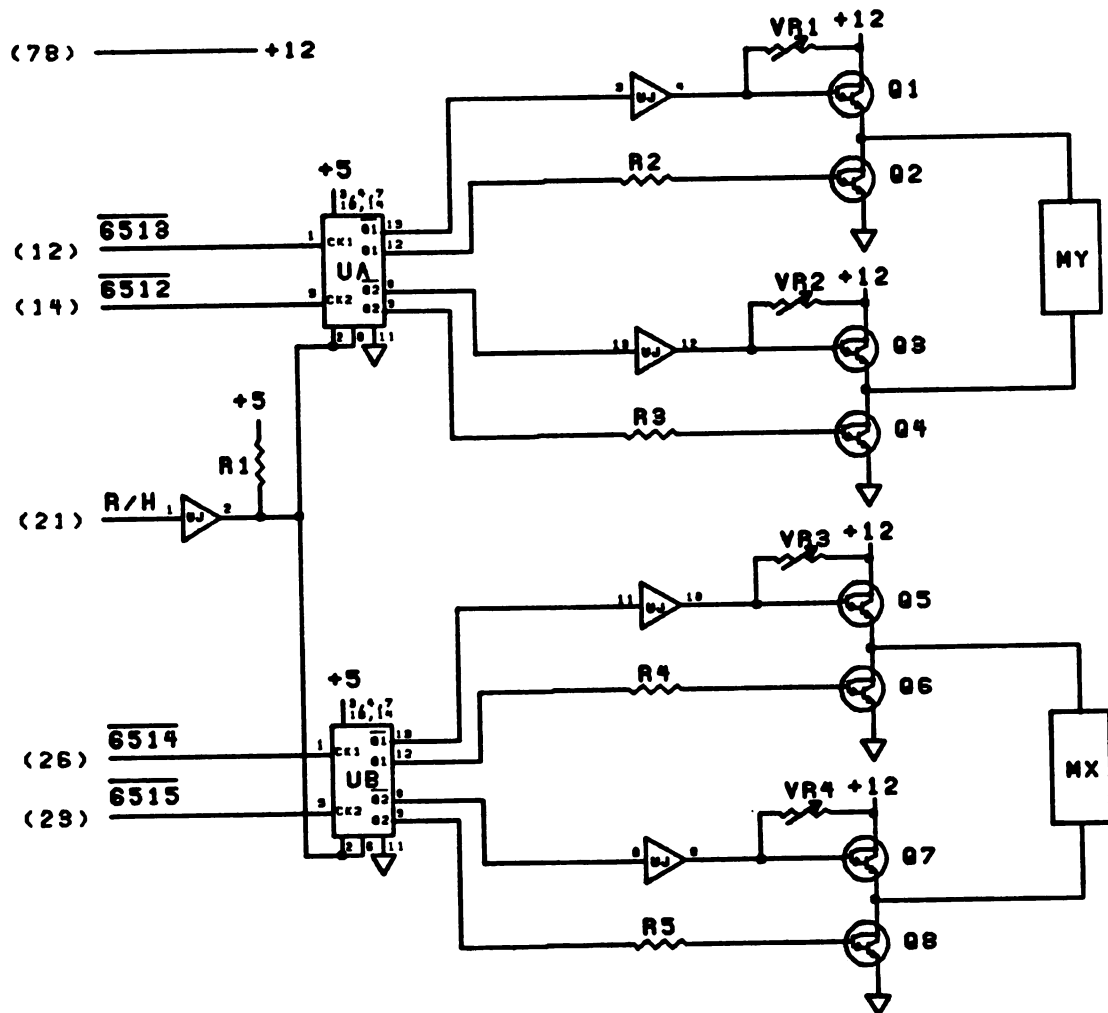


Figure B7. Cell Positioner Control Circuitry. $R1 = 2.2K$, $R2-R5 = VR1 - VR4 = 1K$, $Q1 - Q8 = 2N6043$.

is accomplished by execution of a 6512 instruction. This instruction toggles flip-flop B1 and turns transistors Q3 OFF and Q4 ON. The opposite side of the motor is grounded by this action causing the current and the direction of motor shaft rotation to be reversed. A second 6512 instruction switches the current off. The x motor is controlled in an identical manner by 6514 and 6515 instructions.

c. Control Sequence

(i) Movement to the Origin - To move the fluorescence cell precisely to any point in the x-y plane, it must first be positioned precisely at a reference point. Movement to the x-y origin is accomplished by first applying a DC current to the x motor to move the cell rapidly toward the x coordinate of the origin. When the origin detector beam is blocked by the vane on the positioner, the current is switched off and the motor is allowed to coast to a stop. The same procedure is then executed in the y direction. Next, a 5 Hz pulsed DC current of opposite polarity is applied to the x motor to move the cell slowly away from the origin detector. When the beam of the origin detector becomes unblocked, the pulse train is continued until a HI-to-LO logic transition is observed at the x encoder wheel. This sequence is then repeated for the y motor.

In this manner, the cell approaches all points in x-y space, including the origin, from the same x and y directions. This greatly reduces errors due to the looseness of the dovetail slides and the lead screw threads. Also, the encoder wheels are actually used to define the origin as well as the coordinates of all other

points in the x-y plane. This ensures that all cell positions are highly reproducible. To discriminate against switching transients picked up from the motor power lines, the signals from the origin and position detectors in the sequence described above are always double checked after a 1 ms delay.

(ii) Movement to Other Cell Positions - To move the cell to other positions in the x-y plane, a series of 2.5 ms current pulses of gradually decreasing frequency is applied to the motors. This is accomplished in a three part sequence. The pulsed DC current is first applied at about 100 Hz until the motor shaft is one revolution short of its total rotation for the movement. The pulse frequency is then reduced to about 40 Hz for 0.9 revolution. Finally, current pulses are applied at about 5 Hz until the last encoder signal is counted. During the final part of this sequence, the motor shaft advances about 0.02 revolution with each current pulse and the cell moves about 0.001 cm.

If the cell movement involves a lead screw rotation of one revolution or less, the first part of the sequence is skipped. If a rotation of only 0.1 revolution is involved, only the final part of the sequence is used. For the work described in this thesis, all cell movements between cell positions and between the origin and cell position 1 involved equal movements of 130 encoder logic transitions or 0.65 cm in both the x and y dimensions.

5. Monochromator Control Circuitry - To scan the GCA McPherson monochromators used in the fluorimeter, a TTL square wave is generated under microcomputer control by the circuit shown in Figure B8 and used to drive the external scanning inputs on the monochromator slew boxes. With the slew box scan switches set to 20 Å/s, a 1 nm scan is accomplished by generating 300 cycles of a 600 Hz square wave. The microcomputer does this by executing 6521 instructions at approximately 800 μ s intervals to toggle flip-flop UD1. The square wave is then multiplexed to either or both the excitation and emission monochromators by the action of flip-flops UC1 and UC2 and gate UI. All flip-flops are initially cleared on power-up so that neither monochromator is scan enabled. Execution of a 6523 instruction toggles flip-flop UC1 allowing the square wave from UD to pass gate UI to the excitation monochromator. A second 6523 instruction reverses the state of UC1 and disables the scan. Similarly, the 6522 instruction enables and disables the emission monochromator for scanning. Different wavelength intervals can be scanned by simply generating a different number of cycles of the 600 Hz square wave.

C. Software Structure

1. Fluorimeter Control and Data Collection

A single PAL8 program named DRC3 was written for the IM6100 microcomputer to control all fluorimeter functions. The program is subroutine oriented around a command decoder which calls the various subroutines to execute the fluorimeter control functions.

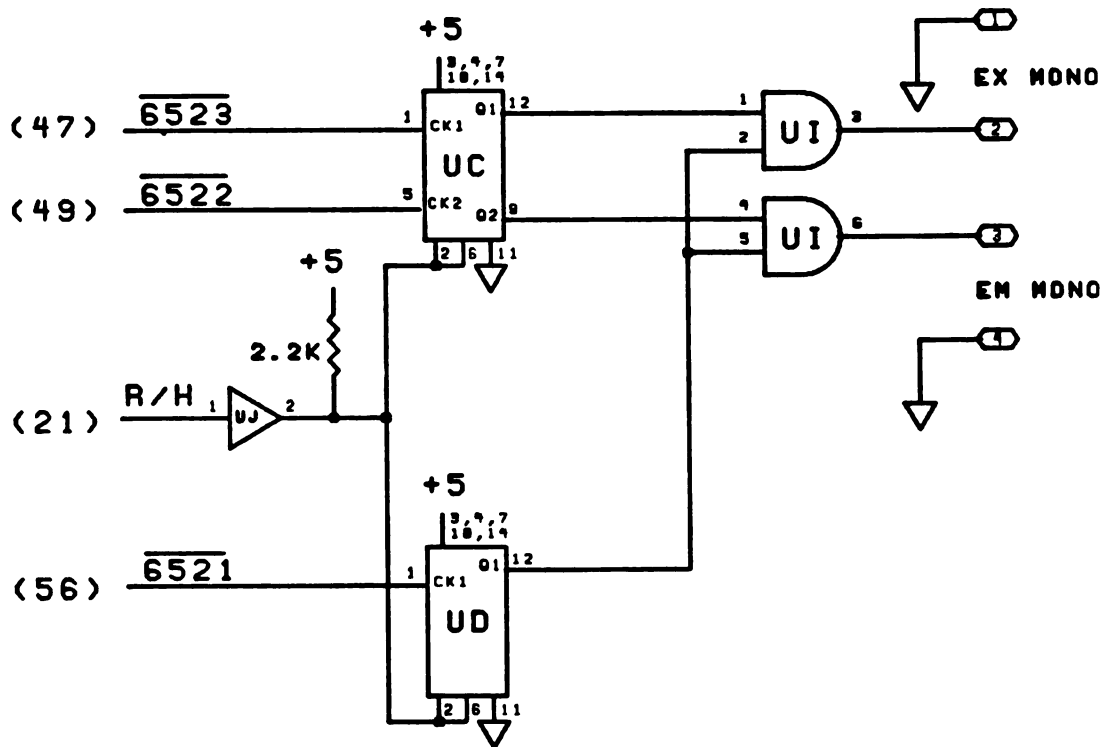


Figure B8. Monochromator Scanning Circuitry

All keyboard commands to DRC3 are single character commands, some of which require an octal argument. Table B3 summarizes the commands and the actions they initiate.

The binary program DRC3.BN is loaded into the microcomputer memory by issuing the following command to the OS/8 keyboard monitor:

_ PU DRC3.BN/B

Loading is executed automatically, and control of the keyboard is turned over to the IM6100 PROM monitor. To start DRC3, one simply types

\$ FO
\$ 0200G

Program DRC3 should respond by typing a "/" on the CRT to indicate that it is running and waiting to receive a command.

2. Data Transfer

Several programs were written in OS/8 Fortran II-SABR for the PDP 8/e to receive, store, and correct fluorescence data collected by program DRC 3. The first of these programs is RCVR2.FT which receives 24-bit integer data transmitted from the IM6100 as fluorescence-reference intensity pairs, converts the numbers to floating point format, normalizes the fluorescence to the reference intensity, and stores the results under a filename specified by the user. RCVR2 operates on a "handshaking" principle with DRC3 during data transfer.

Table B3. Keyboard Commands for Program DRC3.

Command	Resulting Action
A	Executes alignment routine after querying for NNNN _g points to take in the cell profile. Direction of movement and displacement increment should be set prior to command.
B	Measure baselines in each signal channel and type results on CRT (chopper must be on).
D	Measure net fluorescence and reference signals and type results on CRT (chopper must be on).
E	Exit to transparent mode
G	Start scan
LNNNN	Set scan length to NNN _g nanometers.
M	Execute cell movement (direction and displacement must be set prior to command).
O	Move cell to the x-y origin.
R	Collects data at cell positions 1, 2, and 3. Sequence is repeated NNN _g times after querying for this argument.
SN	Set up for scan type N where N = (1) for excitation scan (2) for emission scan (3) for synchronous scan
T	Transmit data to minicomputer (program RCVR2 must be loaded and started on the 8/e prior to command).
XMNNN	Set up for X cell displacement of NNN _g steps in the M direction, M = F(forward) or R(reverse). One step = 0.005 cm.
YMNNN	Set up for Y cell displacement of NNN _g steps in the M direction.

When a data transfer is to be made, the user exits from DRC3 to the OS/8 monitor and loads and starts RCVR2. The program responds by typing "Ready" on the CRT and then waits for an octal 200 character to be transmitted from the microcomputer to signal the beginning of data transfer. The user then restarts DRC3 and types "T" to initiate data transfer. Program DRC3 immediately sends an octal 200 to the 8/e and then transmits data characters in response to octal 100 characters which are sent to the microcomputer by RCVR2 when it is ready to receive a character. Data transfer is terminated when DRC3 sends a second octal 200 character after the last data character.

3. Data Correction

Corrections for primary and secondary absorption errors, reflection effects, and the detection system sensitivity are coordinated by program FLUORO.FT. The corrections are executed according to a list of correction parameters and a list of file specifications supplied to the program by the user. The correction parameters include the fluorimeter window parameters and cell reflectance values. The file specifications include input and output file names, file length, and file type. These specifications are then passed to the correction program STAT.FT if the user has specified static wavelength data, or to the program SPEC.FT if spectral data has been specified. Both of these programs are swapped into core by the Fortran II chaining feature and, in turn, chain back to program FLUORO when execution is finished. More specific information about these programs can be found in the program listings.

4. Program Listings

On the following pages, listings of the source files of programs DRC3.PA, RCVR2.FT, FLUORO.FT, STAT.FT, and SPEC.FT are presented. Some important subroutines are also listed immediately following the Fortran programs in which they are referenced. These include subroutine SUBIN.FT which handles keyboard input for FLUORO.FT, subroutine SUBCORR.FT which performs the absorption and reflection correction calculations for STAT.FT and SPEC.FT, and subroutine SD.FT which computes sample mean and standard deviation values for program STAT.FT.

```

////////////////////////////////////
/
/      PROGRAM DRC3.PA
/
/      FLUORIMETER CONTROL ROUTINES
/
////////////////////////////////////

```

```

CALL=JMS I 0      /INDIRECT SUBROUTINE CALL
SMPL=6506          /SET S/H TO SAMPLE MODE
ADST=6501          /SET S/H TO HOLD MODE AND START ADC
ADRB=6503          /JAM TRANSFER ADC RESULT INTO AC
ADSF=6502          /SKIP ON A-TO-D DONE FLAG
MUXI=6504          /SET MULTIPLEXER TO I CHANNEL
MUF=6505           /SET MULTIPLEXER TO F CHANNEL
XFON=6514          /FORWARD POWER TO X MOTOR ON
XFOF=6509          /FORWARD POWER TO X MOTOR OFF
XRON=6515          /REVERSE POWER TO X MOTOR ON
XROF=6510          /REVERSE POWER TO X MOTOR OFF
YFON=6513          /FORWARD POWER TO Y MOTOR ON
YFOF=6508          /FORWARD POWER TO Y MOTOR OFF
YRON=6512          /REVERSE POWER TO Y MOTOR ON
YROF=6507          /REVERSE POWER TO Y MOTOR OFF
SXEL=6511          /SKIP ON X ENCODER LOW
SYEL=6510          /SKIP ON Y ENCODER LOW
SXOL=6517          /SKIP ON X ORIGIN LOW
SYOL=6516          /SKIP ON Y ORIGIN LOW
SCHL=6524          /SKIP ON CHOPPER LOW
PDPTLS=6146        /COMMANDS FOR SERIAL PORT TO S/E
PDPTSF=6141
PDPKSF=6131
PDPKRB=6136
EXIT=6525          /RETURN TO PROM MONITOR

```

```

/ FREQUENTLY ADDRESSED REGISTERS

```

```

FIELD 0
*10
TDATA, 0
POINTER, 0        / POINTER TO DATA STORAGE
*20
NOPTS, 0000        / MINUS THE NUMBER OF ADC'S TO AVERAGE
HB, 0              / HIGH BYTE OF DIVIDEND
LB, 0              / LOW BYTE OF DIVIDEND
MDIV, 0            / MINUS THE VALUE OF THE DIVISOR
LI, 0              / LOW SUMMATION REGISTER FOR I
HI, 0              / HIGH SUMMATION REGISTER FOR I
LF, 0              / LOW SUMMATION REGISTER FOR F
HF, 0              / HIGH SUMMATION REGISTER FOR F
TEMP, 0            / TEMPORARY CHARACTER STORAGE
DTIME, 0           / NO. OF DELAY TIMING CYCLES
HIB, 0             / BASELINE SUMMATION REGISTERS
LIB, 0
HFB, 0
LFB, 0
SBFLAG, 0          / SIGNAL-BASELINE FLAG
COUNT, 7777       / NUMBER OF ENCODER PULSES TO COUNT
TIME, 0            / DELAY TIME
NOVAL, 0           / NO. OF DATA POINTS
FLAG1, 0
M1, -1             / VARIOUS CONSTANTS
M2, -2
M3, -3
M4, -4
M5, -5
M10, -10
M11, -11
M12, -12
M14, -14
M15, -15

```

M20, -20
 M22, -22
 M30, -30
 M50, -50
 M60, -60
 M76, -76
 M100, -100
 M115, -115
 M144, -144
 M202, -202
 M454, -454
 M1750, -1750
 P3, 3
 P10, 10
 P11, 11
 P77, 77
 P177, 177
 P200, 200
 P256, 256
 P260, 260
 P6510, 6510
 P6511, 6511
 P6512, 6512
 P6513, 6513
 P6514, 6514
 P6515, 6515
 P6777, 6777
 ADCNT1, 0
 ADCNT2, 0
 ADCNT3, 0

/POINTERS TO SUBROUTINES

DIVIDE, DIV /DIVISION SUBROUTINE, ENTER WITH DIVIDEND
 /IN HB-LB AND DIVISOR IN MDIV
 STRING, STR /TYPE OUT ASCII STRING IMMEDIATELY
 /FOLLOWING THE CALL COMMAND
 DECOU, DEC /TYPE OCTAL VALUE IN AC AS A DECIMAL NO.
 TYPE, TY /TYPE ASCII CHARACTER IN THE AC
 CRLF, CR /TYPE A CARRIAGE RETURN AND LINE FEED
 READ, XREAD /INPUT AN OCTAL NUMBER
 IN, XIN /INPUT AN ASCII CHARACTER
 DATA, ADC /DATA ACQUISITION SUBROUTINE
 BASE, BAS /BASELINE ACQUISITION SUBROUTINE
 MOVE, MOV /CELL TRANSLATION SUBROUTINE
 MONITR, MON /COMMAND MONITER
 XSET, XS /PREPARE FOR MOVEMENT IN X DIRECTION
 YSET, YS /PREPARE FOR MOVEMENT IN Y DIRECTION
 ORIGIN, ORG /RETURN TO X-Y ORIGIN
 DELAY, DLA /TIME DELAY SUBROUTINE
 SEND, SND /SEND DATA TO S/E
 NUMIN, NUM /GET 4 DIGIT OCTAL NUMBER
 SAVE, SAV /STORE BASELINE CORRECTED DATA
 OUT, OWT / DISPLAY ADC RESULTS
 ALIGN, ALINE /ALIGNMENT ROUTINE
 RUN, RUNN /THREE POINT ACQUISITION ROUTINE
 STEP, STEPR /APPLY 2.5 MS CURRENT PULSE TO MOTOR
 DIRECT, DIR /SUBR TO ESTABLISH MOTOR DIRECTION
 ARG, ARGU /READ IN 3 DIGIT OCTAL ARGUMENT, RETURN NEG IN AC
 FR, RORF /DETERMINE MOTOR DIRECTION (FOR OR REV)
 LENGTH, LEN /SET SCAN LENGTH
 GOGET, SPEC /START SCAN
 SCMODE, MODE2 /SET SCAN MODE
 SCAN, SCN /SCAN MONOCHROMATORS
 ERROR, ERR /ERROR MESSAGE FOR POSITIONING ERROR
 BELL, RING /RING THE BELL ON THE TTY
 /COMMAND MONITOR

*200

MON, CLA IAC


```

DCA FLAG1
CALL CRLF
TAD (257
CALL TYPE      /TYPES A "/" WHEN READY FOR INPUT
CALL IN        /GET SINGLE CHARACTER COMMAND
TAD (-301
SZA            /"A"?
JMP .+3
CALL ALIGN
JMP MON
TAD M1
SZA            /"B"?
JMP .+4
CALL BASE
CALL OUT
JMP MON
TAD M2
SZA            /"D"?
JMP .+4
CALL DATA
CALL OUT
JMP MON
TAD M1
SZA            /"E"?
JMP .+2
EXIT
TAD M2
SZA            /"G"?
JMP .+3
CALL COGET
JMP MON
TAD M5
SZA            /"L"?
JMP .+3
CALL LENGTH
JMP MON
TAD M1
SZA            /"M"?
JMP .+3
CALL MOVE
JMP MON
TAD M2
SZA            /"O"?
JMP .+4
CALL ORIGIN
CALL BELL
JMP MON
TAD M3
SZA            /"R"?
JMP .+3
CALL RUN
JMP MON
TAD M1
SZA            /"S"?
JMP .+3
CALL SCMODE
JMP MON
TAD M1
SZA            /"T"?
JMP .+3
CALL SEND
JMP MON
TAD M4
SZA            /"X"?
JMP .+3
CALL XSET
JMP MON

```

```

TAD M1
SZA          /"Y"?
JMP .+2
CALL YSET
JMP MON      /NOT A LEGAL COMMAND, IGNORE IT!
              /CELL TRANSLATION SUBROUTINES

MOV, *400
0           /MOVE THE CELL
CALL STEP
TAD COUNT
IAC
SNA
JMP SHORT1

ENC1, 0      /POSITION ENCODER MUST BE HIGH
        /AT START OF MOVEMENT
JMP .+2
CALL ERROR
TAD P11
SMA
JMP SHORT2
DCA CNTRM
TAD TIME
DCA DTIME
JMS GO2

SHORT3, TAD M11
DCA CNTRM
TAD M76
DCA DTIME
JMS GO2

SHORT1, TAD M1
DCA CNTRM
TAD M144
DCA DTIME
JMS GO2
JMP I MOV

SHORT2, SNA
JMP SHORT3
TAD M11
JMP SHORT3+1

GO2, 0
JMS PULSE
ISZ CNTRM
JMP .-2
CLA
JMP I GO2

CNTRM, 0
PULSE, 0      /ROTATE LEAD SCREW 18 DEGREES
ENC2, 0
JMP .+12
CALL STEP
CALL DELAY

ENC3, 0
JMP .+2
JMP .-4

ENC4, 0
JMP I PULSE
JMP .-7
CALL STEP
CALL DELAY

ENC5, 0
JMP .-3

ENC6, 0
JMP .-5
JMP I PULSE

XS, 0        /SET UP FOR X TRANSLATION
CLA
TAD M10
DCA TIME

```

```

TAD P6511
JMS ENC
TAD FLAG1
SZA CLA
CALL FR
JMP XFOR
CLA
TAD P6515
CALL DIRECT
CLA
CALL ARG
DCA COUNT
JMP I XS
XFOR, CLA
TAD P6514
CALL DIRECT
CLA
TAD FLAG1
SNA CLA
JMP .+3
CALL ARG
DCA COUNT
JMP I XS
YS, 0 /SET UP FOR Y TRANSLATION
CLA
TAD M5
DCA TIME
TAD P6510
JMS ENC
TAD FLAG1
SZA CLA
CALL FR
JMP YFOR
CLA
TAD P6512
CALL DIRECT
CLA
CALL ARG
DCA COUNT
JMP I YS
YFOR, CLA
TAD P6513
CALL DIRECT
CLA
TAD FLAG1
SNA CLA
JMP .+3
CALL ARG
DCA COUNT
JMP I YS
ENC, 0 /SET UP DIRECTION OF MOVEMENT
DCA ENC1
TAD ENC1
DCA ENC2
TAD ENC2
DCA ENC3
TAD ENC3
DCA ENC4
TAD ENC4
DCA ENC5
TAD ENC5
DCA ENC6
JMP I ENC
*600
ORG, 0 /RETURN TO ORIGIN
CLA
TAD M144

```

```

DCA DTIME
XRON
SXOL
JMP .-1
XROF
CALL DELAY
SXOL /DOUBLE CHECK X ORIGIN ENCODER
JMP .-6
YRON
SYOL
JMP .-1
YROF
CALL DELAY
SYOL /DOUBLE CHECK Y ORIGIN ENCODER
JMP .-6
TAD M100
DCA DTIME
TAD P6514
JMS DIR
JMS STEPR
CALL DELAY
SXOL
JMP .+2
JMP .-4
SXOL /ANOTHER DOUBLE CHECK
JMP .+2
JMP .-7
TAD M144
DCA DTIME
SXEL
JMP .+2
JMP .+4
JMS STEPR
CALL DELAY
JMP .-5
JMS STEPR
CALL DELAY
SXEL
JMP .+2
JMP .-4
TAD M50
DCA DTIME
TAD P6513
JMS DIR
JMS STEPR
CALL DELAY
SYOL
JMP .+2
JMP .-4
SYOL /ANOTHER DOUBLE CHECK
JMP .+2
JMP .-7
TAD M100
DCA DTIME
SYEL
JMP .+2
JMP .+4
JMS STEPR
CALL DELAY
JMP .-5
JMS STEPR
CALL DELAY
SYEL
JMP .+2
JMP .-4
JMP I ORC
STEPR, 0 /GENERATE CURRENT PULSES

```

```

      CLA                      /TO THE APPROPRIATE MOTOR
      TAD (7500
      DCA CNTRP
ON,    0
      ISZ CNTRP
      JMP .-1
OFF,   0
      JMP I STEPR
CNTRP, 0
DIR,   0                      /SELECT THE MOTOR
      DCA ON
      TAD ON
      DCA OFF
      JMP I DIR
OWT,   0
      CALL CRLF              / OUTPUT RESULTS
      CALL STRING            /OUTPUT F
      0215
      0306
      0275
      0240
      0000
      TAD HF
      CALL DECOUT
      TAD P256
      CALL TYPE
      TAD LF
      CALL DECOUT
      CALL CRLF
      CALL STRING            /OUTPUT I
      0311
      0275
      0240
      0000
      TAD HI
      CALL DECOUT
      TAD P256
      CALL TYPE
      TAD LI
      CALL DECOUT
      JMP I OWT
      /UTILITY SUBROUTINES
DIV,   *1000
      0                      /DIVISION SUBROUTINE, HB LB = DIVIDEND
                                /MDIV = -DIVISOR,... HB=REMAINDER,LB=QUOTIENT
      CLA CLL
      TAD M15
      DCA CNTRD
BEGIN, CLA CLL
      TAD HB
      TAD MDIV
      SZL
      DCA HB
      JMS ROT
      ISZ CNTRD
      JMP BEGIN
      CLA
      JMP I DIV
CNTRD, 0
ROT,   0
      CLA
      TAD LB
      RAL
      DCA LB
      TAD HB
      RAL
      DCA HB

```

STR,	JMP I ROT 0	/TYPE THE ASCII STRING IMMEDIATELY /FOLLOWING THE CALL COMMAND
	CLA TAD I STR ISZ STR NOP SPA SNA JMP I STR JMS TY JMP STR+1	
TY,	0	/TYPE OUT ASCII CHARACTER IN THE AC
	TLS TSF JMP .-1 CLA CLL JMP I TY	
XIN,	0	/READ ASCII CHARACTER INTO AC
	CLA CLL KSF JMP .-1 KRB TLS TSF JMP .-1 JMP I XIN	
XREAD,	0	/READ OCTAL NUMBER INTO AC
	JMS XIN AND P177 TAD M60 SPA JMP I MONITR TAD M10 SMA JMP I MONITR TAD P10 JMP I XREAD	
CR,	0	/TYPE CR LF
	CLA TAD (215 JMS TY TAD (212 JMS TY JMP I CR	
ARGU,	0	/READ 3 DIGIT OCTAL ARGUMENT
	CALL READ BSW DCA TEMP CALL READ RAL RTL TAD TEMP DCA TEMP CALL READ TAD TEMP CIA JMP I ARGU	
RORF,	0	/READ MOTOR DIRECTION
	CALL IN TAD (-306 SNA JMP I RORF TAD M14 SNA JMP .+2 JMP I MONITR ISZ RORF	

```

NOP
JMP I RORF
*1200
DEC, 0 /TYPE OCTAL NO. IN AC AS DECIMAL
DCA TEMP
TAD M1750
DCA MDIV
TAD TEMP
DCA LB
DCA HB
CALL DIVIDE /DIVIDE BY 1000
TAD LB
TAD P260
CALL TYPE /OUTPUT THE INTEGER PART
TAD HB
RAR CLL
DCA LB
DCA HB
TAD M144
DCA MDIV
CALL DIVIDE /DIVIDE REMAINDER BY 100
TAD LB
TAD P260
CALL TYPE /OUTPUT THE INTEGER PART
TAD HB
RAR CLL
DCA LB
DCA HB
TAD M12
DCA MDIV
CALL DIVIDE /DIVIDE REMAINDER BY 10
TAD LB
TAD P260
CALL TYPE /OUTPUT THE INTEGER PART
TAD HB
RAR CLL
TAD P260
CALL TYPE
JMP I DEC
BAS, 0 /MEASURE BASELINE
CALL DATA
TAD HIB
DCA HI
TAD LIB
DCA LI
TAD HFB
DCA HF
TAD LFB
DCA LF
JMP I BAS
DLA, 0 /TIMING LOOP
CLA
TAD DTIME
DCA DCNTR2
CLA
TAD M115
DCA DCNTR1
ISZ DCNTR1
JMP .-1
ISZ DCNTR2
JMP .-6
JMP I DLA
DCNTR1, 0
DCNTR2, 0
SAV, 0 /STORE DATA
TAD HI
JMS STORE

```

```

TAD LI
JMS STORE
TAD HF
JMS STORE
TAD LF
JMS STORE
JMP I SAV
STORE, 0 /STORE IN FIELD 1
CDF 10
DCA I POINTER
CDF 0
JMP I STORE
ALINE, 0 /ALIGNMENT ROUTINE
CALL CRLF
CALL STRING
0316 /NO. POINTS =
0317
0256
0240
0320
0324
0323
0256
0240
0275
0240
0000
CALL NUMIN
DCA NOVAL
TAD NOVAL
CIA
DCA CNTRA
TAD P177
DCA POINTER
AGAIN, CALL DATA
CALL SAVE
CALL MOVE
ISZ CNTRA
JMP AGAIN
CALL BELL
JMP I ALINE
CNTRA, 0
*1400
SND, 0 /TRANSMIT DATA TO THE MINI
CLA
TAD P177
DCA POINTER
TAD NOVAL
CLL RTL
CIA
DCA CNTRT
TAD P200
JMS PDPOUT
A, JMS READY
CDF 10
TAD I POINTER
CDF 0
DCA TEMP
TAD TEMP
BSW
AND P77
JMS PDPOUT
JMS READY
TAD TEMP
AND P77
JMS PDPOUT
ISZ CNTRT

```



```

      JMP A
      CLA
      TAD P200
      JMS PDPOUT
      JMP I SND
CNTRT, 0
READY, 0      /SEE IF MINI IS READY FOR DATA
      JMS PDPIN
      AND P177
      TAD M100
      SZA
      JMP .-4
      JMP I READY
PDPOUT, 0      /SEND CHARACTER TO MINI
      PDPTLS
      PDPTSF
      JMP .-1
      CLA
      JMP I PDPOUT
PDPIN, 0      /READ CHARACTER FROM MINI
      PDPKSF
      JMP .-1
      CLA
      PDPKRB
      JMP I PDPIN
NUM, 0      /READ 4 DIGIT OCTAL ARGUMENT
      CALL READ
      RTR
      RTR
      DCA TEMP
      CALL READ
      BSW
      TAD TEMP
      DCA TEMP
      CALL READ
      RTL
      RAL
      TAD TEMP
      DCA TEMP
      CALL READ
      TAD TEMP
      JMP I NUM
      *1600
RUNN, 0      /DATA ACQUISITION SEQUENCE
      CLA
      DCA FLAG1
      TAD M202
      DCA COUNT
      TAD P177
      DCA POINTER
      DCA NOVAL
      CALL CRLF
      CALL STRING
      'N
      'O
      '.
      '.
      'R
      'U
      'N
      'S
      '.
      '.
      '.
      0000
      CALL ARG
      DCA RCNTR

```

```

R1,      CALL CRLF
          CALL YSET
          CALL MOVE
          CALL XSET
          CALL MOVE
          CALL DATA
          CALL SAVE
          ISZ NOVAL
          CALL OUT
          CALL MOVE
          CALL DATA
          CALL SAVE
          ISZ NOVAL
          CALL OUT
          CALL YSET
          CALL MOVE
          CALL DATA
          CALL SAVE
          ISZ NOVAL
          CALL OUT
          CALL ORIGIN
          ISZ RCNTR
          JMP R1
          CALL BELL
          JMP I RUNN
RCNTR,   0
MODE2,   0      /READ SCAN MODE
          CALL READ
          DCA CHAR
          JMS SET
          JMP I MODE2
CHAR,    0
SET,     0      /SET SCAN MODE
          TAD CHAR
          TAD M1
          SNA
          JMP EXSET
          TAD M1
          SNA
          JMP EMSET
          TAD M1
          SNA
          JMP SYNSET
          JMP I SET
EXSET,   6523
          JMP I SET
EMSET,   6522
          JMP I SET
SYNSET,  6522
          JMP I SET
          JMP I SET
LEN,     0      /READ AND SET SCSAN LENGTH
          CALL ARC
          DCA CNTRS
          TAD CNTRS
          CIA
          DCA NOVAL
          JMP I LEN
CNTRS,   0
SPEC,    0      /SCANNING SEQUENCE
          CLA
          TAD P177
          DCA POINTER
          CALL DATA
          CALL SAVE
          CALL SCAN
          ISZ CNTRS

```

	JMP SPEC+4	
	CLA	
	JMS SET	
	CALL BELL	
	JMP I SPEC	
SCN,	0	/STEP THE MONOCHROMATORS
	CLA	
	TAD M454	
	DCA CNT	
	6521	
	JMS WAIT	
	6521	
	JMS WAIT	
	ISZ CNT	
	JMP .-5	
	JMP I SCN	
CNT,	0	
WAIT,	0	/TIMING LOOP FOR STEPPING PULSES
	CLA	
	TAD M76	
	DCA CNTRW	
	ISZ CNTRW	
	JMP .-1	
	JMP I WAIT	
CNTRW,	0	
	*2000	
ADC,	0	/A-TO-D SEQUENCE
	CLA CLL	
	SMPL	
	TAD NOPTS	
	DCA ADCNT1	
	DCA HF	/INITIALIZE SUMMATION REGISTERS
	DCA LF	
	DCA HI	
	DCA LI	
	DCA HFB	
	DCA LFB	
	DCA HIB	
	DCA LIB	
OK,	CLA CLL	
	TAD M30	/DELAY TIME
	DCA ADCNT2	
	DCA SBFLAG	/SET FLAG FOR DARK SIGNAL
	SCHL	/LOOK FOR DARK SIGNAL
	JMP .+2	
	JMP .-2	
	ISZ ADCNT2	
	JMP .-1	
	JMS GET	/TAKE DATA
	STA	
	DCA SBFLAG	/SET FLAG FOR LIGHT SIGNAL
	TAD M30	
	DCA ADCNT2	
	SCHL	
	JMP .-1	
	ISZ ADCNT2	
	JMP .-1	
	JMS GET	/TAKE DATA
	ISZ ADCNT1	/COUNT NO. OF POINTS
	JMP OK	
	CLA CLL	
	TAD LIB	/COMPUTE NET SIGNALS
	CIA	
	TAD LI	
	DCA LI	
	SZL	
	ISZ HI	

	NOP	
	CLL	
	TAD HIB	
	CMA	
	TAD HI	
	DCA HI	
	TAD LFB	
	CIA	
	TAD LF	
	DCA LF	
	SZL	
	ISZ HF	
	NOP	
	TAD HFB	
	CMA	
	TAD HF	
	DCA HF	
	JMP I ADC	
GET,	0	/A-TO-D CONVERSION
	CLA	
	TAD P6777	
	DCA TDATA	/POINTER TO DATA STORAGE
	TAD M1	
	DCA ADCNT3	
GO,	SMP1	/SET MUX TO REFERENCE CHANNEL
	MUXI	
	NOP	
	ADST	/CONVERT
	ADSF	
	JMP .-1	
	MUXF	/SET MUX TO FLUORESCENCE CHANNEL
	ADRB	
	NOP	
	ADST	/CONVERT
	DCA I TDATA	/STORE I TEMPORARILY
	ADSF	
	JMP .-1	
	ADRB	
	DCA I TDATA	/STORE F TEMPORARILY
	ISZ ADCNT3	/DONE?
	JMP GO	
	TAD P6777	
	DCA TDATA	
	TAD M1	
	DCA ADCNT3	
	ISZ SBFLAG	
	JMP SIG	/GO TO INTEGRATION ROUTINES
	JMP BASL	
SIG,	CLL	/INTEGRATE LIGHT SIGNALS
	TAD I TDATA	
	CMA	
	TAD LI	
	DCA LI	
	SZL	
	ISZ HI	
	NOP	
	CLL	
	TAD I TDATA	
	CMA	
	TAD LF	
	DCA LF	
	SZL	
	ISZ HF	
	NOP	
	ISZ ADCNT3	
	JMP SIG	
	JMP I GET	

```

BASL,  CLL          /INTEGRATE DARK SIGNALS
      TAD I TDATA
      CMA
      TAD LIB
      DCA LIB
      SZL
      ISZ HIB
      NOP
      CLL
      TAD I TDATA
      CMA
      TAD LFB
      DCA LFB
      SZL
      ISZ HFB
      NOP
      ISZ ADCNT3
      JMP BASL
      JMP I GET
      *2200
ERR,   0          /TYPE ERROR MESSAGE ON CRT
      CALL CRLF
      CALL STRING
      "P
      "O
      "S
      "I
      "T
      "I
      "O
      "N
      "
      "E
      "R
      "R
      "O
      "R
      0000
      JMP I MONITR
RING,  0          /RING THE BELL
      CLA
      TAD P207
      CALL TYPE
      JMP I RING
P207, 207
      ****

```

```

CCCCCCCCCCCCCCCCCCCCCCCCCCCCCCCCCCCCCCCCCCCCCCCCCCCCCCCC
C
C      PROGRAM RECEIVER
C      FILE: RCVR2.FT
C
C      PURPOSE: RECEIVE AND STORE DATA
C      FROM THE IM6100 MICROCOMPUTER
C
CCCCCCCCCCCCCCCCCCCCCCCCCCCCCCCCCCCCCCCCCCCCCCCCCCCCCCCC
S      OPDEF   BSW      7002
      DIMENSION I(1000),F1(99),F2(99),F3(99)
      WRITE(1,1)
1      FORMAT(/'HELLO'/)
2      READ(1,5)FNAME
5      FORMAT('WHAT IS THE FILENAME?(A6) 'A6)
      CALL OOPEN('FLP2',FNAME)
      READ(1,10)L
10     FORMAT(' IS THIS A SPECTRUM?(Y/N)'A1)
      IF(L-1632)15,250,15
15     READ(1,20)NSETS
20     FORMAT('HOW MANY 3 PT. DATA SETS IN THIS FILE?(12) '12)
      WRITE(1,25)
25     FORMAT('OK! TYPE CONTROL-A TO ENTER LOCAL MODE. ')
S      JMS DATA
      MK=1
      DO 100 K=1,NSETS
      F1(K)=FLOAT(I(MK+2))+2048.+(FLOAT(I(MK+3))+2048.)/4096.
      F1(K)=F1(K)/(FLOAT(I(MK))+2048.+(FLOAT(I(MK+1))+2048.)/4096.)
      F2(K)=FLOAT(I(MK+6))+2048.+(FLOAT(I(MK+7))+2048.)/4096.
      F2(K)=F2(K)/(FLOAT(I(MK+4))+2048.+(FLOAT(I(MK+5))+2048.)/4096.)
      F3(K)=FLOAT(I(MK+10))+2048.+(FLOAT(I(MK+11))+2048.)/4096.
      F3(K)=F3(K)/(FLOAT(I(MK+8))+2048.+(FLOAT(I(MK+9))+2048.)/4096.)
      MK=MK+12
100    CONTINUE
      DO 150 K=1,NSETS
      WRITE(4,110)F1(K),F2(K),F3(K)
110    FORMAT(3E15.9)
150    CONTINUE
175    CALL OCLOSE
      READ(1,200)L
200    FORMAT('DO YOU HAVE ANOTHER FILE?(Y/N)'A1)
      IF(L-1632)400,2,400
250    WRITE(1,25)
S      JMS DATA
      X=0.
      DO 300 N=1,J,4
      N1=N+1
      N2=N+2
      N3=N+3
      F1(1)=FLOAT(I(N))+2048.+(FLOAT(I(N1))+2048.)/4096.
      F1(1)=(FLOAT(I(N2))+2048.+(FLOAT(I(N3))+2048.)/4096.)/F1(1)
      X=X+1.
      WRITE(4,275)X,F1(1)
275    FORMAT('RD',2E15.5)
300    CONTINUE
      GO TO 175
400    STOP
SDATA, 0
      J=0
SA,    JMS IN
S      JMP GET
S      JMP A
SGET,  JMS PROMPT
S      JMS IN
S      JMP EOF
S      BSW
S      DCA TEMP

```

```

S      JMS PROMPT
S      JMS IN
S      JMP EOF
S      TAD TEMP
S      TAD (4000
S      DCA m
          J=J+1
          I(J)=M
S      JMP GET
STEMP, 0
SEOF,  CLA
S      JMP I DATA
SIN,   0
S      CLA
SB,    KSF
S      JMP B
S      KRB
S      TAD (-200
S      SNA
S      JMP I IN
S      ISZ IN
S      NOP
S      AND (77
S      JMP I IN
SPROMPT,0
S      CLA
S      TAD (100
S      TLS
SC,    TSF
S      JMP C
S      CLA
S      JMP I PROMPT
END

```

```

CCCCCCCCCCCCCCCCCCCCCCCCCCCCCCCCCCCCCCCCCCCCCCCCCCCCCCCC
C
C      PROGRAM FLUORO.FT
C
C      FLUORESCENCE CORRECTION
C      COORDINATOR
C
CCCCCCCCCCCCCCCCCCCCCCCCCCCCCCCCCCCCCCCCCCCCCCCCCCCCCCCC
COMMON RHO1,RHO2,W1,W2,W3,W4,TH1,TH2,TH3,TH4
COMMON IXMIN,NOPTS,INTVAL,K,FILE1,FILE2,FILE3,LTYPE

C
C      BEGINNING OF COMMAND MODE
C
      WRITE(1,1)
1      FORMAT(/6X,'PROGRAM FLUORO   VERSION 1'/)
2      CALL IN(L)
C
C      COMMAND DECODER
C
5      IF(L-513)10,170,10
10     IF(L-344)11,235,11
11     IF(L-333)12,236,12
12     IF(L-1241)15,237,15
15     IF(L-1236)20,240,20
20     IF(L-784)25,189,25
25     IF(L-774)30,194,30
30     IF(L-463)35,200,35
35     IF(L-396)40,205,40
40     IF(L-433)45,210,45
45     IF(L-434)50,211,50
50     IF(L-435)55,212,55
55     IF(L-262)60,213,60
60     IF(L-590)65,216,65
65     IF(L-1239)70,220,70
70     IF(L-1201)75,294,75
75     IF(L-1202)80,296,80
80     IF(L-1521)85,297,85
85     IF(L-1522)90,298,90
90     IF(L-1523)95,299,95
95     IF(L-1524)100,300,100
100    IF(L-1329)105,301,105
105    IF(L-1330)110,302,110
110    IF(L-1331)115,303,115
115    IF(L-1332)120,304,120
120    WRITE(1,125)
125    FORMAT(3X'ILLEGAL COMMAND!  TRY AGAIN.'/)
      GO TO 2
C
C      HA = HALT
C
170    STOP
C
C      LP = LIST PARAMETERS
C
189    WRITE(1,190)RHO1,RHO2,W1,TH1,W2,TH2,W3,TH3,W4,TH4
190    FORMAT(/5X,6HRHO = ,F5.3/5X,6HRHO' = ,F5.3//5X,'OMEGA1 = '
1F5.3,10X'THETA1 = 'F5.3/5X'OMEGA2 = 'F5.3,10X'THETA2 = '
2F5.3/5X'OMEGA3 = 'F5.3,10X'THETA3 = 'F5.3/5X'OMEGA4 = '
3F5.3,10X'THETA4 = 'F5.3/)
      GO TO 2
C
C      LF = LIST FILES
C
194    WRITE(1,195)FILE1,NOPTS,FILE2,IXMIN,FILE3,LTYPE,INTVAL
195    FORMAT(/5X'FILE1 = 'A6,10X'FILE LENGTH = 'I3/
15X'FILE2 = 'A6,10X'STARTING WAVELENGTH = 'I3/
25X'FILE3 = 'A6,10X'FILE TYPE = 'A2/

```



```

329X' WAVELENGTH INTERVAL = '12/)
GO TO 2

C
C      GO = EXECUTE CURRENT INSTRUCTION SET
C
200    IF(K)202,202,201
201    GO TO (500,600,600,600),K
202    WRITE(1,203)
203    FORMAT(3X,'WHICH CORRECTION MODE, ST, EX, EM, OR SY?'/)
GO TO 2

C
C      FL = FILE LENGTH
C
205    READ (1,206)NOPTS
206    FORMAT(13)
GO TO 2

C
C      F1 = DATA FILE FOR POSITION 1
C      F2 = " " " " " 2
C      F3 = " " " " " 3
C
210    READ(1,215)FILE1
GO TO 2
211    READ(1,215)FILE2
GO TO 2
212    READ(1,215)FILE3
GO TO 2

C
C      DF = SET DEFAULT PARAMETERS
C
213    RHO1=.04
RHO2=.04
W1=.05
W2=.265
W3=.70
W4=.915
TH1=.05
TH2=.29
TH3=.7
TH4=.94
NOPTS=1
K=0
LTYPE=1236
IXMIN=200
INTVAL=2
GO TO 2
215    FORMAT(A6)

C
C      IN = WAVELENGTH INTERVAL
C
216    READ(1,217)INTVAL
217    FORMAT(12)
GO TO 2

C
C      SW = STARTING WAVELENGTH (EMISSION)
C
220    READ(1,221)IXMIN
221    FORMAT(13)
GO TO 2

C
C      EX = EXCITATION PHASE
C      EM = EMISSION PHASE
C      SY = SYNCHRONOUS PHASE
C
235    K=2
LTYPE=L
GO TO 2

```

```

236      K=3
          LTYPE=L
          GO TO 2
237      K=4
          LTYPE=L
          GO TO 2

C
C          ST = STATIC PHASE
C
240      K=1
          LTYPE=L
          GO TO 2

C
C          CORRECTION PARAMETERS
C
294      READ(1,295) RH01
295      FORMAT(F5.3)
          GO TO 2
296      READ(1,295) RH02
          GO TO 2
297      READ(1,295) W1
          GO TO 2
298      READ(1,295) W2
          GO TO 2
299      READ(1,295) W3
          GO TO 2
300      READ(1,295) W4
          GO TO 2
301      READ(1,295) TH1
          GO TO 2
302      READ(1,295) TH2
          GO TO 2
303      READ(1,295) TH3
          GO TO 2
304      READ(1,295) TH4
          GO TO 2
500      CALL CHAIN('STAT')
600      CALL CHAIN('SPEC')
          END

```

```

CCCCCCCCCCCCCCCCCCCCCCCCCCCCCCCCCCCCCCCCCCCCCCCCCCCCCCCC
C
C      SUBROUTINE FOR KEYBOARD INPUT      C
C      FOR PROGRAM FLUORO.FT              C
C                                          C
CCCCCCCCCCCCCCCCCCCCCCCCCCCCCCCCCCCCCCCCCCCCCCCCCCCCCCCC
S      OPDEF   KCC      6032
S      OPDEF   BSW      7002
S      SUBROUTINE IN(L)
S      CLA
S      TAD K212
S      JMS OUT
S      TAD K215
S      JMS OUT
S      TAD K276
S      JMS OUT
S      TAD K207
S      JMS OUT
S      KCC
S      JMS GET
S      BSW
S      DCA TEMP
S      JMS GET
S      TAD TEMP
S      DCA I 1
S      RETURN
SK276, 276
SK212, 212
SK215, 215
SK207, 207
SK77, 77
STEMP, 0
SCET, 0
SA, KSF
S      JMP A
S      KRB
S      TLS
SB, TSF
S      JMP B
S      AND K77
S      JMP I GET
SOUT, 0
S      TLS
SC, TSF
S      JMP C
S      CLA
S      JMP I OUT
S      STOP
S      END

```

```

CCCCCCCCCCCCCCCCCCCCCCCCCCCCCCCCCCCCCCCCCCCCCCCCCCCCCCCCCCCC
C          PROGRAM STAT.FT          C
C          STATIC ABSORPTION CORRECTION      C
C          C          C          C
CCCCCCCCCCCCCCCCCCCCCCCCCCCCCCCCCCCCCCCCCCCCCCCCCCCCCCCCCCCC
      DIMENSION F1(200),F2(200),F3(200)
      COMMON RHO1,RHO2,W1,W2,W3,W4,TH1,TH2,TH3,TH4
      COMMON IXMIN,NOPTS,INTVAL,K,FILE1,FILE2,FILE3
500      CALL IOPEN('FLP2',FILE1)
      DO 510 I=1,NOPTS
505      READ(4,505)F1(I),F2(I),F3(I)
      FORMAT(3E15.9)
510      CONTINUE
      M=0
515      S1=0.
      SS1=0.
      S2=0.
      SS2=0.
      S3=0.
      SS3=0.
      DO 520 I=1,NOPTS
      S1=S1+F1(I)
      SS1=SS1+F1(I)*F1(I)
      S2=S2+F2(I)
      SS2=SS2+F2(I)*F2(I)
      S3=S3+F3(I)
      SS3=SS3+F3(I)*F3(I)
520      CONTINUE
      XN=FLOAT(NOPTS)
      SD1=SD(SS1,S1,XN)
      SD2=SD(SS2,S2,XN)
      SD3=SD(SS3,S3,XN)
      S1=S1/XN
      S2=S2/XN
      S3=S3/XN
      IF(M)550,521,550
521      READ(1,522)OFILE
522      FORMAT('OUTPUT FILE:'A6)
      CALL OOPEN('FLP2',OFILE)
      WRITE(4,530)FILE1
      WRITE(4,535)S1,SD1,S2,SD2,S3,SD3
530      FORMAT('FILE: 'A6/16X'RAW MEANS'/)
535      FORMAT('F1= 'E15.9' +/- 'E15.9/'F2= 'E15.9' +/- 'E15.9/
      1'F3= 'E15.9' +/- 'E15.9/)
      M=1
      DO 540 I=1,NOPTS
      CALL CORR(F1(I),F2(I),F3(I))
540      CONTINUE
      GO TO 515
550      WRITE(4,555)
555      FORMAT(16X'CORRECTED MEANS'/)
      WRITE(4,560)S1,SD1,S2,SD2,S3,SD3
560      FORMAT('F= 'E15.9' +/- 'E15.9/'A= 'E15.9' +/- 'E15.9/
      14HA'= ,E15.9' +/- 'E15.9/)
      CALL OCLOSE
      CALL CHAIN('FLUORO')
      END

```

```

CCCCCCCCCCCCCCCCCCCCCCCCCCCCCCCCCCCCCCCCCCCCCCCCCCCCCCCC
C                                C
C    PROGRAM SPEC.FT            C
C    SPECTRAL ABSORPTION CORRECTION    C
C                                C
CCCCCCCCCCCCCCCCCCCCCCCCCCCCCCCCCCCCCCCCCCCCCCCCCCCCCCCC
      DIMENSION F1(200),F2(200),F3(200),PM(501)
      COMMON RHO1,RHO2,W1,W2,W3,W4,TH1,TH2,TH3,TH4
      COMMON IXMIN,NOPTS,INTVAL,K,FILE1,FILE2,FILE3
600    CALL IOPEN('FLP2',FILE1)
      READ(4,615)(F1(I),I=1,NOPTS)
615    FORMAT(17X,E15.5)
      CALL IOPEN('FLP2',FILE2)
      READ(4,615)(F2(I),I=1,NOPTS)
      CALL IOPEN('FLP2',FILE3)
      READ(4,615)(F3(I),I=1,NOPTS)
      DO 640 I=1,NOPTS
      CALL CORR(F1(I),F2(I),F3(I))
640    CONTINUE
      IF(K-2)641,700,641
641    NSKP=IXMIN-199
      CALL IOPEN('SYS','PM')
      READ(4,642)(PM(I),I=1,501)
642    FORMAT(9(F6.3,2X)F6.3)
      DO 650 I=1,NOPTS
      F1(I)=F1(I)*PM(NSKP)
      NSKP=NSKP+INTVAL
650    CONTINUE
700    READ(1,701)OFILE
701    FORMAT('OUTPUT FILE:'A6)
      CALL OOPEN('FLP2',OFILE)
      DO 750 I=1,NOPTS
      XI=FLOAT(I)
      WRITE(4,755)XI,F1(I),F2(I),F3(I)
750    CONTINUE
755    FORMAT('RD'4E15.5)
      CALL OCLOSE
800    CALL CHAIN('FLUORO')
      END

```

```

CCCCCCCCCCCCCCCCCCCCCCCCCCCCCCCCCCCCCCCCCCCCCCCCCCCCCCCC
C          ABSORPTION CORRECTION SUBROUTINE          C
C                                                    C
CCCCCCCCCCCCCCCCCCCCCCCCCCCCCCCCCCCCCCCCCCCCCCCCCCCCCCCC
SUBROUTINE CORR(F1,F2,F3)
COMMON RHO1,RHO2,W1,W2,W3,W4,TH1,TH2,TH3,TH4
COMMON IXMIN,NOPTS,INTVAL,K,FILE1,FILE2,FILE3
CLOG=ALOG(10.)
PEXP=1./(W3-W1)
SEXP=1./(TH3-TH1)
T1=(F1/F2)**PEXP
T2=(F3/F2)**SEXP
PRC1=1.+RHO1*T1**(2.-W3-W4)
PRC2=1.+RHO1*T1**(2.-W1-W2)
SRC1=1.+RHO2*T2**(2.-TH3-TH4)
SRC2=1.+RHO2*T2**(2.-TH1-TH2)
T1=T1*(PRC2/PRC1)**PEXP
T2=T2*(SRC2/SRC1)**SEXP
AP=-ALOG(T1)/CLOG
AS=-ALOG(T2)/CLOG
A=AP*AS*(W2-W1)*(TH2-TH1)*CLOG*CLOG
B=T1**W2-T1**W1
C=T2**TH2-T2**TH1
F1=F1*A/(C*(T1**W4-T1**W3))
F2=F2*A/(C*B)
F3=F3*A/(B*(T2**TH4-T2**TH3))
RC=(1.-RHO1*RHO1*T1*T1)*(1.-RHO2*RHO2*T2*T2)/(1.-RHO1)/(1.-RHO2)
F1=F1*RC/PRC1/SRC2
F2=F2*RC/PRC2/SRC2
F3=F3*RC/PRC2/SRC1
F1=(F1+F2+F3)/3.
F2=AP
F3=AS
RETURN
END

```

```

CCCCCCCCCCCCCCCCCCCCCCCCCCCCCCCCCCCCCCCCCCCCCCCCCCCCCCCC
C          SUBROUTINE SD          C
C          COMPUTE STANDARD DEVIATION FROM          C
C          SUM AND SUM OF SQUARES          C
CCCCCCCCCCCCCCCCCCCCCCCCCCCCCCCCCCCCCCCCCCCCCCCCCCCCCCCC
FUNCTION SD(SS,S,X)
SD=SQRT(ABS(SS-S*S/X)/(X-1.))
RETURN
END

```